ESTIMATION OF PETROLEUM RESERVOIR PROPERTIES

Thesis by

Tai-yong Lee

In Partial Fulfillment of the Requirements

for the Degree of

Doctor of Philosophy

California Institute of Technology

Pasadena, California

1987

(Submitted October 20, 1986)

Acknowledgements

I would like to express my deepest appreciation to my advisor, Professor John H. Seinfeld, who was most patient and generous throughout the course of this research, and was always able to provide timely suggestions when they were needed. I thank Dr. Costas Kravaris for his invaluable discussions and Lenore Kerner for her excellent typing during the preparation of the paper reported in Chapter II. I am indebted to Drs. Wen H. Chen and Mel L. Wasserman and Chevron Oil Field Research Company for providing many vital suggestions and access to their Cray X-MP/48 for the two-phase problems.

Last but not least, I thank my family for their love and wish my father could have shared in this.

Abstract

Numerical algorithms are developed to estimate petroleum reservoir properties such as absolute permeability, porosity, and relative permeabilities based on the noisy pressure and flow data. Regularization and spline approximation of spatially varying parameters are employed to convert the ill-posed nature of the problem to a well-posed one. A stabilizing functional with gradient operator is used to measure the non-smoothness of the parameter estimates. The number of spline coefficients along each spatial direction is chosen to be as much as the number of meshes for the reservoir PDE's. New history matching algorithms are developed that determine the regularization parameter during the computation without requiring *a priori* information and improve the parameter estimates stepwise. A partial conjugate gradient method is employed for the estimation of a single set of parameters, and the steepest descent algorithm is used for the simultaneous estimation of absolute and relative permeabilities. A rough parametric sensitivity analysis is carried out for the simultaneous estimation to improve the convergence. Numerical tests are carried out to estimate the parameters in single- and two-phase reservoirs for the different choices of the stabilizing functionals, the regularization parameters, and the degrees of spline approximation; and the effects of the observation error, the observation time, and the configuration of the observation points are investigated. The results show that the new algorithms generate better parameter estimates over the various possible choices of the estimation conditions.

Table of Contents

List of Figures

Page

Chapter II

Chapter III

Chapter IV

Appendix A

Appendix B

List of Tables

Chapter IV

Appendix A

Chapter I

Introduction

The knowledge of petroleum reservoir properties such as absolute and relative permeabilities and porosity forms the bases for determining the optimal strategy of oil recovery. Estimation of the reservoir properties appearing as the coefficients of reservoir PDE's from the noisy pressure and production data is an ill-posed inverse problem due to the insensitivity of the measured data to the reservoir properties associated with its large dimensionality. Regularization of an ill-posed problem refers to solving a well-posed regularized problem of the original problem of estimating inhomogeneous coefficients of integral or partial differential equations, where the regularized solution approximates the solution of the original problem. More precisely, the parameter estimation by regularization is carried out by minimizing the smoothing functional, that is a weighted sum of the conventional least-squares discrepancy function and the stabilizing functional, with respect to the parameter estimates. The weighting coefficient, called the regularization parameter, represents the relative importance given to the stabilizing functional. Spline approximation is another way of alleviating the ill-posed nature of estimating spatially varying parameters in PDE's, and it also provides a convenient way of representing the parameters. By introducing the concept of regularization and spline approximation to the optimal control algorithms of reservoir history matching, the problems become to involve additional unknowns, namely, the form of the stabilizing functional, the regularization parameter, and the degree of spline approximation that should be determined before or during the estimation processes. In this dissertation, history matching algorithms are developed to estimate absolute permeability and porosity by the regularization and the spline approximation and relative permeabilities that resolve the additional unknowns in a quantitative manner.

In Chapter II, the estimation of absolute permeability and porosity in the single-phase, two-dimensional reservoirs or aquifers is considered. Tikhonov's stabilizing functional is used to measure the non-smoothness of the parameter estimates. The smoothing functional is minimized by the partial conjugate gradient algorithm of Nazareth. Estimation of spatially varying parameter starts with the single-valued parameter that is spatially uniform and minimizes the least-squares discrepancy term. The estimation results are demonstrated for the various degrees of spline approximation and for the different regularization parameters. The quasi-optimality condition of the regularization parameter is investigated for both the estimation of absolute permeability and porosity. It is shown that the use of Tikhonov's stabilizing functional leads to the underestimation of the parameters due to inclusion of the Euclidean norm of the parameter itself.

In Chapter III, a history-matching algorithm is developed to estimate the absolute permeability from the pressure data in two-phase, two-dimensional petroleum reservoirs. The number of spline coefficients along each spatial direction is specified to be as much as the number of grid cells of the governing PDE's. The algorithm employs Locker and Prenter's stabilizing functional with a differential (gradient) operator that does not include the Euclidean norm. The regularization parameter is determined from the ratio of the discrepancy term to the stabilizing functional calculated from the results of the conventional least-squares estimation and additional regularized estimation is followed. The numerical test shows the superiority of the regularized estimation to the conventional estimation.

In Chapter IV, the estimation of the absolute permeability and the exponents of relative permeability expressions are estimated simultaneously. The algorithm developed in Chapter III is extended for the simultaneous estimation of the parameters. The steepest descent algorithm is used as the core minimization technique, and a rough parametric sensitivity analysis is carried to improve the convergence

of the minimization. Numerical examples show the identifiability conditions on the observation time in estimating relative permeabilities.

In Appendix A, an additional example to Chapter III is tested that estimates the absolute permeability, which varies stiffly. The example shows the identifiability condition on the configuration of the observation points. In Appendix B, numerical details of the algorithm developed in Chapter IV are described.

Chapter II

History Matching by Spline Approximation and Regularization in Single-Phase Areal Reservoirs

---

The text of Chapter II consists of an article coauthored with C. Kravaris and J. H. Seinfeld, which has appeared in *SPE Reservoir Engineering* **1** 521 (1986).

History Matching by Spline Approximation and Regularization in Single-Phase Areal Reservoirs

Tai-yong Lee, California Inst. of Tech.
Costas Kravaris, U. of Michigan
John H. Seinfeld, SPE, California Inst. of Tech.

Summary. An automatic history-matching algorithm is developed from bicubic spline approximations of permeability and porosity distributions and from the theory of regularization to estimate permeability or porosity in a single-phase, two-dimensional (2D) areal reservoir from well pressure data. The regularization feature of the algorithm, the theoretical details of which are described by Kravaris and Seinfeld,[1,2] is used to convert the ill-posed history-matching problem into a well-posed problem. The algorithm uses Nazareth's[3] conjugate gradient method as its core minimization method. A number of numerical experiments are carried out to evaluate the performance of the algorithm. Comparisons with conventional (nonregularized) automatic history-matching algorithms indicate the superiority of the new algorithm with respect to the parameter estimates obtained. A quasioptimal regularization parameter is determined without requiring *a priori* information on the statistical properties of the observations.

Introduction

The process of estimating unknown properties, such as permeability and porosity, in a mathematical reservoir model to give the best fit to measured well pressure and production data is commonly called history matching. Because the properties in an inhomogeneous reservoir vary with location, an infinite number of parameters is required conceptually for a full description of the reservoir. From a computational point of view, a reservoir simulator contains only a finite number of parameters, corresponding to each gridblock or element in the spatial domain. In field-scale simulations, it is not unusual for the reservoir domain to consist of about 10,000 gridblocks, and consequently 20,000 or more parameters may need to be estimated simultaneously. This potential large dimensionality of the unknown parameters distinguishes the reservoir history-matching problem from other parameter-estimation problems in science and engineering. Moreover, the standard reservoir history-matching problem is mathematically ill-posed, and this ill-posed nature, coupled with such a large number of unknown parameters, lies at the root of the difficulties in its solution. The ill-posed nature of the history-matching problem is manifested by numerical instabilities in the estimated parameters. Such instabilities are well documented in the petroleum engineering and hydrology literature.[4,5]

The principal approach that has been used to alleviate ill-conditioning in the parameter estimates is to decrease the number of unknown parameters and, if possible, to utilize any available information to constrain the space of unknown parameters. One commonly used approach for reducing the number of unknown parameters is to divide the reservoir into a relatively small number of zones and to assume uniform properties within each zone. While this approach is effective in reducing the number of unknowns, sufficient *a priori* information usually is not available to enable specification of the zones on any physical basis. Moreover, although it limits the dimension of the parameter space, zonation does not alleviate the fundamental ill-posed nature of the problem. An alternative to zonation is to use prior information expressed in the form of an assumed probability distribution for the reservoir properties. If certain *a priori* knowledge is assumed about the parameter mean values and correlations, the history-matching objective function can be modified to include a term that penalizes the weighted deviations of the parameters from their assumed mean values.[4] A form of Bayesian estimation can then be used to determine the unknown parameters. While it has been shown that better-conditioned estimates may be obtained when *a priori* statistical information is used, sufficient knowledge of the nature of the unknown parameters generally is not available to specify the parameters needed to carry out a Bayesian estimation.

The critical problems in generating an effective algorithm for history matching are two-fold: (1) the original problem must be defined in a manner that alleviates the ill-posed nature of the problem; and (2) an efficient computational algorithm must be developed for solving the large, constrained, nonlinear minimization problem that results from any history-matching problem.

With respect to the inherent ill-posed nature of the history-matching problem, Kravaris and Seinfeld[1,2] have shown that the concept of regularization can be applied rigorously to the estimation of spatially varying parameters in partial-differential equations of parabolic type. The regularization idea, first advanced by Tikhonov and Arsenin,[6] has been widely used in the solution of ill-posed integral equations, but had not been developed for the estimation of parameters in partial-differential equations.

Regularization of a problem is solving a related problem (called the regularized problem) with a solution that is more "regular" (in a certain sense) than the solution of the original problem and approximates (in a certain sense) the solution of the original problem. More precisely, regularization of an ill-posed problem refers to solving a well-posed problem, the solution of which gives a physically meaningful answer to the original ill-posed problem. The regularization formulation of parameter estimation measures the "nonsmoothness" of the estimated parameter as a norm of the parameter in an appropriate Hilbert space. No prior information about the parameter is required other than a general idea of the degree of smoothness desired in the estimated field. The only unspecified parameter is that reflecting the relative weight given to the smoothness norm vs. the usual least-squares objective function.

Researchers[7-10] have found that the use of spline representations for spatially varying parameters in one-dimensional (1D) partial-differential equations of both parabolic and hyperbolic type leads to well-conditioned estimates. Although their numerical results were obtained for low levels of spline discretization, it seems that the spline representation may impart a degree of smoothness to the parameter distribution that could circumvent some of the ill-conditioning inherent in the finite-difference or zonation representation of the unknown parameters. The use of 2D bicubic spline approximations for reservoir history matching is an additional new feature of the work reported here.

The object of this work is to present an automatic history-matching algorithm that is based on the concept of regularization together with bicubic spline approximations for the estimation of permeability and porosity in a single-phase, 2D areal reservoir simulation. The two critical problems cited previously are addressed in the algorithm. First, the regularization formulation converts the history-matching problem to a mathematically well-posed problem. Second, we use a particularly efficient numerical minimization method, Nazareth's[3] conjugate gradient method, as the core technique for the minimization. We present the results of extensive numerical testing of the algorithm in which both permeability and porosity distributions are estimated. The effects of the degree of regularization and of the order of the spline approximation on the behavior of the estimates will be of particular interest.

History Matching by Regularization

The problem of history matching may be viewed in a general way by expressing the reservoir model, or simulator, as the nonlinear operator equation,

$$K\alpha = u, \quad \ldots\ldots\ldots\ldots\ldots\ldots\ldots\ldots\ldots\ldots (1)$$

where α represents the reservoir parameters, K is the operator representing the reservoir model, and u is the observed portion of the model's output, such as the well pressures. The history-matching problem is just the inverse problem to Eq. 1—i.e., given u and K, find α. This inverse problem is well-posed if for every u there exists a solution α, if the solution is unique, and if the solution is stable—i.e., small perturbations in u imply small perturbations in α.

If any of these conditions are not met, the inverse problem is ill-posed. Establishing uniqueness of α given u for operators K typical of reservoir simulators is an extremely difficult problem, and at this time uniqueness results are available only for very special cases.[11] It can be shown readily, however, that the inverse problem to Eq. 1 for spatially varying parameters in parabolic partial-differential equations is unstable,[1] and the estimation of α from u is an ill-posed problem. As we noted, the ill-posed nature of the problem manifests itself by highly ill-conditioned estimates in conventional automatic history-matching approaches.

Let us now be more specific and consider unsteady flow of a slightly compressible oil with viscosity μ in a 2D, areal reservoir of unit thickness, spatial domain Ω, and boundary $\partial\Omega$ in which fluid is being withdrawn from n_w wells located at (x_w, y_w), $w = 1,2 \ldots n_w$. The fluid properties, μ and c, are assumed to be known, whereas the porosity, ϕ, and permeability, k, are assumed to be unknown. The pressure distribution in the reservoir is governed by

$$c\phi \frac{\partial p}{\partial t} = \nabla\left(\frac{k}{\mu}\nabla p\right) + \sum_{w=1}^{n_w} q_w \delta(x - x_w)\delta(y - y_w) \quad . (2)$$

in $\Omega \times (0,T)$,

$$\frac{\partial p}{\partial n} = 0 \quad \ldots\ldots\ldots\ldots\ldots\ldots\ldots\ldots\ldots\ldots (3)$$

on $\partial\Omega \times (0,T)$, and

$$p(x,y,0) = p_0(x,y) \quad \ldots\ldots\ldots\ldots\ldots\ldots\ldots\ldots (4)$$

in Ω, where $\partial p/\partial n$ is the outward normal derivative of p on the boundary $\partial\Omega$ and $(0,T)$ is the time interval over which data are available. Because of the small size of the wellbores relative to the reservoir dimensions, the well flow rates are represented as point sink terms in the pressure equation. If there exist observed pressures at n_{OBt} times at n_{OB} locations, $p_{k,n_{OB}}$, $k = 1,2 \ldots n_{OB}$, $n = 1, 2 \ldots n_{OBt}$, then the customary history-matching least-squares objective function is

$$J_{LS} = \sum_{n=1}^{n_{OBt}} \sum_{k=1}^{n_{OB}} [p_{k,n_{OB}} - p(x_k, y_k, t_n)]^2. \quad \ldots\ldots (5)$$

The conventional history-matching problem can be viewed therefore as a nonlinear optimization problem of minimizing the sum of squares of differences between the observed and predicted pressures subject to the constraint of the reservoir model (Eqs. 2 through 4).

In the regularization approach, we minimize an augmented objective function, called the smoothing functional, denoted by J_{SM}, that consists of the sum of the least-squares term, J_{LS}, and a stabilizing functional, J_{ST}. The stabilizing functional for a parameter α ($\alpha = \phi$ or k) is of the form

$$J_{ST} = ||\alpha||^2 H^3(\Omega), \quad \ldots\ldots\ldots\ldots\ldots\ldots (6)$$

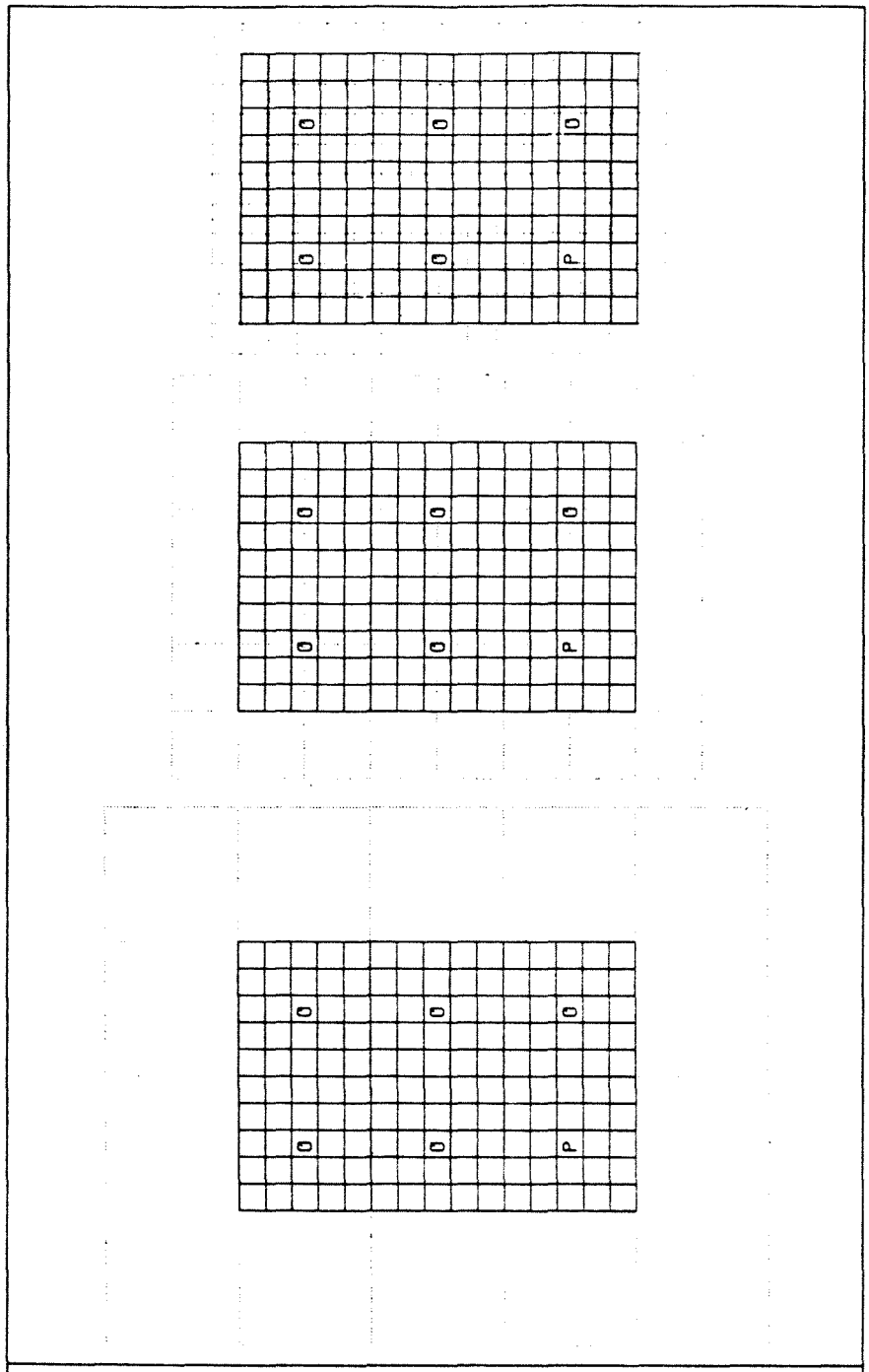

Fig. 1—Pressure and spline grid system, pressure grid: 10 x 15; spline grid: 5 x 6; 7 x 9; 12 x 17 (O = observation well; P = production well).

where $||\ ||^2_{H^3(\Omega)}$ is a norm defined in the Sobolev space $H^3(\Omega)$. [The Sobolev space $H^3(\Omega)$ is the set of functions that are square-integrable over Ω and have square-integrable derivatives up to order 3. The norm of $H^3(\Omega)$ is given by Eq. A-12.] Thus the overall objective function to be minimized is

$$J_{SM}=J_{LS}+\beta_\alpha J_{ST}, \quad \ldots\ldots\ldots\ldots\ldots\ldots\ldots (7)$$

where β_α is a weighting coefficient chosen to reflect the degree of importance given to J_{ST}.

The minimization of J_{SM} is performed over an appropriate finite-dimensional subspace of $H^3(\Omega)$, the so-called space of approximants, which can be spanned by cubic spline functions. Thus the infinite-dimensional parameter spaces for k and ϕ are reduced to finite-dimensional spaces by cubic spline approximations, and the finite-

TABLE 1—SPECIFICATIONS OF RESERVOIR FOR HISTORY-MATCHING EXAMPLE

Dimension of reservoir, miles [km]	12.4 x 18.6 [20 x 30]
Compressibility of system, atm^{-1} [Pa^{-1}]	1.2×10^{-5} [1.2×10^{-10}]
Viscosity of fluid, cp [Pa·s]	2.0 [2.0×10^{-3}]
Number of production wells	1
Production rate, ft^2/D [m^2/s]	500 [5.376×10^{-4}]
Initial pressure, atm [Pa]	150 [1.52×10^{7}]
Pressure grid	10 x 15
Number of observation wells	6
Number of well pressure data per well	35
Time interval of well pressure data, days	10
Total number of data points	210

dimensional minimization of J_{SM} is carried out by an appropriate numerical minimization method.

Bicubic Spline Approximation of Permeability and Porosity

A general approach to representing the spatial variation of reservoir properties is through the use of bicubic spline functions in which a parameter, $\alpha(x,y)$, is represented as

$$\alpha(x,y)=\sum_{\ell_y=1}^{n_{ys}}\sum_{\ell_x=1}^{n_{xs}} b_x(\ell_x,x)W^{\alpha}{}_{\ell_x,\ell_y}b_y(\ell_y,y), \quad \ldots (8)$$

where

$$b_x(\ell_x,x)=\chi^{*4}\left(4-\ell_x+\frac{x}{\Delta x_s}\right), \quad \ell_x=1,2\ldots n_{xs}, \quad .(9)$$

$$b_y(\ell_y,y)=\chi^{*4}\left(4-\ell_y+\frac{y}{\Delta y_s}\right), \quad \ell_y=1,2\ldots n_{ys}, \quad .(10)$$

and where $\chi^{*4}(\ )$ is the cubic B-spline function,

$$\chi^{*4}(x)=\begin{cases}\dfrac{x^3}{6} & x\in(0,1)\\ \tfrac{1}{6}+\dfrac{x-1}{2}+\dfrac{(x-1)^2}{2}-\dfrac{(x-1)^3}{2} & x\in(1,2)\\ \tfrac{4}{6}-(x-2)^2+\dfrac{(x-2)^3}{2} & x\in(2,3)\\ \tfrac{1}{6}-\dfrac{x-3}{2}+\dfrac{(x-3)^2}{2}-\dfrac{(x-3)^3}{6} & x\in(3,4)\\ 0 & \text{otherwise.}\end{cases} \quad \ldots (11)$$

Here, Δx_s and Δy_s are the grid distances of the spline grid along the x and y directions, respectively. With this approximation, $\alpha(x,y)$ is replaced by the set of unknown coefficients, $W^{\alpha}{}_{\ell_x,\ell_y}$, $\ell_x=1,2\ldots n_{xs}$ and $\ell_y=1,2\ldots n_{ys}$.

The grid used for spline representation of the unknown properties need not coincide with that on which the actual reservoir model is solved. The reservoir model will be solved numerically by use of finite-difference approximations on the block-centered grid system shown in Fig. 1. Fig. 1 also shows the spline grid system. The finite-difference grid can be expressed compactly as $I_x=\{i_x\,|\,i_x=1,2\ldots n_x\}$, $I_y=\{i_y\,|\,i_y=1,2\ldots n_y\}$, and $I_n=\{i\,|\,i=i_x+n_x(i_y-1),\ i_x\in I_x,\ i_y\in I_y\}=\{i\,|\,i=1,2\ldots n_t\}$, where $n_t=n_xn_y$.

The finite-difference approximation of the pressure equation can be written in compact notation as

$$Qc\phi_i(p_i^{\,n}-p_i^{\,n-1})=\sum_{j\in J_i}Q_{LJ}\frac{k(i,j)}{\mu}(p_j^{\,n}-p_i^{\,n})+\sum_{w=1}^{n_w}q_w\delta_{i,i_w} \quad \ldots (12)$$

for $i\in I_n$, $n=1,2\ldots n_t$, where

$$I_i=\{j\,|\,j=i-n_x,\ i-1,\ i+1,\ i+n_x\}\cap I_N,$$

$Q=\Delta x\Delta y/\Delta t$, and

$$Q_{LJ}=\begin{cases}\Delta y/\Delta x, & \text{if } j=i-1,\ i+1, \text{ and } j\in I_n\\ \Delta x/\Delta y, & \text{if } j=i-n_x,\ i+n_x, \text{ and } j\in I_n,\end{cases}$$

δ_{i,i_w} is the Kronecker delta, and $k(i,j)=(k_i+k_j)/2$. The initial condition is $p_i^{\,0}=p_0$, $i\in I_N$.

The least-squares objective function is then written as

$$J_{LS}=\sum_{i=1}^{n_t}\sum_{n=1}^{n_{OBt}}\sum_{k=1}^{n_{OB}}(p_{k,n_{OB}}-p_i^{\,n})^2\delta_{i,i_k}, \quad \ldots (13)$$

where we assume that $t_n-t_{n-1}=\Delta t$ for $n=1\ldots n_{OBt}$.

History-Matching Algorithm

The problem we now seek to solve is to minimize the augmented objective function, J_{SM}, given by Eq. 7 with respect to the spline coefficients $W^{\alpha}{}_{\ell_x,\ell_y}$, $\ell_x=1,2\ldots n_{xs}$ and $\ell_y=1,2\ldots n_{ys}$, subject to the pressure equation (Eq. 12). To obtain an algorithm to solve this problem, two steps are required. First, we must compute the gradient of J_{SM} with respect to each $W^{\alpha}{}_{\ell_x,\ell_y}$. Second, that gradient is then used in a numerical minimization method to minimize J_{SM}. The calculation of these gradients repre-

TABLE 2—TRUE VALUES OF POROSITY AND PERMEABILITY, THE UNIFORM VALUES OF ϕ AND k THAT MINIMIZE J_{LS}, AND THE CORRESPONDING STARTING VALUES OF J_{LS}, J_{ST}, AND J_{SM}

Parameter To Be Estimated	ϕ (fraction)		k (darcies)	
True value	$0.2-0.05\sin(\pi x/x_L)\times\sin(2\pi y/y_L)$		$0.3-0.1\sin(\pi x/x_L)\times\sin(2\pi y/y_L)$	
Initial guess	0.25 and 0.15		0.25 and 0.35	
$\bar{\alpha}$ that minimizes J_{LS}	0.184		0.241	
J_{LS}	44.6		41.0	
J_{ST}	5.1		8.7	
J_{SM}	β_α, atm^2 = 0	44.6	β_k, atm^2/darcies^2 = 0	41.0
	0.01	44.7	0.01	41.1
	0.1	45.1	0.1	41.9
	1	49.7	1	49.7
	10	95.6	10	128.0

sents the most time-consuming part of updating the parameter iterates. In a problem as large as history matching in a candidate algorithm, these derivatives must be able to be calculated directly, not requiring the individual derivatives $\partial p_i^n/\partial W^\alpha{}_{t_x,t_y}$.[12,13] Those algorithms based on an optimal control or variational formulation possess this necessary property.[14–16] First, we solve the reservoir simulator equation (Eq. 13) from $t=0$ to $t=T$. Then we solve the adjoint system equation (Eq. A-7) backward, starting from $t=T$ with the terminal condition (Eq. A-8) to $t=0$, and at the end of each timestep during the solution of adjoint system, compute the functional derivative of J_{LS} with respect to permeability (Eq. A-9) or porosity (Eq. A-10) at the simulator grid cells. Then we compute the derivative of J_{LS} with respect to the spline coefficient W^α (Eq. A-11), the derivative of J_{ST} with respect to W^α (Eqs. A-12 through A-19), and the derivative of J_{SM} with respect to W^α (Eq. A-20).

Because of the large dimensionality of $W^\alpha{}_{t_x,t_y}$, one seeks to use an algorithm that is as efficient as possible. The essential consideration in the choice of a method is the computational time needed to minimize the objective function. Most multivariate minimization methods can be divided into two groups: conjugate gradient methods and quasi-Newton methods. The quasi-Newton methods are preferred for moderate-sized problems, but the conjugate gradient methods become superior to the quasi-Newton methods as the number of variables gets large (Scales[17] suggested 250 as a turning point). Although we treat 30 to 204 variables in our examples, the number is larger for field applications. Nazareth's[3] conjugate gradient algorithm of was chosen as the core-minimization method in the current code.

The remainder of this work is devoted to the numerical evaluation of the algorithm on the estimation of permeability and porosity distributions in a single-phase, 2D areal reservoir as modeled by Eq. 2. We want to evaluate the algorithm on a well-defined test problem for which the "true" property distributions are known *a priori*. For this reason, we will specify the true parameter values, generate our own pressure data by solving the reservoir model with these values, and then try to recover the true parameter values by using the history-matching algorithm.

Permeability level and distribution is the principal reservoir property used to match pressure behavior. Porosity is usually better known than permeability, and values from log and core data are often used as initial guesses for ϕ. (Porosity in the aquifer is generally less well known than in the reservoir itself and can be more readily varied than ϕ in the reservoir.) Aside from aquifer permeability and porosity, which are generally not well known, reservoir permeability is usually more uncertain than porosity.

It is difficult to determine the optimal value of the regularization parameter even if we know the statistical properties of measurement error of the well pressure data. We will choose a set of values of the regularization parameter so that they form a geometric sequence and determine the optimal regularization parameter from the quasioptimal value of the regularization parameter[6] that minimizes $||\beta_\alpha \partial w^\alpha/\partial\beta_\alpha||_2$.

The data for the cases we will study are given in Table 1. Although this set of data is hypothetical, every effort has been made to have the example conform to an actual field simulation.

An important question concerns starting the algorithm. Convergence difficulties are sometimes experienced when

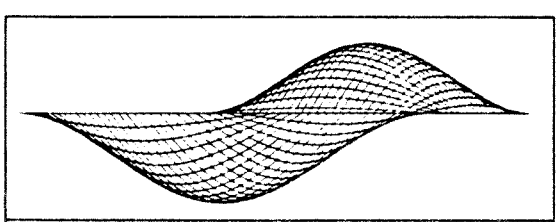

Fig. 2—True $\phi(x,y)$ surface; $\phi(x,y)=0.2-0.05\sin(\pi x/x_L)\sin(2\pi y/y_L)$.

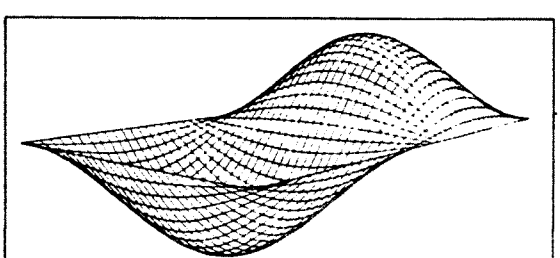

Fig. 3—True $k(x,y)$ surface; $k(x,y)=0.3-0.1\sin(\pi x/x_L)\sin(2\pi y/y_L)$ darcies.

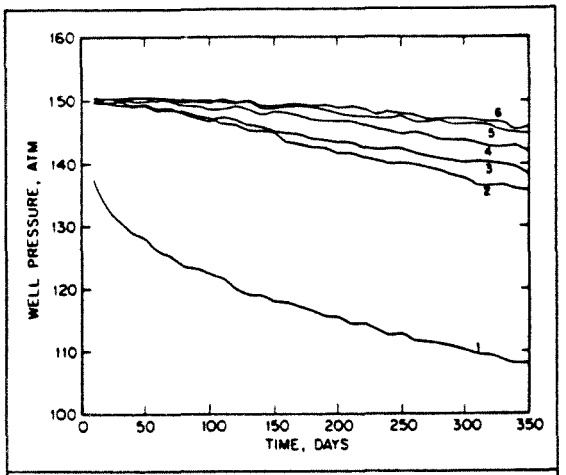

Fig. 4—Simulated pressure data vs. time for $\sigma = 0.3$ atm: (1) (3.1, 3.1); (2) (9.3, 3.1); (3) (3.1, 9.3); (4) (9.3, 9.3); (5) (3.1, 15.5); and (6) (9.3, 15.5) (units are miles).

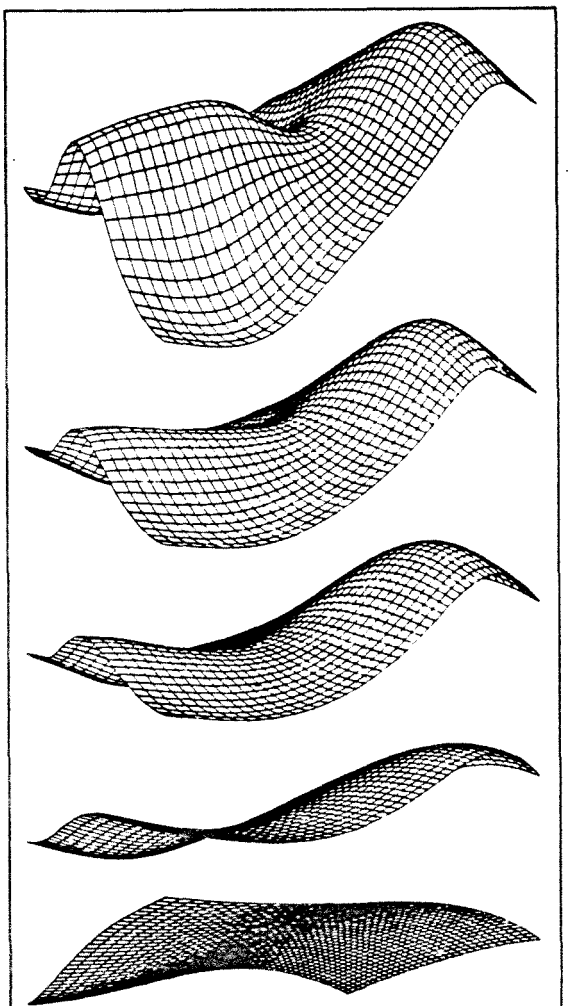

Fig. 5—Estimated ϕ surface for $\sigma = 0.3$ atm, $n_{xs} \times n_{ys} = 7 \times 9$, and from top down: $\beta_\phi = 0$ atm^2, 0.01, 0.1, 1, and 10.

the initial guesses of the parameters are far from their actual values. To attempt to alleviate this problem and to generate an algorithm that is as "hands-off" as possible, we begin the estimation by determining the unknown parameters as uniform over the entire region. Thus, to start, we estimate single values of k and ϕ for the entire region, called $\bar{k}$ and $\bar{\phi}$, that minimize J_{LS}. These values then serve as starting points for the full history-matching algorithm. The rationale behind this strategy is that convergence problems should not be encountered in estimating a single parameter. The single value, while not accurate in its spatial detail, nevertheless serves as a good starting point for the full algorithm. This strategy has been used in the results to be presented shortly. The single-variable minimization is carried out in our code by the secant method.

Table 2 gives the results of this first step for the estimation of ϕ when k is known and the estimation of k when ϕ is known. Listed in Table 2 are the true values of ϕ and k, the initial guesses to start the secant method, the minimizing parameter value α ($\alpha = \phi$ or k), and the values of J_{LS}, J_{ST}, and J_{SM} for various values of the regularization parameter β at the minimum. The true ϕ and k surfaces are shown in Figs. 2 and 3, respectively. To simulate measurement error, uniformly distributed random numbers are added to the pressure data generated from our presumed true permeability and porosity distributions. The resulting data are shown in Fig. 4.

Estimation of Spatially Varying Permeability and Porosity

We will investigate the effect of the choice of regularization parameter (β_α), degree of spline approximation ($n_{xs} \times n_{ys}$), and the number of observation wells in the estimation of ϕ when k is known and the estimation of k when ϕ is known.

We will use six observation wells for values of the regularization parameter $\beta_\phi = 0$, 0.01, 0.1, 1, and 10 atm^2 [0, 1×10^9, 10×10^9, and 100×10^9 Pa^2] for the estimation of ϕ and $\beta_k = 0$, 0.01, 0.1, 1, and 10 atm^2/darcies^2 [0, 0.01×10^{34}, 0.1×10^{34}, 1×10^{34}, and 10×10^{34} Pa^2/m^4] for the estimation of k and spline grids $n_{xs} \times n_{ys} = 5 \times 6$, 7×9, and 12×17, where 12×17 is the maximum possible value for the pressure grid we are using for both the estimation of ϕ and the estimation of k. As a special case, we will use 18 observation wells for the estimation of k, with $\beta_k = 1$ atm^2/darcies^2 [1.054×10^{34} Pa^2/m^4] and $n_{xs} \times n_{ys} = 7 \times 9$. Finally, in all our simulations, we assumed that the root-mean-square (RMS) error in pressure measurements was $\sigma = 0.3$ atm [30.4 kPa] (thus $\sigma/p_0 = 0.2\%$ and the corresponding J_{LS} value is 18.96 atm^2 [195×10^9 Pa^2]).

The estimation of ϕ started with a uniform value of $\bar{\phi} = 0.184$ and the smoothing functional J_{SM} was minimized until the change in spline coefficient, W^ϕ, and the gradient of J_{SM} with respect to W^ϕ satisfied the convergence criteria given by

$$||W^{\phi,\text{new}} - W^{\phi,\text{old}}|| < \epsilon_1 \quad \ldots\ldots\ldots\ldots\ldots\ldots (14a)$$

and

$$||G_{SM}{}^{W^\phi}|| < \epsilon_2. \quad \ldots\ldots\ldots\ldots\ldots\ldots (14b)$$

TABLE 3—ESTIMATION OF ϕ

a. Final values of performance indices for $\sigma = 0.3$ atm and $n_{xs} \times n_{ys} = 7 \times 9$ as a function of β_ϕ (atm^2)

β_ϕ	J_{SM}	J_{LS}	J_{ST}*	J_{ST}^1	$J_{ST}^2 \times 10^2$	$J_{ST}^3 \times 10^3$	$J_{ST}^4 \times 10^3$
0	20.67	20.67	15.55	6.47	5.30	30.24	193.63
0.01	20.86	20.76	9.47	6.47	2.67	10.96	61.64
0.1	21.60	20.85	7.48	6.44	1.76	5.11	18.75
1	27.61	21.16	6.45	6.28	0.75	1.47	1.79
10	81.69	24.09	5.76	5.74	0.20	0.12	0.09
true			7.09	6.17	2.63	7.48	1.88

b. Final values of performance indices for $\sigma = 0.3$ atm and $\beta_\phi = 1$ atm^2 as a function of $n_{xs} \times n_{ys}$

$n_{xs} \times n_{ys}$	h	J_{SM}	J_{LS}	J_{ST}	J_{ST}^1	$J_{ST}^2 \times 10^2$	$J_{ST}^3 \times 10^3$	$J_{ST}^4 \times 10^3$
5 × 6	5	27.86	21.38	6.47	6.29	0.50	0.04	0.002
7 × 9	2.5	27.61	21.16	6.45	6.28	0.75	1.47	1.79
12 × 17	1.09	27.17	20.78	6.40	6.31	3.11	18.38	14.78

*$\zeta_1 = 1, \zeta_2 = h^2, \zeta_3 = h^4, \zeta_4 = h^6$, with $h = 2.5$.
**$\xi_1 = 1, \xi_2 = h^2, \xi_3 = h^4, \xi_4 = h^6$.

The same strategy was used for the estimation of k, where the starting value of $\bar{k} = 0.241$ darcies (0.243 darcies for 18 observation wells) was used. Tables 3 and 4 summarize the history-matching results for all the cases studied.

Effect of Regularization. We expect that, as the regularization parameter increases, the value of the least-squares objective function, J_{LS}, at convergence will increase, but the stabilizing functional, J_{ST}, will decrease because a larger value of regularization parameter means more smoothing of the parameter to be estimated at the expense of less exact fitting of the observed well pressure data.

This expectation turned out to be true with some exceptions for the terms $J_{ST}{}^{m+1}$, $m = 0$ and 1, in the stabilizing functional during the estimation of k as shown in Table 4a. That is, $J_{ST}{}^1$ for $\beta_k = 0.1$ atm^2/darcies^2 [1.054×10^{33} Pa^2/m^4] is slightly greater than that for $\beta_k = 0.01$ atm^2/darcies^2 [1.054×10^{32} Pa^2/m^4], and $J_{ST}{}^2$ for $\beta_k = 10$ atm^2/darcies^2 [10.5×10^{35} Pa^2/m^4] is greater than those for $\beta_k = 0.1$ and 1 atm^2/darcies^2 [1.054×10^{33} and 1.054×10^{34} Pa^2/m^4]. But the total stabilizing functional, J_{ST}, and its component, $J_{ST}{}^4$, that represents the third-order derivative term and is most important among the four terms, $J_{ST}{}^{m+1}$, $m = 0$, 1, 2, and 3, decreases strictly without exception as β_k increases.

Table 3a shows that $J_{ST}{}^4$ terms for true ϕ are close to that for estimated ϕ, with $\beta_\phi = 1$ atm^2 [1.03×10^{10} Pa^2] for which J_{LS} and $\beta_\phi J_{ST}$ are balanced; but Table 4a shows that $J_{ST}{}^4$ terms for true k are close to that for estimated k with β_ϕ between 0.1 and 0.01 atm^2/darcies^2

TABLE 4—ESTIMATION OF k

a. Final values of performance indices for $\sigma = 0.3$ atm and $n_{xs} \times n_{ys} = 7 \times 9$ as a function of β_k (atm^2/darcies^2)

β_k	J_{SM}	J_{LS}	J_{ST}*	J_{ST}^1	$J_{ST}^2 \times 10^2$	$J_{ST}^3 \times 10^3$	$J_{ST}^4 \times 10^3$
0	21.26	21.26	20.46	11.68	7.81	36.75	28.05
0.01	21.59	21.44	14.86	11.36	5.56	18.14	9.99
0.1	22.82	21.49	13.36	11.38	4.79	12.33	4.84
1	33.42	22.18	11.24	10.54	3.83	5.36	1.04
10	114.7	35.70	7.90	7.39	4.98	2.86	0.33
True			17.54	13.88	10.50	29.97	7.50

b. Final values of performance indices for $\sigma = 0.3$ atm and $\beta_k = 1$ atm^2/darcies^2 as a function of $n_{xs} \times n_{ys}$

$n_{xs} \times n_{ys}$	h	J_{SM}	J_{LS}	J_{ST}	J_{ST}^1	$J_{ST}^2 \times 10^2$	$J_{ST}^3 \times 10^3$	$J_{ST}^4 \times 10^3$
5 × 6	5	35.70	23.48	12.22	11.30	1.30	0.39	0.02
7 × 9	2.5	33.42	22.18	11.24	10.54	3.83	5.36	1.04
12 × 17	1.09	31.59	21.68	9.91	9.53	12.43	81.60	68.91

c. Final values of performance indices for $\sigma = 0.3$ atm, $\beta_k = 1$ atm^2/darcies^2, and $n_{xs} \times n_{ys} = 7 \times 9$ with different number of observation wells

No. of Wells	J_{SM}	J_{LS}	J_{ST}*	J_{ST}^1	$J_{ST}^2 \times 10^2$	$J_{ST}^3 \times 10^3$	$J_{ST}^4 \times 10^3$
6	33.42	22.18	11.24	10.54	3.83	5.36	1.04
18	76.96	63.33	13.62	11.96	5.00	11.28	3.74

*$\zeta_1 = 1, \zeta_2 = h^2, \zeta_3 = h^4, \zeta_4 = h^6$, with $h = 2.5$.
**$\zeta_1 = 1, \zeta_2 = h^2, \zeta_3 = h^4, \zeta_4 = h^6$.

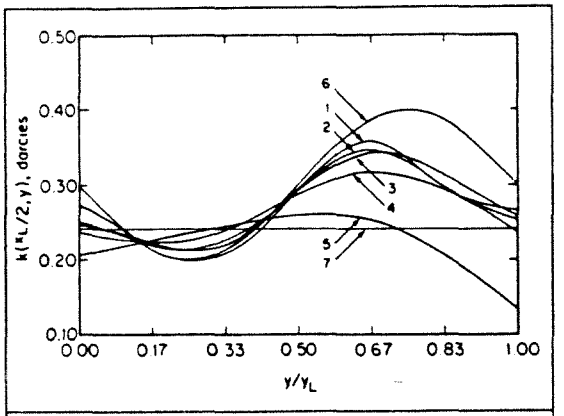

Fig. 6—Cross-sectional plot of $k(x_L/2, y)$ vs. y for $\sigma = 0.3$ atm, $n_{xs} \times n_{ys} = 7 \times 9$ and (1) $\beta_k = 0$ atm^2/darcies^2, (2) 0.01, (3) 0.1, (4) 1, (5) 10, (6) true values, and (7) initial guess.

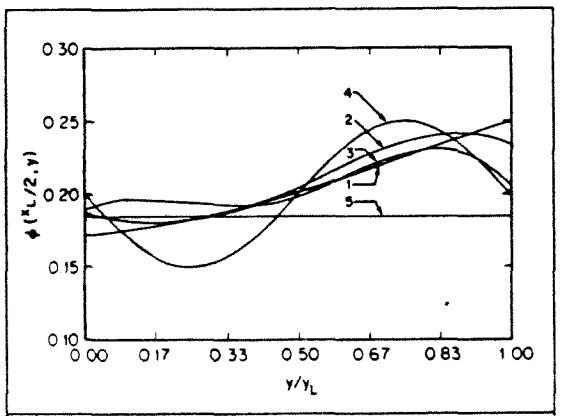

Fig. 7—Cross sectional plot of $\phi(x_L/2, y)$ vs. y for $\sigma = 0.3$ atm, $\beta_\phi = 1$ atm^2, and (1) $n_{xs} \times n_{ys} = 5 \times 6$, (2) 7×9, (3) 12×17, (4) true values, and (5) initial guess.

$[1.054 \times 10^{33}$ and 1.054×10^{32} Pa^2/m$^4]$ for which J_{LS} is 10 to 100 times as large as $\beta_k J_{ST}$. This means k can be regularized more easily than ϕ can. It is interesting to compare these numerical indicators of performance with the surfaces and profiles in Figs. 5 and 6. The estimated parameter surfaces are too bumpy compared with the true surfaces (Figs. 2 and 3) when small regularization parameters are used and in the nonregularized case. Note the "bump" in Fig. 5a or the inflection point at $y/y_L \approx 0.8$ in curves 1 ($\beta_k = 0$) and 2 ($\beta_k = 0.01$ atm^2/darcies^2 $[0.01 \times 10^{34}$ Pa^2/m$^4]$) of Fig. 6. On the other hand, the parameter estimates become too flat for large values of regularization parameters, as shown in Fig. 5c and Curve 5 in Fig. 6, as compared to Fig. 2 and Curve 6 in Fig. 6.

To determine the optimal regularization parameter, $||\beta_\alpha dW^\alpha/d\beta_\alpha||_2$ can be approximated by $||(W_2{}^\alpha - W_1{}^\alpha)/(\ln \beta_{\alpha,2} - \ln \beta_{\alpha,1})||$, where $\beta_{\alpha,1}$ and $\beta_{\alpha,2}$ denote two different regularization parameters, $W_1{}^\alpha$ and $W_2{}^\alpha$ are the corresponding spline coefficients that minimize J_{SM}, and $||\cdot||_2$ denotes Euclidean vector norm. Table 5 summarizes the results for the estimation of ϕ and the estimation of k. The optimal $\beta_\phi \approx 0.1$ to 1

TABLE 5—VALUES OF $||\beta_\alpha \frac{dW^\alpha}{d\beta_\alpha}||_2$

a. Estimation of ϕ

β_ϕ	$\|\|\beta_\phi dW^\phi/d\beta_\phi\|\|_2$
0.01, 0.1	0.167
0.1, 1	0.148
1, 10	0.169

b. Estimation of k

β_k	$\|\|\beta_k dW^k/d\beta_k\|\|_2$ (darcies)
0.01, 0.1	0.211
0.1, 1	0.229
1, 10	0.456

atm^2 for the estimation of ϕ and the optimal $\beta_k \approx 0.01$ to 0.1 atm^2/darcies^2 $[1.054 \times 10^{32}$ to 1.054×10^{33} Pa^2/m$^4]$ for the estimation of k, which agree with the above investigation.

Table 4 also shows that in the estimation of k, the $J_{ST}{}^1$ term, which is proportional to the Euclidean norm of $k(x,y)$, in the domain Ω, is smaller than that calculated from the true k. This behavior can be explained from Eq. 2, which shows that the pressure value is governed by the gradient of k with respect to the spatial variables rather than the value of k itself. Thus the value of k can be reduced to some extent without changing the values of pressure significantly during the estimation of k.

Effect of Spline Approximation ($n_{xs} \times n_{ys}$). The measurement error (J_{LS} for true parameters) is 18.96 atm^2, while J_{LS} for $\beta_\phi = 0$ is 20.67 atm^2 $[212 \times 10^9$ Pa$^2]$ for the estimation of ϕ, and J_{LS} for $\beta_k = 0$ is 21.26 atm^2 $[218 \times 10^9$ Pa$^2]$ for the estimation of k. This can be explained because the spline approximation has the effect of smoothing instead of fitting the noisy measured data in detail.

It is clear that the measured data can be better fit with more parameters, thus we expect that values of J_{LS} should decrease as the dimension of spline grid, $n_{xs} \times n_{ys}$, increases. At the same time, the estimated parameters are expected to be less regular for larger values of $n_{xs} \times n_{ys}$. This expectation turns out to be true in our examples in the estimation of both ϕ and k. The value of $J_{ST}{}^4$ for the true ϕ is closer to that for the estimated ϕ when $n_{xs} \times n_{ys} = 7 \times 9$, and the values of $J_{ST}{}^4$ for the true k lies between those of the estimated k for $n_{xs} \times n_{ys} = 7 \times 9$ and 12×17. If we want the values of $J_{ST}{}^4$ not to be greater than that of true k, however, we conclude that $n_{xs} \times n_{ys} = 7 \times 9$ is the best value for the 10×15 pressure grid in our example.

Figs. 7 and 8 show the effect of spline approximation on the estimation of ϕ and k, respectively. We can observe ill-conditioning in the estimation of k from Fig. 8c ($n_{xs} \times n_{ys} = 12 \times 17$), which can be explained because the ratio of spline grid to pressure grid (h) is only 1.09, so that we have 204 unknown spline coefficients to be estimated as compared with 210 measured pressure data.

Effect of the Number of Observation Wells. The regularization effect is relatively less important for more observation wells and thus the values of J_{ST} and the terms in J_{ST}, $J_{ST}{}^{m+1}$, $m = 0$, 1, 2, and 3 are larger, as shown

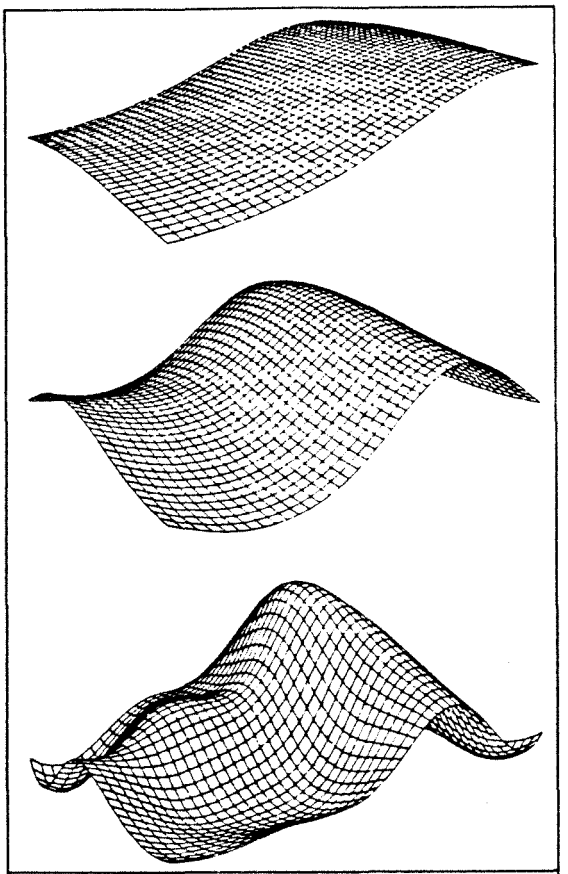

Fig. 8—Estimated k surface for $\sigma = 0.3$ atm, $\beta_k = 1$ atm^2/darcies^2 and from top down: $n_{xs} \times n_{ys} = 5 \times 6$, 7×9, and 12×17.

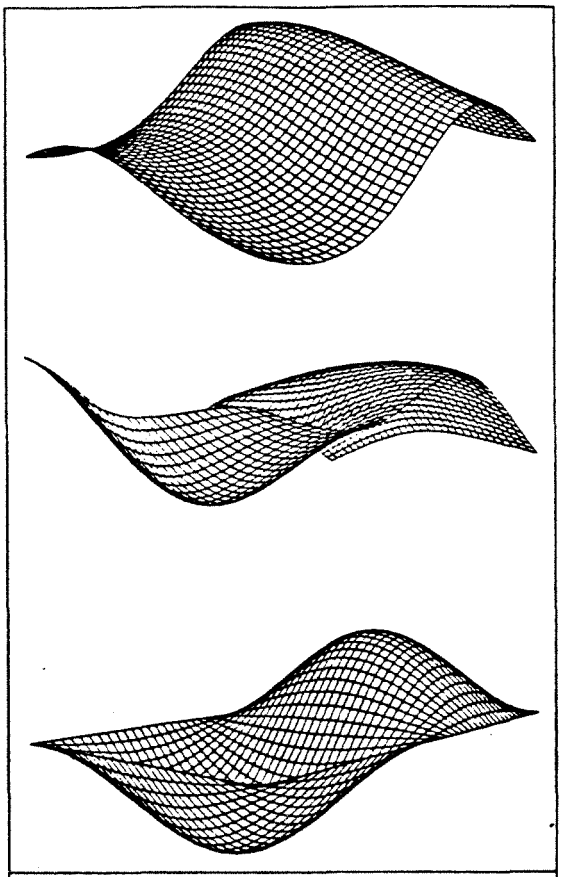

Fig. 9—Estimated and true k surfaces for $\sigma = 0.3$ atm, $\beta_k = 1$ atm^2/darcies^2, $n_{xs} \times n_{ys} = 7 \times 9$, and from top down: 6 observation wells, 18 observations wells, and true k.

in Table 4c. As one can see in Fig. 9, the estimated k for 18 observation wells is closer to the true k than that for 6 observation wells. Note that J_{LS} for 18 observation wells is closer to the true value than that for 6 observation wells with any set of k and $n_{xs} \times n_{ys}$.

Convergence of the Algorithm

When we seek the minimum of J_{SM} with respect to W^α ($\alpha = \phi$ or k) with the conjugate gradient algorithm, we need up to $n_{xs} \times n_{ys}$ conjugate directions to find the approximation of the inverse of the Hessian matrix. The algorithm used here, however, uses 5 to 10 conjugate directions to find the approximation of the inverse of the Hessian matrix. On the whole, the algorithm requires 10 to 20 different inverse Hessian matrix evaluations, or 0.5 to 1 hour of CPU time on a VAX11-780 for a single history match.

The algorithm determines the minimum of $J_{SM}(W^\alpha + s\delta W^\alpha)$ along s, the step size, by trial and error. In some cases, if s is too large, some elements of $W^\alpha + s\delta W^\alpha$ have negative values that are physically impossible. Thus, in the implementation of the algorithm, a limit on the size of s was used.

Conclusions

In this study we have developed and tested an automatic history-matching algorithm for estimating spatially varying porosity and permeability in a single-phase areal reservoir. The algorithm is based on spline approximations of the parameters and a regularization formulation. In the regularization approach to parameter estimation by introduction of the stabilizing functional as a measure of nonsmoothness, one can control the properties of the parameter estimates as well as the history match.

We have presented results of a detailed numerical evaluation of the performance of the history-matching method. In this example, we found that the permeability distribution is estimated somewhat better than the porosity distribution at comparable levels of spline approximation and degree of regularization. It was also found that increasing the value of the regularization parameter leads to estimated property distributions that are smoother than those obtained for smaller values of the regularization parameter. Some exceptions to this behavior were found at small values of the regularization parameter and can be attributed to inherent numerical ill-conditioning in estimation problems of this size. There appears to be an optimal level of spline approximation in the case of the example studied. The optimum was a 7×9 grid for which the ratio of the size of the spline grid to that of the pressure grid is 2.5. This optimal value of approximation appears to represent a tradeoff between a low-dimensional spline grid that has as few unknown parameters as possible and a high-

dimensional spline grid that is better able to represent the details of property distributions but introduces more unknowns and therefore inherently more ill-conditioning in the optimization step.

On the basis of the optimal spline approximation, the optimal regularization parameters are $\beta_\phi = 0.1$ to 1 atm^2 [1.03×10^9 to 10×10^9 Pa^2] for the estimation of ϕ and $\beta_k = 0.01$ to 0.1 atm^2/darcies^2 [1.054×10^{32} to 1.054×10^{33} Pa^2/m^4] for the estimation of k. These values were determined from the quasioptimal condition of regularization and have the same magnitude of the values of measure of nonsmoothness as the true profiles.

Finally, we can suggest a history-matching strategy as follows.

1. Choose simulator and spline grid systems. The number of the spline coefficients need not be as large as the number of simulator grid cells.
2. Find a uniform initial guess of a parameter to be estimated that minimizes J_{LS} and calculate J_{LS}/J_{ST} at convergence.
3. Choose the regularization parameter value about the same as J_{LS}/J_{ST} above and find a set of spline coefficients that minimizes J_{SM}.
4. Step 3 can be repeated to evaluate the result for the different regularization parameter values around the J_{LS}/J_{ST} value determined in Step 2, so that we can find the optimum value of regularization parameter discussed in the previous section.

Nomenclature

A_x^m = matrix defined by Eq. A-19, $m=0$, 1, 2, and 3

A_y^m = matrix defined by Eq. A-19, $m=0$, 1, 2, and 3

$A_{\ell_x m_x}^{mx}$ = quantity defined by Eq. A-17

$A_{\ell_y m_y}^{my}$ = quantity defined by Eq. A-18

$b_x(\ell_x,x)$ = cubic spline function defined by Eq. 9

$b_y(\ell_y,y)$ = cubic spline function defined by Eq. 10

B_x = $n_{xs}\times n_x$ matrix of spline function values

B_y = $n_{ys}\times n_y$ matrix of spline function values

c = compressibility, atm^{-1} [Pa^{-1}]

$G_{LS,i}^k$, $G_{LS,i}^\phi$ = derivative of J_{LS} with respect to the values of k and ϕ at the grid point of the simulator, $i=1,2\ldots n_t$

$G_{LS}^k(x,y)$, $G_{LS}^\phi(x,y)$ = functional derivative of J_{LS} with respect to k and ϕ at (x,y)

$G_{LS,\ell_x,\ell_y}^{W^k}$, $G_{LS,\ell_x,\ell_y}^{W^\phi}$ = derivative of J_{LS} with respect to the values of W_{ℓ_x,ℓ_y}^k and W_{ℓ_x,ℓ_y}^ϕ

$G_{SM,\ell_x,\ell_y}^{W^k}$, $G_{SM,\ell_x,\ell_y}^{W^\phi}$ = derivative of J_{SM} with respect to the values of W_{ℓ_x,ℓ_y}^k and W_{ℓ_x,ℓ_y}^ϕ

$G_{ST,\ell_x,\ell_y}^{W^k}$, $G_{ST,\ell_x,\ell_y}^{W^\phi}$ = derivative of J_{ST} with respect to the values of W_{ℓ_x,ℓ_y}^k and W_{ℓ_x,ℓ_y}^ϕ

$H^3(\Omega)$ = Sobolev space of order 3 on the domain Ω

$H_{ST,\ell_x,\ell_y,m_y,m_y}$ = quantity defined by Eq. A-14

h = $(h_x h_y)^{1/2}$

h_x = $\Delta x_s/\Delta x$

h_y = $\Delta y_s/\Delta y$

i,i_x,i_y = indices for simulator grid, $i=i_x+n_x(i_y-1)$

I_i = a set of integers that indicate the neighborhood of ith gridblock

I_n = set of integers from 1 to n_t

I_x,I_y = set of integers from 1 to n_x and n_y

J_{LS} = least-squares objective function, Eq. 5

J_{SM} = smoothing functional, Eq. 7

J_{ST} = stabilizing functional, Eq. 6

J_{ST}^{m+1} = terms in stabilizing functional defined by Eq. A-12, $m=0$, 1, 2, and 3

k = permeability, darcies

k_i = permeability values at the ith simulator grid, $i=1\ldots n_t$, darcies

ℓ_x,ℓ_y = indices for bicubic spline approximation grid, $\ell_x=1\ldots n_{xs}$; $\ell_y=1\ldots n_{ys}$

n = unit normal to boundary

n_{OB} = number of observation locations

n_{OBt} = number of observation times

n_t = $n_x n_y$, total number of simulator gridblocks

n_w = number of wells

n_x,n_y = number of simulator gridblocks among x and y directions

n_{xs},n_{ys} = number of nodes along x and y direction of spline grid

p = pressure, atm [Pa]

p_i = pressure at Gridblock i, atm [Pa]

p_j = pressure at Gridblock j, atm [Pa]

p_{OB} = observed pressure, atm [Pa]

p_0 = initial pressure, atm [Pa]

q_w = volumetric flow rate per thickness of reservoir of Well w, ft^2/day [m^2/s]

Q = $\Delta x\Delta y/\Delta t$

Q_L = $\Delta y/\Delta x$ or $\Delta x/\Delta y$

s = step size

t = time, days

Δt = time interval of observation, days

T = time periods over which observations are available, days

W^α = spline coefficients for Parameter α

W^k, W^ϕ = $n_{xs}\times n_{ys}$ matrix of spline coefficient of k and ϕ

x = spatial variable, miles [km]

x_L = extent of domain in x direction, miles [km]
$\Delta x, \Delta y$ = simulator grid spacings, miles [km]
$\Delta x_s, \Delta y_s$ = spline grid spacings, miles [km]
y = spatial variable, miles [km]
y_L = extent of domain in y direction, miles [km]
α = unknown parameter to be estimated ($\alpha = k$ or ϕ)
β_α = regularization parameter for the estimation of α
β_k = regularization parameter for the estimation of k, atm^2/darcies^2 [Pa^2/m^4]
β_ϕ = regularization parameter for the estimation of ϕ, atm^2 [Pa^2]
$\delta(\cdot)$ = Dirac delta function
δ_{ij} = Kronecker delta
Δ = difference
ϵ_i = convergence criterion, $i=1,2$
ζ_{m+1} = weighting factor of Sobolev norm $\|\cdot\|_{H^3(\Omega)}$, $m=0$, 1, 2, and 3
η = $y/\Delta y$
μ = viscosity, cp [Pa·s]
ξ = $x/\Delta x$
σ = standard deviation of measurement error, atm
ϕ = porosity
$\chi^{*4}(\cdot)$ = cubic B-spline function, Eq. 11
ψ = adjoint variable
Ω = spatial domain of reservoir
$\partial\Omega$ = boundary of reservoir
∇ = gradient
$\| \|$ = norm
$\bar{}$ = average

References

1. Kravaris, C. and Seinfeld, J.H.: "Identification of Parameters in Distributed Parameter Systems by Regularization," *SIAM J. Control and Optimization*, **23**, No. 2, 217–41.
2. Kravaris, C. and Seinfeld, J.H.: "Identification of Spatially-Varying Parameters in Distributed Parameter Systems by Discrete Regularization," *J. Mathematical Analysis and Appl.* (1986) **118**, No. 9.
3. Nazareth, L.: "A Conjugate Direction Algorithm Without Line Searchers," *J. Optimization Theory and Application* (Nov. 1977) 373–87.
4. Shah, P.C., Gavalas, G.R., and Seinfeld, J.H.: "Error Analysis in History Matching: The Optimum Level of Parametrization," *SPEJ* (June 1978) 219–28.
5. Yakowitz, S. and Duckstein, L.: "Instability in Aquifer Identification: Theory and Case Studies," *Water Resources Research*, **16**, No. 198, 1054–64.
6. Tikhonov, A.N. and Arsenin, V.Y.: *Solutions of Ill-posed Problems*, H. Winston & Sons, Washington, DC (1977).
7. Banks, H.T.: "Distributed System Optimal Control and Parameter Estimation: Computational Techniques Using Spline Approximations," *Proc.*, Third Intl. Federation of Automatic Control Symposium on Control of Distributed Parameter Systems, Toulouse (June 29–July 2, 1982).
8. Banks, H.T. and Crowley, J.M.: "Parameter Identification in Continuum Models," *Proc.*, American Control Conference, San Francisco (June 1983).
9. Banks, H.T. and Murphy, K.A.: "Estimation of Coefficients and Boundary Parameters in Hyperbolic Systems," Div. of Applied Mathematics, Brown U., Providence, RI, report LCDS No. 84-5 (Feb. 1984).
10. Banks, H.T. and Lamm, P.D.: "Estimation of Variable Coefficients in Parabolic Distributed Systems," *I.E.E.E. Trans. Auto. Control*, **30**, No. 4, 386–98.
11. Kravaris, C. and Seinfeld, J.H.: "Identifiability of Spatially-Varying Conductivity from Point Observation as an Inverse Sturm-Liouville Problem," *SIAM J. Control and Optimization*, **24**, No. 3, 522–42.
12. Carter, R.D., Kemp, L.F., and Williams, D.: "Performance Matching With Constraints," *SPEJ* (April 1974) 187–96; *Trans.*, AIME, **257**.
13. Dogru, A.H. and Seinfeld, J.H.: "Comparison of Sensitivity Coefficient Calculation Methods in Automatic History Matching," *SPEJ* (Oct. 1981) 551–57.
14. Chen, W.H. *et al.*: "A New Algorithm for Automatic History Matching," *SPEJ* (Dec. 1974) 593–608; *Trans.*, AIME, **257**.
15. Chavent, G., Dupuy, M., and Lemonnier, P.: "History Matching by Use of Optimal Control Theory," *SPEJ* (Feb. 1975) 74–86; *Trans.*, AIME, **259**.
16. Wassermann, M.L., Emanuel, A.S., and Seinfeld, J.H.: "Practical Applications of Optimal-Control Theory to History-Matching Multiphase Simulator Models," *SPEJ* (Aug. 1975) 347–55; *Trans.*, AIME, **259**.
17. Scales, L.E.: *Introduction to Non-Linear Optimization*, Springer-Verlag New York Inc., New York City (1985).

Appendix A—Gradient of the Objective Function With Respect to the Unknown Parameters

Let us begin by supposing that we want to minimize the least-squares objective function, J_{LS}, given by Eq. 5 with respect to permeability k and porosity ϕ subject to Eqs. 2 through 4. By adjoining the model of Eq. 2 to J_{LS} by means of an adjoint function $\psi(x,y,t)$,

$$\bar{J}_{LS} = \int_{\Omega 0}\int\int^{T}\left(\sum_{n=1}^{n_{OBt}} \sum_{k=1}^{n_{OB}} [p_{OBk,n} - p(x,y,t)]^2 \times \delta(x-x_k)\delta(y-y_k)\delta(t-t_n) + \psi(x,y,t)\left\{ -c\phi\frac{\partial}{\partial t}p \times (x,y,t) + \nabla\cdot\left[\frac{k}{\mu}\nabla p(x,y,t)\right] + \sum_{w=1}^{n_w} q_w\delta(x-x_w) \times \delta(y-y_w)\right\}\right) d\tau dx dy. \quad \text{(A-1)}$$

Minimizing $\bar{J}_{LS}$ leads to the following equations governing $\psi(x,y,t)$.

$$c\phi\frac{\partial}{\partial t}\psi(x,y,t) = -\nabla\cdot\left[\frac{k}{\mu}\psi(x,y,t)\right] - 2\sum_{n=1}^{n_{OBt}}\sum_{k=1}^{n_{OB}} \times \left\{ [p_{OBk,n} - p(x,y,t)]\delta(x-x_k)\delta(y-y_k)\delta(t-t_n)\right\} \quad \text{(A-2)}$$

in $\Omega\times[0,T]$,

$$\frac{\partial\psi}{\partial n} = 0 \quad \text{(A-3)}$$

on $\partial\Omega\times[0,T]$, and

$$\psi(x,y,T)=0 \quad \text{(A-4)}$$

in Ω, where n has the direction outward normal to the boundary, and the functional derivatives of J_{LS} with respect to k and ϕ at $(x,y)\epsilon\Omega$ are

$$G_{LS}^{k}(x,y)=-\frac{1}{\mu}\int_0^T \nabla\psi(x,y,t)\cdot\nabla p(x,y,t)dt \quad \text{(A-5)}$$

in Ω, and

$$G_{LS}^{\phi}(x,y)=-c\int_0^T \psi(x,y,t)\frac{\partial}{\partial t}p(x,y,t)dt=c\psi(x,y,0)$$

$$\times p_0(x,y)+c\int_0^T\left\{\left[\frac{\partial}{\partial t}\psi(x,y,t)\right]p(x,y,t)\right\}dt \quad \text{(A-6)}$$

in Ω.

The first-order necessary condition for a local minimum of J_{LS} is that p and ψ satisfy Eqs. 2 through 4 and A-2 through A-4, respectively, and that $G_{LS}^{k}(x,y)=0$ (for the estimation of k) or $G_{LS}^{\phi}(x,y)=0$ (for the estimation of ϕ) for all $(x,y)\epsilon\Omega$. The gradients $G_{LS}^{k}(x,y)$ and $G_{LS}^{\phi}(x,y)$ are used in the so-called optimal control algorithms for history matching. As noted, because these gradients can be calculated directly without requiring the sensitivity coefficients, $\partial p/\partial k$ and $\partial p/\partial\phi$, these optimal-control algorithms are computationally attractive for history matching.

The adjoint equations (Eqs. A-2 through A-4) can be written in a finite-difference form corresponding to Eq. 12 as

$$Qc\phi_i(\psi_i^{n+1}-\psi_i^n)=-\sum_{j\epsilon I_i}Q_{Lj}(\psi_j^n-\psi_i^n)$$

$$-2\sum_{k=1}^{n_{OB}}(p_{OBk,n}-p_i^n)\delta_{i,i_k} \quad \text{(A-7)}$$

for $i\epsilon I_n$ and $n=1,2\ldots n_{OBt}$, and

$$\psi_i^{n_{OBt}+1}=0 \quad \text{(A-8)}$$

for $i\epsilon I_n$, where $I_i=\{i-n_x,\ i-1,\ i+1,\ i+n_x\}\cap I_n$ and the derivatives of J_{LS} with respect to k_i and ϕ_i are

$$G_{LS,i}^{k}=-\frac{1}{\mu}\sum_{n=1}^{n_{OBt}}\sum_{j\epsilon I_i}Q_{Lj}(\psi_j^n-\psi_i^n)(p_j^n-p_i^n) \quad \text{(A-9)}$$

for $i\epsilon I_n$, and

$$G_{LS,i}^{\phi}=-Qc\sum_{n=1}^{n_{OBt}}\psi_i^n(p_i^n-p_i^{n-1})$$

$$=Qc\left[\psi_i^1+\sum_{n=1}^{n_{OBt}}(\psi_i^{n+1}-\psi_i^n)p_i^n\right] \quad \text{(A-10)}$$

for $i\epsilon I_n$.

In our algorithm, k and ϕ are represented by the bicubic spline approximation (Eq. 8), and the actual unknown parameters are the coefficients W_{ℓ_x,ℓ_y}^{k} and W_{ℓ_x,ℓ_y}^{ϕ}. Thus, we need to obtain the derivatives of the overall objective functional J_{SM} with respect to W_{ℓ_x,ℓ_y}^{k} and W_{ℓ_x,ℓ_y}^{ϕ}. These gradients are then the values used directly in the conjugate gradient minimization method.

Let the $n_{xs}\times n_x$ matrix B_x have elements $B_{x,\ell_x,i_x}=b_x[\ell_x,(i_x-½)\Delta x]$ and the $n_{ys}\times n_y$ matrix B_y have elements $B_{y,\ell_y,i_y}=b_y[\ell_y,(i_y-½)\Delta y]$. Then the derivative of J_{LS} with respect to the elements of W^{α} ($\alpha=k$ or ϕ) is

$$G_{LS,\ell_x\ell_y}^{W^\alpha}=\sum_{i_x=1}^{n_x}\sum_{i_y=1}^{n_y}B_{x,\ell_x,i_x}G_{LS,i}^{\alpha}B_{y,\ell_y,i_y},$$

$$\ell_x=1\ldots n_{xs} \text{ and } \ell_y=1\ldots n_{ys}, \quad \text{(A-11)}$$

where $i=i_x+n_x(i_y-1)$. Thus Eq. A-11 relates the gradient of the least-squares objective function with respect to the spline coefficients to that with respect to the individual reservoir parameters at each grid point of the simulator.

Eq. A-11 expresses the gradient of the least-squares portion, J_{LS}, of the overall objective function, J_{SM}. We need to obtain the gradient of J_{SM}. Let us consider the second component of J_{SM}, namely the stabilizing functional, J_{ST}, given by Eq. 6, which is

$$J_{ST}=\zeta_1J_{ST}^1+\zeta_2J_{ST}^2+\zeta_3J_{ST}^3+\zeta_4J_{ST}^4, \quad \text{(A-12a)}$$

where

$$J_{ST}^1=\int_0^{n_x}\int_0^{n_y}\alpha^2(\xi,\eta)d\xi d\eta, \quad \text{(A-12b)}$$

$$J_{ST}^2=\int_0^{n_x}\int_0^{n_y}\left[\left(\frac{\partial\alpha}{\partial\xi}\right)^2+\left(\frac{\partial\alpha}{\partial\eta}\right)^2\right]d\xi d\eta, \quad \text{(A-12c)}$$

$$J_{ST}^3=\int_0^{n_x}\int_0^{n_y}\left[\left(\frac{\partial^2\alpha}{\partial\xi^2}\right)^2+2\left(\frac{\partial^2\alpha}{\partial\xi\partial\eta}\right)^2\right.$$

$$\left.+\left(\frac{\partial^2\alpha}{\partial\eta^2}\right)^2\right]d\xi d\eta, \quad \text{(A-12d)}$$

and

$$J^4_{ST}=\int_0^{n_x}\int_0^{n_y}\left[\left(\frac{\partial^3\alpha}{\partial\xi^3}\right)^2+3\left(\frac{\partial^3\alpha}{\partial\xi^2\partial\eta}\right)^2+3\left(\frac{\partial^3\alpha}{\partial\xi\partial\eta^2}\right)^2\left(\frac{\partial^3\alpha}{\partial\eta^3}\right)^2\right]d\xi d\eta, \quad \ldots(A\text{-}12e)$$

where $\zeta_1>0$, $\zeta_2\geq 0$, $\zeta_3\geq 0$, $\zeta_4>0$ and $\xi=x/\Delta x$ and $\eta=y/\Delta y$. With ξ and η rather than x and y, $b_x(\ell_x,x)$ and $b_y(\ell_y,y)$ in Eqs. 9 and 10 and their derivatives are

$$b_x(\ell_x,x)=\chi^{*4}(4-\ell_x+\xi/h_x), \quad \ldots\ldots\ldots\ldots(A\text{-}13a)$$

$$b_y(\ell_y,y)=\chi^{*4}(4-\ell_y+\eta/h_y), \quad \ldots\ldots\ldots\ldots(A\text{-}13b)$$

$$\frac{d^m}{d\xi^m}b_x(\ell_x,x)=\frac{1}{h_x^m}\chi^{*4(m)}(4-\ell_x+\xi/h_x),$$

$$m=1,2,3, \quad \ldots\ldots\ldots\ldots\ldots\ldots\ldots\ldots(A\text{-}13c)$$

and

$$\frac{d^m}{d\eta^m}b_y(\ell_y,y)=\frac{1}{h_y^m}\chi^{*4(m)}(4-\ell_y+\eta/h_y),$$

$$m=1,2,3, \quad \ldots\ldots\ldots\ldots\ldots\ldots\ldots\ldots(A\text{-}13d)$$

where $\chi^{*4(m)}(\cdot)$ denotes mth derivatives of $\chi^{*4}(\cdot)$, $h_x=\Delta x_s/\Delta x$, and $h_y=\Delta y_s/\Delta y$. By combining Eqs. 8, A-12, and A-13 we obtain

$$\begin{aligned}H_{ST,\ell_x,\ell_y,m_x,m_y}&=2\zeta_1 A^{0x}_{\ell_x,m_x}A^{0y}_{\ell_y,m_y}\\&+\zeta_2\left(A^{1x}_{\ell_x,m_x}A^{0y}_{\ell_y,m_y}+A^{0x}_{\ell_x,m_x}A^{1y}_{\ell_y,m_y}\right)\\&+\zeta_3\left(A^{2x}_{\ell_x,m_x}A^{0y}_{\ell_y,m_y}+2A^{1x}_{\ell_x,m_x}A^{1y}_{\ell_y,m_y}+A^{0x}_{\ell_x,m_x}A^{2y}_{\ell_y,m_y}\right)\\&+\zeta_4\left(A^{3x}_{\ell_x,m_x}A^{0y}_{\ell_y,m_y}+3A^{2x}_{\ell_x,m_x}A^{1y}_{\ell_y,m_y}+3A^{1x}_{\ell_x,m_x}A^{2y}_{\ell_y,m_y}+A^{0x}_{\ell_x,m_x}A^{3y}_{\ell_y,m_y}\right), \quad \ldots\ldots(A\text{-}14)\end{aligned}$$

$$G^{w^\alpha}_{ST,\ell_x,\ell_y}=\sum_{m_x=1}^{n_{xx}}\sum_{m_y=1}^{n_{yy}}H_{ST,\ell_x,\ell_y,m_x,m_y}W^{\alpha}_{m_x,m_y}, \quad \ldots\ldots\ldots\ldots(A\text{-}15)$$

$$J_{ST}=\sum_{\ell_x=1}^{n_{xx}}\sum_{\ell_y=1}^{n_{yy}}\tfrac{1}{2}G^{W}_{ST,\ell_x,\ell_y}W^{\alpha}_{\ell_x,\ell_y}, \quad \ldots\ldots\ldots(A\text{-}16)$$

where

$$A^{(m)x}_{\ell_x,m_x}=h_x^{1-2m}\int_0^{n_{xx}-3}\chi^{*4(m)}\left(4-\ell_x+\frac{\xi}{h_x}\right)\chi^{*4(m)}\left(4-m_x+\frac{\xi}{h_x}\right)d\left(\frac{\xi}{h_x}\right), \quad m=0,1,2,3, \quad \ldots\ldots(A\text{-}17)$$

and

$$A^{(m)y}_{\ell_y,\ell_y}=h_y^{1-2m}\int_0^{n_{yy}-3}\chi^{*4(m)}\left(4-\ell_y+\frac{\eta}{h_y}\right)\chi^{*4(m)}\left(4-m_y+\frac{\eta}{h_y}\right)d\left(\frac{\eta}{h_y}\right), \quad m=0,1,2,3, \quad \ldots\ldots(A\text{-}18)$$

or in the matrix form,

$$A^{0x}=\frac{h_x}{7!}\begin{bmatrix}20&129&60&1&&&&&\\129&1208&1062&120&1&&&&\\60&1062&2396&1191&120&1&&&\\1&120&1191&2416&1191&120&1&&\\&&&1&120&1191&2416&1191&120&1\\&&&&1&120&1191&2396&1062&60\\&&&&&1&120&1062&1208&129\\&&&&&&1&60&129&20\end{bmatrix}$$

$$A^{1x}=\frac{1}{5!h_x}\begin{bmatrix}6&7&-12&-1&&&&&\\7&40&-22&-24&-1&&&&\\-12&-22&74&-15&-24&-1&&&\\-1&-24&-15&80&-15&-24&-1&&\\&&&-1&-24&-15&80&-15&-24&-1\\&&&&-1&-24&-15&74&-22&-12\\&&&&&-1&-24&-22&40&7\\&&&&&&-1&-12&7&6\end{bmatrix}$$

$$A^{2x}=\frac{1}{3!h_x^3}\begin{bmatrix}2&-3&0&1&&&&&\\-3&8&-6&0&1&&&&\\0&-6&14&-9&0&1&&&\\1&0&-9&16&-9&0&1&&\\&&&1&0&-9&16&-9&0&1\\&&&&1&0&-9&14&-6&0\\&&&&&1&0&-6&8&-3\\&&&&&&1&0&-3&2\end{bmatrix}$$

$$A^{3x}=\frac{1}{h_x^5}\begin{bmatrix}1&-3&3&-1&&&&&\\-3&10&-12&6&-1&&&&\\3&-12&19&-15&6&-1&&&\\-1&6&-15&20&-15&6&-1&&\\&&&-1&6&-15&20&-15&6&-1\\&&&&-1&6&-15&19&-12&3\\&&&&&-1&6&-12&10&-3\\&&&&&&-1&3&-3&1\end{bmatrix}, \quad \ldots\ldots\ldots\ldots(A\text{-}19)$$

and A^{0y}, A^{1y}, A^{2y}, and A^{3y} have the analogous expressions to Eq. A-19.

Finally, we obtain the gradient of overall objective function J_{SM} with respect to W^{α} as

$$G^{W^{\alpha}}_{SM,t_x t_y} = G^{W^{\alpha}}_{LS,t_x t_y} + \beta_{\alpha} G^{W^{\alpha}}_{ST,t_x t_y} \quad \ldots\ldots\ldots\ldots (A\text{-}20)$$

Weighting Factor ζ_{m+1}, $m=0$, 1, 2, and 3 in Eq. A-12a. In the stabilizing functional in Eq. A-12a, we have four undetermined constants, namely the weighting factors, ζ_{m+1}, $m=0$, 1, 2, and 3, which are arbitrary except for the conditions that $\zeta_1 > 0$, $\zeta_2 \geq 0$, $\zeta_3 \geq 0$, and $\zeta_4 > 0$. We can set these constants in a systematic way by using the fact that we want the four terms in Eq. A-12a, each of which is a weighting factor ζ_{m+1} multiplied by $J^{(m+1)}_{ST}$ described in Eqs. A-12b through A-12e, to be of about equal magnitude. We assume that h_x, the ratio of the size of the spline grid to that of the simulator grid along the x direction is not much different from h_y, the ratio along the y direction, and we let $h=(h_x h_y)^{1/2}$. Then, the ratio of terms $J^{(m+1)}_{ST}$, $m=0$, 1, 2, and 3 in Eqs. A-12 is about

$$J^1_{ST} : J^2_{ST} : J^3_{ST} : J^4_{ST} = h^2 : 1 : \frac{1}{h^2} : \frac{1}{h^4}, \quad \ldots\ldots (A\text{-}21)$$

and this suggests values for the weighting factors, ζ_{m+1}, $m=0$, 1, 2, and 3 as $\zeta_1 = 1$, $\zeta_2 = h^2$, $\zeta_3 = h^4$, $\zeta_4 = h^6$, where ζ_1 is independent of h.

SI Metric Conversion Factors

atm	×	1.013 250*	E+05	= Pa
atm^2	×	1.026 676	E+10	= Pa^2
atm^2/darcies^2	×	1.054	E+34	= Pa^2/m^4
atm^{-1}	×	0.986 923	E−05	= Pa^{-1}
cp	×	1.0*	E−03	= Pa·s
ft^2	×	9.290 304	E−02	= m^2
mile	×	1.609 344*	E+00	= km

*Conversion factor is exact.

SPERE

Original manuscript (SPE 13931) received in the Society of Petroleum Engineers office Jan. 2, 1985. Paper accepted for publication Dec. 30, 1985. Revised manuscript received Feb. 20, 1986.

Chapter III

Estimation of Two-Phase Petroleum Reservoir Properties by Regularization

Abstract. An algorithm is developed, based on the theory of regularization and on spline approximation, to estimate the absolute permeability in two-phase petroleum reservoirs from noisy well pressure data. The regularization feature of the algorithm converts the ill-posed estimation problem to a well-posed one. The algorithm, which employs the partial conjugate gradient method of Nazareth as its core minimization technique, automatically chooses the regularization parameter based on the non-regularized estimation. It is shown that regularized estimation is more stable and insensitive to the choice of an initial guess as compared to a non-regularized conventional estimation.

The text of Chapter III consists of an article coauthored with J. H. Seinfeld, which has been accepted for publication in the *Journal of Computational Physics.*

1. Introduction

The spatial distribution of the properties of petroleum reservoirs cannot be measured directly; rather, they must be inferred from matching the observed reservoir behavior to that predicted by a mathematical model. A reservoir that can be modeled as containing a single phase, e.g. oil, leads to a single linear PDE of heat conduction type for the pressure. Although the single-phase reservoir is clearly the first step in addressing reservoir parameter estimation problems, from the point of view of practical application, one really must consider two- (oil and water) and three- (gas, oil, and water) phase reservoirs. In this paper we present a comprehensive study of the estimation of two-phase petroleum reservoir properties.

The estimation of reservoir properties such as permeability and porosity based on measurements of pressure and production data at wells is an ill-posed problem, as it is neither unique nor continuously dependent on the measured data. Considerable effort has been devoted recently to attempting to develop well-posed algorithms for estimating petroleum reservoir properties. The critical problems in generating an effective algorithm for reservoir parameter estimation are twofold: (1) The original problem must be defined in a manner that alleviates the ill-posed nature of the problem; and (2) An efficient computational algorithm must be developed for solving the large, constrained, nonlinear minimization problem that results.

With respect to the inherent ill-posedness of the reservoir parameter estimation problem, Kravaris and Seinfeld (1985, 1986) have shown that the concept of regularization can be extended to the estimation of spatially varying parameters in partial differential equations of parabolic type, and Lee et al. (1986) applied the approach to estimating parameters in single-phase (oil) reservoirs. The regularization idea, first advanced by Tikhonov (Tikhonov and Arsenin, 1977) has been widely used in the solution of ill-posed integral equations, but had not heretofore been developed for the estimation of parameters in partial differential equations.

In short, regularization of a problem refers to solving a related problem, called the regularized problem, whose solution is more "regular" (in a certain sense) than the solution of the original problem and approximates (in a certain sense) the solution of the original problem. More precisely, regularization of an ill-posed problem refers to solving a well-posed problem, whose solution gives a physically meaningful answer to the original ill-posed problem. The regularization formulation of parameter estimation measures the "non-smoothness" of the estimated parameter as a norm of the parameter in an appropriate Hilbert space. No prior information about the parameter is required other than a general idea of the degree of smoothness desired in the estimated field. The only unspecified parameter is that reflecting the relative weight given to the smoothness norm versus the usual least-squares objective function.

In the present context, the regularized problem is to find the parameters that minimize a performance index, called the smoothing functional, J_{SM}, that consists of the weighted sum of the conventional least-squares discrepancy term, J_{LS}, and a term that penalizes non-smoothness of the parameters, called the stabilizing functional, J_{ST}. Thus

$$J_{SM} = J_{LS} + \beta J_{ST} \tag{1}$$

where β is the weighting coefficient, called the regularization parameter, chosen to reflect the degree of importance ascribed to J_{ST}.

The second major problem posed above is that of generating an efficient computational algorithm. Because the properties in an inhomogeneous reservoir vary with location, conceptually an infinite number of parameters are required for a full description of the reservoir. From a computational point of view, a reservoir model contains only a finite number of parameters, corresponding to each grid block or element in the spatial domain. In field scale simulations, it is not unusual for the reservoir domain to consist of the order of 10,000 grid cells, and consequently, 20,000

or more parameters may need to be estimated simultaneously.

Banks and coworkers (1982, 1983 1984, 1985) and Kravaris and Seinfeld(1986) have shown that an effective way to represent the spatial variation of unknown parameters in PDE's is by spline approximation. Then the parameter estimation problem reduces to determining the coefficients in the spline approximation. An important computational question concerns the choice of the spline parameter grid relative to the grid employed for the numerical solution of the governing PDE's.

This paper is a comprehensive study of the estimation of parameters in two-phase (oil/water) petroleum reservoirs. The numerical aspects of the problem will be considered in detail including (1) the choice of the stabilizing functional, (2) the choice of the regularization parameter, (3) the choice of the spline grid, and (4) the development of a computationally efficient algorithm.

2. Mathematical Model of Two-Phase Petroleum Reservoir

We consider a two-phase water-oil reservoir which has a sufficiently large areal extent so that we can assume that the pressure change and hence the flow in the vertical direction is negligible compared to flow in the other two directions (Aziz and Settari, 1983). If the water and oil phases are immiscible, then the equations of mass conservation for water and oil phases are given by

$$R_w \equiv -\frac{\partial}{\partial t}(\rho_w \phi S_w) - \nabla \cdot (\rho_w \mathbf{v}_w) + \sum_{\kappa=1}^{N_w} \rho_w q_{w\kappa} \frac{\delta(x-x_\kappa)\delta(y-y_\kappa)}{h} = 0 \qquad (2.a)$$

$$R_o \equiv -\frac{\partial}{\partial t}(\rho_o \phi S_o) - \nabla \cdot (\rho_o \mathbf{v}_o) + \sum_{\kappa=1}^{N_w} \rho_o q_{o\kappa} \frac{\delta(x-x_\kappa)\delta(y-y_\kappa)}{h} = 0 \qquad (2.b)$$

for $(x,y) \in \Omega \subset \Re^2$ and for $0 < t < T$ and the linear velocities of the two fluid phases are represented by Darcy's Law for flow in porous media

$$\mathbf{v}_w = -\frac{k k_{rw}}{\mu_w} \nabla p \qquad (3.a)$$

$$\mathbf{v}_o = -\frac{k k_{ro}}{\mu_o} \nabla p, \tag{3.b}$$

where

$$S_w + S_o = 1\,. \tag{4}$$

The initial conditions are

$$p(x, y, 0) = p_0 \tag{5}$$

$$S_w(x, y, 0) = S_{iw} \tag{6}$$

for $(x, y) \in \Omega$, and the no flux boundary condition

$$\mathbf{n} \cdot \nabla p = 0 \tag{7}$$

is assumed to hold for $(x, y) \in \partial\Omega$ and for $0 < t < T$. The relative permeabilities of water and oil phases are functions of saturation, relatively general forms of which, and those employed here, are

$$k_{rw}(S_w) = a_w \left(\frac{S_w - S_{iw}}{1 - S_{ro} - S_{iw}} \right)^{b_w} \tag{8.a}$$

$$k_{ro}(S_w) = a_o \left(\frac{1 - S_{ro} - S_w}{1 - S_{ro} - S_{iw}} \right)^{b_o}, \tag{8.b}$$

respectively, where the coefficients a_w, a_o, b_w, and b_o are constants independent of location.

3. Definition of the Parameter Estimation Problem

The reservoir parameter estimation problem can be considered as solving an inverse problem involving the nonlinear operator equation

$$K\alpha = u_\delta \tag{9}$$

where α is the unknown reservoir parameter, u_δ is the noisy pressure and production data measured at the observation wells, and the operator K is the reservoir model.

In a multiphase petroleum reservoir, the parameter α being estimated can in theory be the absolute permeability (k), porosity (ϕ), or coefficients appearing in the expressions for the relative permeabilities (k_{rw} and k_{ro}). In general, the porosity is better known from log and well data than is the absolute permeability, and the functional form of relative permeabilities are frequently given as shown in Eq. (8), so that the unknowns are the coefficients in the relative permeability expressions (a_w or a_o, b_w, and b_o), which are independent of location. In the present work we focus on the estimation of absolute permeability assuming that the porosity and relative permeabilities are known so that the reservoir model K includes the reservoir model equations, Eqs. (2–8), known parameters (ϕ, k_{rw}, and k_{ro}), and the numerical solution scheme. This inverse problem is often referred to in the petroleum literature as "history matching" since the parameter is to be estimated from the measured transient history of pressure and production data at wells distributed over the reservoir domain.

Often there is no solution α that satisfies Eq. (9) exactly, nor is the operator K directly invertible. Thus, the inverse problem is stated as one of minimizing the error in approximating Eq. (9). As we have noted, the parameter is usually replaced by a finite (but usually large) number of new parameters by finite difference (Chen et al. 1974, Shah et al. 1978) or spline approximation (Banks, 1982, Banks and Crowley, 1983, Banks and Murphy, 1984, Banks and Lamm, 1985).

Conventional least-squares estimation seeks the parameter that minimizes the discrepancy between pressure and production data,

$$J_{LS} = \|K\alpha - u_\delta\|^2 . \tag{10}$$

The performance function J_{LS} is generally non-convex, minimized over a large number of variables, and insensitive to changes in the parameters. As a consequence, the parameter estimates are (1) dependent on the given initial guess, (2) highly oscillatory and dependent on the grid system chosen for numerical solution, and (3)

not continuously dependent on the measured data. Thus, the inverse problem is "ill-posed" in the sense that the estimation of the parameters is neither unique nor stable.

Regularization of an ill-posed parameter estimation problem leads to penalizing the undesired features (non-smoothness) of the parameter estimates. In regularization the stabilizing functional represents non-smoothness of the parameter,

$$J_{ST} = \|L\alpha\|^2_{H^{(L)}(\Omega)} , \tag{11}$$

where L is either identity or a differential operator and $H^{(L)}(\Omega)$ is an appropriate Sobolev space. The total performance index is then the smoothing functional given in Eq. (1), which now becomes

$$J_{SM} = \|K\alpha - u_\delta\|^2 + \beta\|L\alpha\|^2_{H^{(L)}(\Omega)} \tag{12}$$

where the regularization parameter, β, measures the relative weight of the penalty on the non-smoothness compared to the discrepancy in matching data.

Tikhonov's stabilizing functional (Tikhonov, 1963, Tikhonov and Arsenin, 1977) is defined as the Sobolev norm of the unknown parameter. When we use spline approximation with cubic B-spline functions for representing the unknown parameter, $\alpha(x,y)$, Tikhonov's stabilizing functional is given by $\|\alpha\|^2_{H^3(\Omega)}$, where the Sobolev space $H^3(\Omega)$ is the set of functions that are square-integrable over Ω and have square-integrable derivatives up to order 3 (Kravaris and Seinfeld 1986, Lee et al. 1986). More precisely, this stabilizing functional is given by

$$J_{ST} = \sum_{m=0}^{3} \varsigma_m {J_{ST}}^{(m)} \tag{13}$$

where ${J_{ST}}^{(m)}$, $m = 0,\ldots,3$, represents m-th order derivative terms given by

$${J_{ST}}^{(m)} = \iint_\Omega \sum_{\nu=0}^{m} \binom{m}{\nu} \left(\frac{\partial^m \alpha(\xi,\eta)}{\partial\xi^\nu \partial\eta^{m-\nu}}\right)^2 d\xi d\eta \tag{14}$$

with dimensionless space variables $\xi = x/\Delta x$ and $\eta = y/\Delta y$, and the coefficients ς_m, $m = 0$, 1, 2, and 3 satisfy (1) $\varsigma_m > 0$ for $m = 0, \ldots, 3$ (Tikhonov, 1963); or (2) $\varsigma_m \geq 0$ for $m = 0$, 1, and 2 and $\varsigma_3 > 0$ (Tikhonov and Arsenin, 1977).

In practical applications of theory of regularization, as Trummer (1984) has pointed out, Tikhonov's stabilizing functional can lead to underestimation of the parameter value itself owing to the term ${J_{ST}}^{(0)}$ in Eq. (13), which is the usual Euclidean norm of the parameter. Locker and Prenter (1980) suggested regularization with a differential operator defined by $\|Lk\|^2_{H(L)(\Omega)}$ for the linear least-squares problem, so that the stabilizing functional is the norm of derivatives of the parameter in the Sobolev space. When the operator L in Eq. (11) is equal to the two-dimensional gradient ∇, Locker and Prenter's stabilizing functional becomes

$$J_{ST} = \sum_{m=1}^{3} \varsigma_m {J_{ST}}^{(m)} \tag{15}$$

where ${J_{ST}}^{(m)}$, $m = 1, \ldots, 3$ is the same as above, and the coefficients ς_m, $m = 1, \ldots, 3$ satisfy $\varsigma_1 \gtrless 0$, $\varsigma_2 \geq 0$, and $\varsigma_3 > 0$ so that it does not include the Euclidean norm of the parameter.

The choice of values of the ς_m's in Eqs. (13) and (15) is arbitrary except for the inequality conditions given above. One possible choice of ς_m's is based on the length scales used for the finite difference approximation of the PDE's, Δx and Δy. We will subsequently use $\varsigma_1 = \varsigma_2 = \varsigma_3 = 1$ in Eqs. (13) and (15), while the choice of ς_0 will be examined in the computational results.

A traditional question in the use of regularization to solve ill-posed problems is the choice of the regularization parameter β. Clearly, $\beta = 0$ corresponds to the non-regularized problem, while $\beta \to \infty$ would lead to a physically unrealistic solution. Miller (1970) suggested a way of determining the regularization parameter β from the ratio of an upper bound of J_{LS} values evaluated from the measured data (say $\overline{J_{LS}}$) to an upper bound of J_{ST} (say $\overline{J_{ST}}$). In this study, assuming that neither $\overline{J_{LS}}$

nor $\overline{J_{ST}}$ is available *a priori*, we will develop "a rule of thumb" to determine Miller's choice of β within our framework of regularization and spline approximation. Extensive numerical tests show that, for the solutions of non-regularized ($\beta = 0$) and regularized ($\beta > 0$) problems when the spline approximation is used for both cases,

(a) J_{LS} does not vary significantly for a wide range of $\beta \geq 0$, and the values of J_{LS} are close to the observation error in magnitude.

(b) J_{ST} generally decreases as β increases and J_{ST} at $\beta = 0$ is somewhat larger than the values of J_{ST} evaluated for the true profile.

This observation suggests that the value J_{LS}/J_{ST} calculated from the non-regularized ($\beta = 0$) estimation can be used as an approximation of the optimal regularization parameter. We will discuss later in this paper how this idea can be implemented in the estimation algorithm.

One might define a "quasi-optimal" value of the regularization parameter as a $\beta > 0$ such that parameter estimates are minimally sensitive to the (logarithmic) change of β; i.e., $J_{ST}(\beta \frac{\partial \alpha}{\partial \beta})$ is a minimum (Tikhonov and Arsenin, 1977). The numerical algorithm to find such a quasi-optimal β requires repeated solution of the regularized problem for different β's. Although we will later examine the effect on the estimates of the value of β, we will not use this particular strategy.

The intuitive idea of Generalized Cross Validation (GCV) is to find a β at which the parameter estimate gives the best prediction of unobserved data values. For that purpose, a GCV function is defined and minimized over $\beta > 0$ (Craven and Wahba, 1979). To apply this idea to reservoir parameter estimation, one needs the parametric sensitivity of pressure and production data, the calculation of which is specifically avoided in our estimation algorithm for computational efficiency. Thus, we will not consider the selection of β by GCV.

4. Spline Approximation of Unknown Parameters

A general approach to representing the spatial variation of the unknown parameters is through the use of bi-cubic spline functions, in which the parameter $\alpha(x,y)$ is represented as

$$\alpha(x,y) = \sum_{l_y=1}^{N_{ys}} \sum_{l_x=1}^{N_{xs}} b_x(l_x,x) W_{l_x,l_y} b_y(l_y,y) \tag{16}$$

where

$$b_x(l_x,x) = \chi^{*4}(4 - l_x + \frac{x}{\Delta x_s}) \qquad l_x = 1,2,\ldots,N_{xs} \tag{17}$$

$$b_y(l_y,y) = \chi^{*4}(4 - l_y + \frac{y}{\Delta y_s}) \qquad l_y = 1,2,\ldots,N_{ys} \tag{18}$$

and where $\chi^{*4}(\cdot)$ is the cubic B-spline function. Δx_s and Δy_s are the grid distance of the spline grid along x- and y-directions, respectively. With this approximation, $\alpha(x,y)$ is replaced by the set of unknown coefficients, W_{l_x,l_y}, $l_x = 1,2,\ldots,N_{xs}$ and $l_y = 1,2,\ldots,N_{ys}$.

The grid used for spline representation of the unknown properties need not necessarily coincide with that on which the actual reservoir model is solved. In general, the number of coefficients for spline representation should not exceed either the number of grid cells for the PDE or the number of available data. If too few coefficients are employed for the spline approximation, the functional derivative of J_{LS} with respect to the absolute permeability given by Eq. (B.7) in Appendix B cannot be properly represented by the derivative of J_{LS} with respect to the spline coefficients during the minimization of J_{SM}, and this may slow the rate of convergence. Hence, we will employ a spline grid system as dense as that for the reservoir PDE's with a minimizing algorithm that is suitable for a system with large dimensionality.

5. Numerical Algorithm

The problem we now seek to solve is to minimize the augmented objective function J_{SM} with respect to the spline coefficoents W_{l_x,l_y}, $l_x = 1,2,\ldots,N_{xs}$ and $l_y =$

$1, 2, \ldots, N_{ys}$, subject to Eqs. (2–8). To obtain an algorithm to solve this problem, two steps are required. First, we must compute the gradient of J_{SM} with respect to each W_{l_x,l_y}, and second, that gradient is then used in a numerical minimization method to minimize J_{SM}. The calculation of these gradients represents the most time-consuming part of updating the parameter iterates. In a problem as large as the current one these derivatives must be able to be calculated directly. Seinfeld and coworkers (Chen et al., 1974, Wasserman et al., 1975, Van den Bosch and Seinfeld, 1977) and Chavent, et al. (1975) have developed algorithms for estimating parameters in PDE's based on optimal control theory so that the algorithm requires only first-order functional derivatives of the performance functional with respect to the parameter to be estimated, and this approach is used here. To compute the functional derivative of J_{LS} with respect to the absolute permeability, first solve the reservoir PDE's with given initial conditions at $t = 0$; then, as shown in Appendix B, solve the adjoint system equations, Eqs. (B.3–4), backward with terminal constraints given by Eqs. (B.5–6). At the end of each time step during the solution of adjoint system equations, compute $\partial J_{LS}/\partial k_i$, $i = 1, \ldots, N$ by Eq. (B.7).

For most multivariate minimization problems, from the point of view of computational efficiency, methods that require second-order derivatives of the performance function are not recommended. As a result, various methods have been developed that utilize only first order derivatives, among which are conjugate gradient, quasi-Newton, and partial conjugate gradient methods. The conjugate gradient algorithm requires an exact line search to compute the length of each descent direction vector. Quasi-Newton methods use the inverse Hessian matrix to compute the descent vector, which requires a substantial amount of memory, although it does not require an exact line search. In general, quasi-Newton methods are preferred for relatively small problems, and conjugate gradient methods for large problems (Scales, 1985).

On the other hand, partial conjugate gradient methods use about the same amount of memory as does the conjugate gradient method, without requiring an exact line search, and show good performance over a range of problem sizes. In this study the partial conjugate gradient method of Nazareth (1977) is used as the core minimization technique.

An important question concerns starting the algorithm. Convergence difficulties are sometimes experienced when the initial guesses of the parameters are far from their actual values. To attempt to alleviate this problem and to generate an algorithm that is as "automatic" as possible, we begin the estimation by determining the unknown parameter as uniform over the entire region. Thus, to start, we estimate a single value of k for the entire region, which minimizes J_{LS}. This value then serves as a starting point for the full estimation algorithm. The rationale behind this strategy is that convergence problems should not be encountered in estimating a single parameter. The single value, while not accurate in its spatial detail, nevertheless serves as a good starting point for the full algorithm

Based on the foregoing discussion we suggest the following algorithm:

Step 1 In the absence of *a priori* information on the unknown parameters, find the flat initial guess of the parameter, i.e., one whose values are the same over the whole spatial domain, that minimizes J_{LS}.

Step 2 Using the initial guess of the parameter determined from Step 1, find the spatially varying parameter that minimizes J_{LS} and compute the values of J_{LS} and J_{ST}.

Step 3 Using the parameter profile and the values of J_{LS} and J_{ST} determined in Step 2, let $\beta = J_{LS}/J_{ST}$ and find the spatially-varying parameter that minimizes J_{SM}.

6. Computational Examples

The remainder of this work is devoted to the numerical evaluation of the algorithm on the estimation of absolute permeability in a two-phase, two-dimensional reservoir, as described by Eqs. (2–8). We want to evaluate the algorithm on a well-defined test problem for which the "true" absolute permeability distribution is known *a priori*. For this reason, we will specify the true parameter values, generate the pressure data by solving the reservoir model with these values, and then try to recover the true parameter values by using the estimation algorithm.

The specification of the reservoir is given in Table I, and its shape and well locations are shown in Figure 1. The production rate at each of two production wells (denoted by "P") is 3×10^{-3} m^3/s, and the injection rate at each of six injection wells (denoted by "I") is 10^{-3} m^3/s. The data were chosen so that the system is representative of actual reservoirs. To generate noisy measured pressure data at the observation wells, we solve the reservoir PDE's for the presumed true absolute permeability profile and add a set of uniformly distributed pseudo-random numbers (which are generated by the IMSL subroutine GGNML on a VAX 11/780).

The ill-posed nature of parameter estimation problems often leads to irregular estimated surfaces. In order to demonstrate this ill-conditioning, we will use the inclined plane shown in Figure 2.a as the true absolute permeability profile. We will also test the ability to recover a k surface of complicated geometry such as that shown in Figure 2.b. Since the k profile shown in Figure 2.a yields ${J_{ST}}^{(2)} = {J_{ST}}^{(3)} = 0$ and that shown in Figure 2.b is inadequate to test ill-conditioned estimation in the middle of the domain, we use yet a third k surface, shown in Figure 2.c, for which ${J_{ST}}^{(2)}$ and ${J_{ST}}^{(3)}$ have nonzero finite values and for which irregular behavior of the estimates can be visualized over the whole reservoir domain.

Throughout the numerical example, we use Locker and Prenter's (1980) stabilizing functional with differential operator ($L \equiv \nabla$ and $\varsigma_1 = \varsigma_2 = \varsigma_3 = 1$), the

Table I Specification of Reservoir Shown in Figure 1

(1) Fluid properties

	Water	Oil
Compressibility, Pa^{-1}	1.94×10^{-9}	0.97×10^{-9}
Viscosity, $Pa \cdot s$	10^{-3}	3×10^{-3}
Relative permeability	$a_w = 0.9$	$a_o = 1.0$
	$b_w = 2.5$	$b_o = 2.0$
	$S_{iw} = 0.1$	$S_{ro} = 0.2$
Well flow rate:		
$q_\kappa < 0$ for production wells	$q_{w\kappa} = \frac{\lambda_w}{\lambda_w + \lambda_o} q_\kappa$	$q_{o\kappa} = q_\kappa - q_{w\kappa}$
$q_\kappa > 0$ for injection wells	$q_{w\kappa} = q_\kappa$	$q_{o\kappa} = 0$

(2) Rock and reservoir properties

Compressibility, Pa^{-1}	2.91×10^{-9}
Porosity	$\phi_{SC} = 0.2 - 0.05 \sin(2\pi x/x_L) \sin(\pi y/y_L)$
Initial pressure, Pa	1.52×10^7
Reservoir Dimension, m^3	$1500 \times 1000 \times 10$

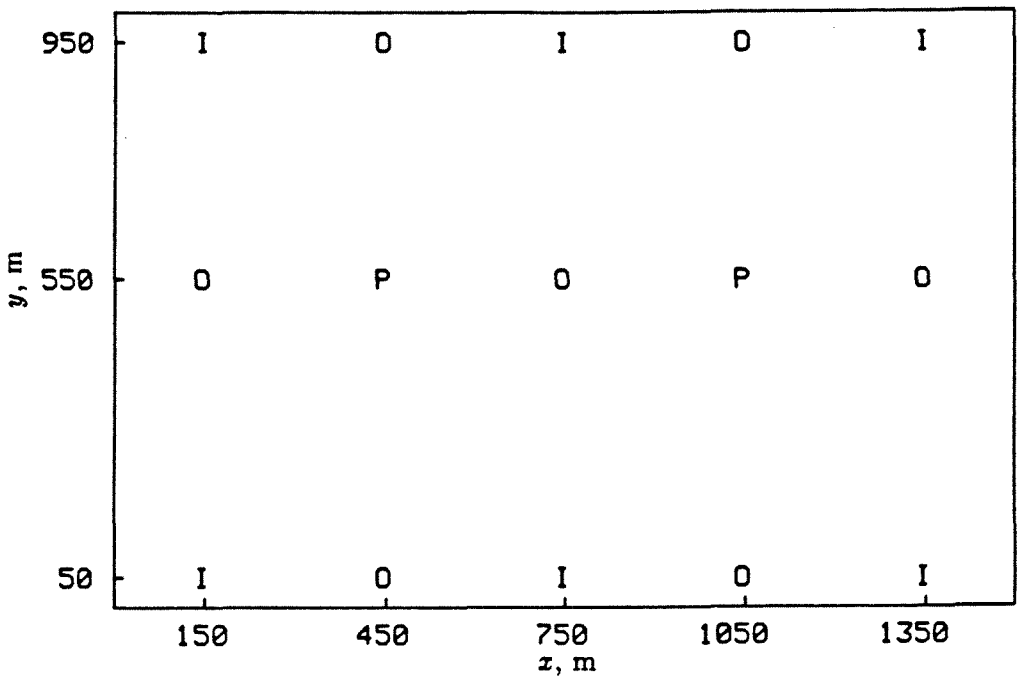

Figure 1 Shape of reservoir and location of wells

I injection and observation well

P production and observation well

O observation well

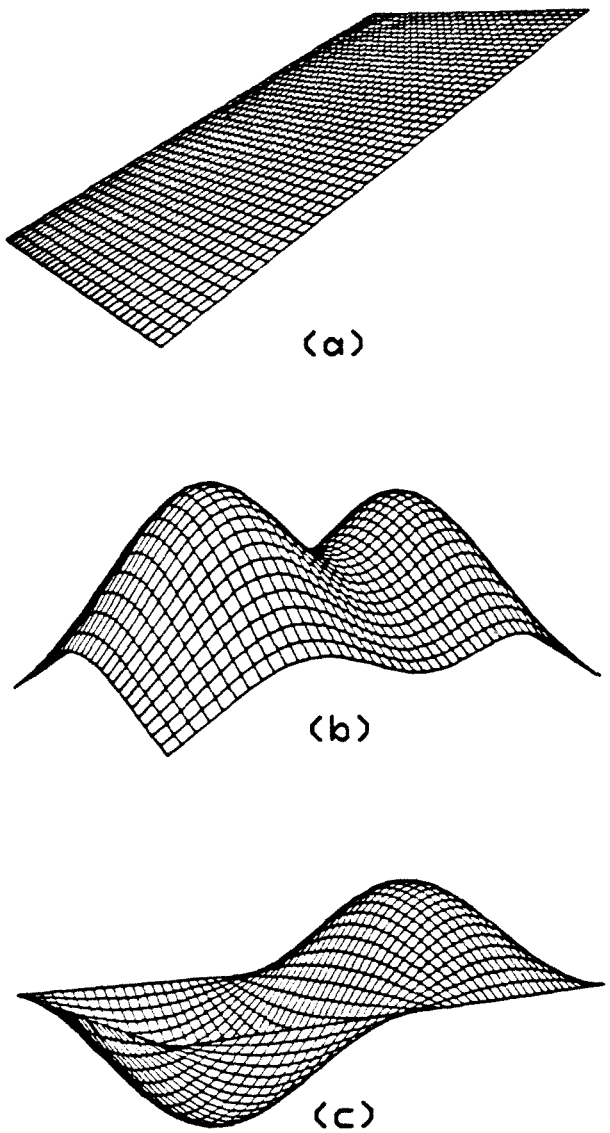

Figure 2 Assumed absolute permeability profiles

(a) $k = 0.2 + 0.2x/x_L$

(b) $k = 0.2 + 0.2e^{-(4x/x_L-1)^2-(2y/y_L-1)^2} + 0.2e^{-(4x/x_L-3)^2-(2y/y_L-1)^2}$

(c) $k = 0.3 - 0.1\sin(2\pi x/x_L)\sin(\pi y/y_L)$

regularization parameter based on J_{LS}/J_{ST} calculated from the non-regularized estimation, and a 15 × 10 grid system for spline approximation, unless specified otherwise, with a PDE grid system of 15 × 10. Since absolute permeability can be estimated from pressure data alone (Van den Bosch and Seinfeld 1977), we use only pressure data in this study. The smoothing functional is minimized until the maximum value of the derivative of J_{SM} with respect to the spline coefficients is less than 1/1000 of that for the flat initial guess of k. All computations were carried out on a CRAY X-MP/48.

6.1 Effect of Initial Guess

Since the uniqueness of the solution of the parameter estimation problem is not guaranteed and there may exist unidentifiable regions based on the configuration of measurements and the time period over which the data are available, convergence of the algorithm may depend on the given initial guess.

The assumed true absolute permeability profile shown in Figure 2.a,

$$k(x,y) = 0.2 + 0.2\frac{x}{x_L}\,, \tag{19}$$

was estimated using 300 noisy pressure data from 15 wells (20 data from each well) measured over the period $0 \leq t \leq 1.3$ years. (The conventional unit of the absolute permeability, and used in Eq. (19) and thereafter, is the darcy $= 0.987 \times 10^{-12}\mathrm{m}^2$. For consistency of units, k in Eq. (3) is in units of m^2.) The flat k value described in Step 1 of our algorithm that minimizes J_{LS} is 0.29 darcies and the J_{LS} value at this value of k is 28.8 times as large as the J_{LS} value calculated from the observation error. For an initial guess of $k(x,y) = 0.29$ darcies and $k(x,y) = 0.1 + 0.4x/x_L$ darcies, the smoothing functional was minimized for $\beta = 0$ (the suggested β's based on our algorithm are 2.25 and 1.88 darcies^{-2}, respectively) and again minimized for $\beta = 2.3$ darcies^{-2} starting from the result of the non-regularized estimation. Table

Table II Effect of Initial Guess on the Estimation of k given by Eq. (19)

	Initial Guess of k	β darcies^{-2}	J_{SM}	J_{LS}	J_{ST}	$J_{ST}^{(0)}$	$J_{ST}^{(1)}$	$J_{ST}^{(2)}$	$J_{ST}^{(3)}$	CPU time seconds*
(a)	0.29	0	0.997	0.997	0.443	13.7	0.088	0.105	0.250	21.9
(b)	$0.1 + 0.4x/x_L$	0	1.000	1.000	0.531	14.7	0.170	0.117	0.243	27.7
(c)	Converged solution of (a)	2.3	1.077	1.003	0.032	13.8	0.022	0.007	0.003	36.4
(d)	Converged solution of (b)	2.3	1.067	0.999	0.030	13.9	0.023	0.004	0.003	35.4
	True k		1.160†	1.099	0.027	14.0	0.027	0	0	

* CRAY X-MP/48.

† For $\beta = 2.3$ darcies^{-2}.

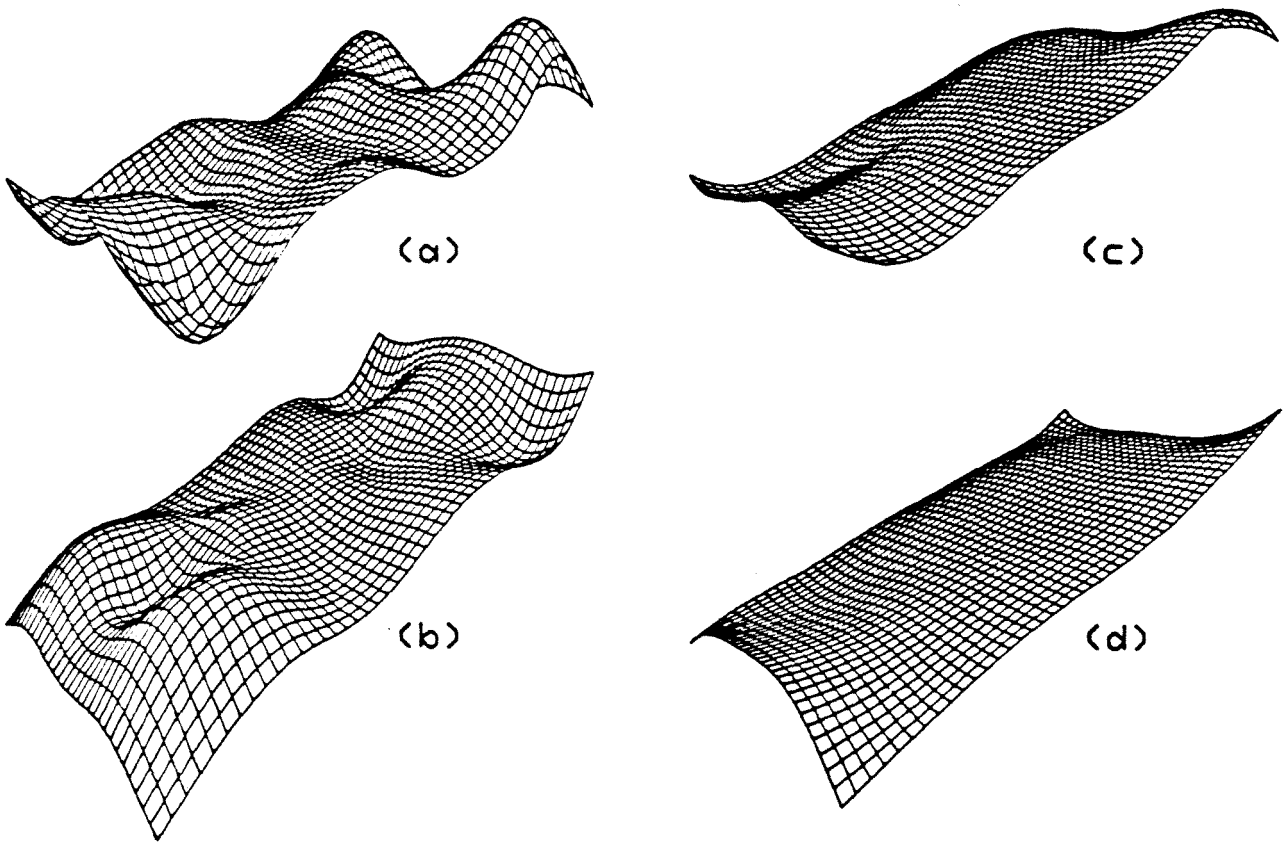

non-regularized $\beta = 2.3$ darcies^{-2}

Figure 3 Effect of initial guess on the estimation of k given by Eq. (19) for $\beta = 0$ (non-regularized) and $\beta = 2.3$ darcies^{-2}

(a) initial guess of $k = 0.29$

(b) initial guess of $k = 0.1 + 0.4x/x_L$

(c) initial guess of k from (a)

(d) initial guess of k from (b)

II shows the results of the estimation, and Figure 3 shows the parameter estimates. Figure 3 shows multiple solutions for non-regularized estimation, whereas for regularized estimation, the regions of multiple solution exist only near the boundaries of $x = 0$ and $x = x_L$, where flows of both oil and water are too small to provide meaningful data.

6.2 Effect of Spline Grid

To study the effect of the choice of spline grid, we consider 15×10, 12×9, 9×7, and 6×5 spline grid systems, where the grid cells are square for the last three cases. In all cases the PDE grid remains as 15×10. The assumed true profile of absolute permeability shown in Figure 2.b,

$$k(x,y) = 0.2 + 0.2\exp\left(-\left(4\frac{x}{x_L} - 1\right)^2 - \left(2\frac{y}{y_L} - 1\right)^2\right) + 0.2\exp\left(-\left(4\frac{x}{x_L} - 3\right)^2 - \left(2\frac{x}{y_L} - 1\right)^2\right) \tag{20}$$

was estimated. The flat initial guess of $k = 0.31$ darcies results from Step 1. We then carry out the estimation for $\beta = 0$ and $\beta = 1.7$ darcies^{-2} starting from the converged solution of the $\beta = 0$ case. Figure 4 show the parameter estimates for the cases given in Table III. Based on the non-regularized estimation, our algorithm suggests β's as 1.7, 2.5, 2.2, and 5.0 darcies^{-2} for the spline grid systems given above. Non-regularized estimates shows ill-conditioning near the boundaries for the $N_{xs} \times N_{ys} = 15 \times 10$ and 12×9 cases, but the regularized estimates are insensitive to the choice of spline grid except for 6×5 spline grid, for which the parameter estimates are incorrect no matter whether or not regularization is applied. (See Table III.) CPU times in Table III show that reducing the number of spline coefficients, $N_{xs} \times N_{ys}$, does not increase the rate of convergence. Thus a grid system on the order of that used to solve the PDE's can be employed for the parameter estimation by

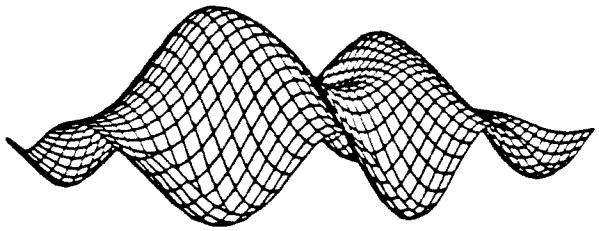

$N_{xs} \times N_{ys} = 15 \times 10$

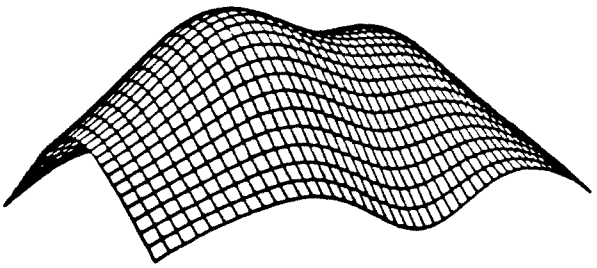

$N_{xs} \times N_{ys} = 15 \times 10$

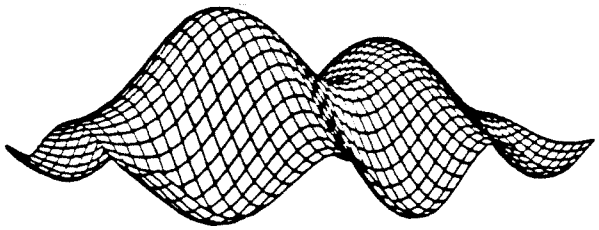

$N_{xs} \times N_{ys} = 12 \times 9$

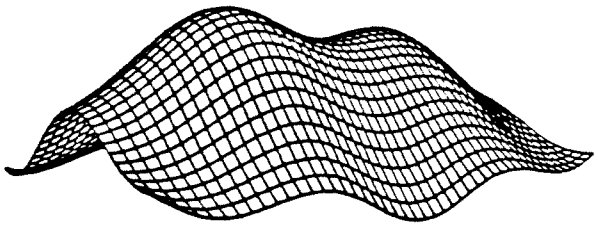

$N_{xs} \times N_{ys} = 12 \times 9$

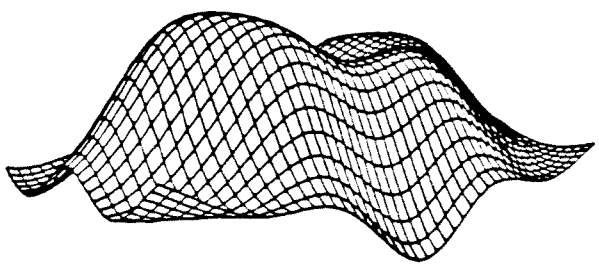

$N_{xs} \times N_{ys} = 9 \times 7$

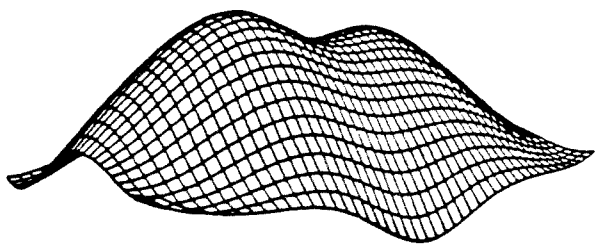

$N_{xs} \times N_{ys} = 9 \times 7$

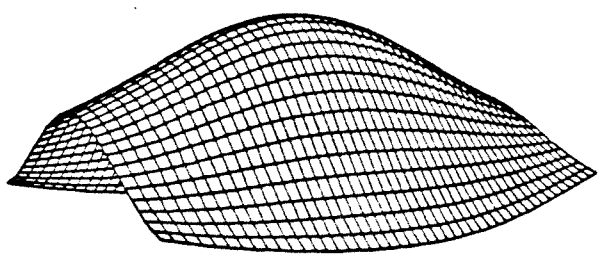

$N_{xs} \times N_{ys} = 6 \times 5$

non-regularized

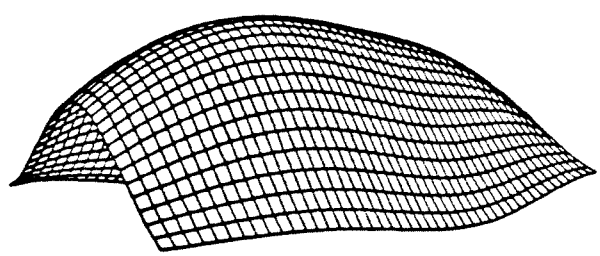

$N_{xs} \times N_{ys} = 6 \times 5$

$\beta = 1.7$ darcies^{-2}

Figure 4 Effect of spline grid on the estimation of k given by Eq. (20) for $\beta = 0$ (non-regularized) and $\beta = 1.7$ darcies^{-2}

Table III Effect of Spline Grid on the Estimation of k given by Eq. (20)

$N_{xs} \times N_{ys}$	β darcies^{-2}	J_{SM}	J_{LS}	J_{ST}	$J_{ST}^{(0)}$	$J_{ST}^{(1)}$	$J_{ST}^{(2)}$	$J_{ST}^{(3)}$	CPU time seconds*
15 × 10	0	0.927	0.927	0.548	16.0	0.144	0.151	0.253	14.0
12 × 9	0	0.933	0.933	0.370	16.1	0.133	0.108	0.128	12.8
9 × 7	0	0.911	0.911	0.407	16.3	0.169	0.106	0.132	28.3
6 × 5	0	0.982	0.982	0.197	16.4	0.153	0.031	0.013	18.2
15 × 10	1.7	1.221	0.954	0.157	16.1	0.118	0.025	0.014	31.3
12 × 9	1.7	1.229	0.957	0.160	16.1	0.113	0.029	0.017	21.2
9 × 7	1.7	1.253	0.954	0.176	16.0	0.126	0.032	0.018	13.9
6 × 5	1.7	1.276	0.980	0.174	16.3	0.140	0.024	0.009	31.5
True k		1.438†	1.070	0.217	15.8	0.162	0.036	0.019	

* CRAY X-MP/48.

† For $\beta = 1.7$ darcies^{-2}.

regularization without introducing the ill-conditioning that is prevalent in non-regularized algorithms. The regularization parameter depends on the spline grid system, such that a finer grid system generally yields a smaller value of β.

6.3 Effect of Stabilizing Functional

The main difference between Tikhonov's and Locker and Prenter's stabilizing functionals is the value of the weighting coefficient ς_0. We will test the cases $\varsigma_0 = 1, 0.3,$ 0.1, and 0 and $\varsigma_1 = \varsigma_2 = \varsigma_3 = 1$ for the true k shown in Figure 2.c,

$$k(x,y) = 0.3 - 0.1 \sin\left(\frac{2\pi x}{x_L}\right) \sin\left(\frac{\pi y}{y_L}\right) . \tag{21}$$

In this case it is advantageous to have a large amount of data so that effects of the number of data are absent. Consequently, we use 1500 noisy pressure data measured over a period $0 \leq t \leq 6.3$ years (100 data at each of the 15 wells). Step 1 produces the flat initial guess of $k = 0.28$ darcies. The regularization parameter is then chosen based on our algorithm using $\varsigma_0 = 0$, which is 2.1 darcies^{-2}. Table IV shows that the larger ς_0 leads to a mismatch of data (J_{LS}), an underestimate of the parameter ($J_{ST}{}^{(0)}$), and ill-conditioning of parameter estimates ($J_{ST}{}^{(2)}$ and $J_{ST}{}^{(3)}$). It can be deduced from this example that, with Tikhonov's stabilizing functional, increasing β will amplify the mismatch of data and the underestimate of the parameter; while decreasing β increases ill-conditioning of the estimates. One possible way to improve the parameter estimates is by decreasing ς_0, the limiting case of which is use of a stabilizing functional with the differential operator given by Eq. (15). Figure 5 shows how the estimates vary as ς_0 changes.

6.4 Effect of the Regularization Parameter

We now wish to study the effect of the value of the regularization parameter β on the estimation. To do so we employ the true k given by Eq. (21) and return to

Table IV Effect of Stabilizing Functional on the Estimation of k given by Eq. (21)

ς_0	β darcies^{-2}	J_{SM}	J_{LS}	J_{ST}	$J_{ST}^{(0)}$	$J_{ST}^{(1)}$	$J_{ST}^{(2)}$	$J_{ST}^{(3)}$	CPU time seconds*
	0	0.952	0.952		13.6	0.102	0.100	0.247	150.5
1	2.1	26.69	2.877	11.21	10.8	0.169	0.129	0.158	124.3
0.3	2.1	9.563	1.237	3.920	12.5	0.088	0.041	0.038	79.6
0.1	2.1	4.078	1.006	1.447	13.4	0.075	0.023	0.012	66.4
0	2.1	1.187	0.963	0.105	13.8	0.075	0.020	0.010	81.1
True k			0.973		13.9	0.106	0.030	0.008	

* CRAY X-MP/48.

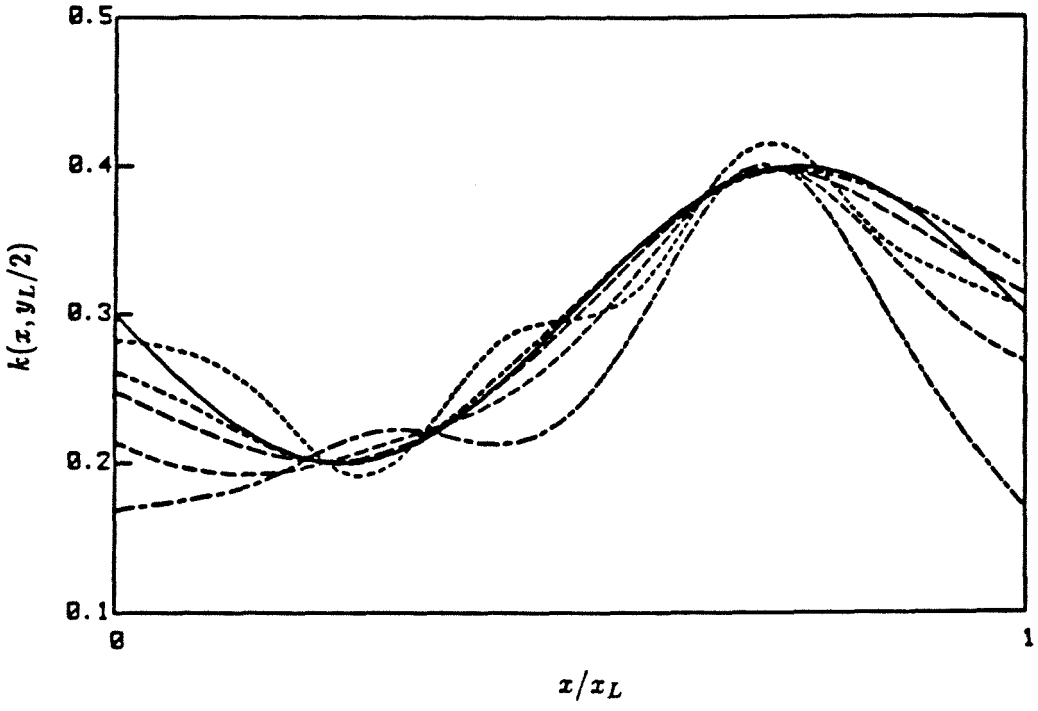

Figure 5 Effect of stabilizing functional on the estimation of k given by Eq. (21)

———— true k

····· $\beta = 0$

·—·—·—· $\varsigma_0 = 1$ and $\beta = 2.1$ darcies^{-2}

– – – – – $\varsigma_0 = 0.3$ and $\beta = 2.1$ darcies^{-2}

— — — —· $\varsigma_0 = 0.1$ and $\beta = 2.1$ darcies^{-2}

– – – – · $\varsigma_0 = 0$ and $\beta = 2.1$ darcies^{-2}

Table V Effect of Regularization Parameter on the Estimation of k given by Eq. (21)

β darcies^{-2}	J_{SM}	J_{LS}	J_{ST}	$J_{ST}^{(0)}$	$J_{ST}^{(1)}$	$J_{ST}^{(2)}$	$J_{ST}^{(3)}$	CPU time seconds*
0	0.924	0.924	0.630	13.6	0.118	0.139	0.372	33.7
0.091	0.946	0.925	0.231	13.7	0.106	0.059	0.066	21.7
0.183	0.967	0.929	0.207	13.7	0.098	0.054	0.055	13.4
0.367	0.993	0.932	0.166	13.7	0.096	0.040	0.030	16.0
0.734	1.062	0.937	0.170	13.7	0.091	0.043	0.036	8.4
1.468†	1.105	0.950	0.106	13.8	0.075	0.020	0.010	34.2
2.935	1.248	0.973	0.094	13.8	0.067	0.018	0.009	29.2
5.870	1.499	1.023	0.081	13.7	0.058	0.015	0.007	31.5
11.74	1.931	1.126	0.069	13.6	0.045	0.013	0.006	62.8
True k		1.041	0.144	13.9	0.106	0.030	0.008	

* CRAY X-MP/48.

† β based on the proposed algorithm.

the case of 300 data over the period of 1.3 years. The results are summarized in Table V. The value of β based on the non-regularized estimation is 1.468 darcies^{-2}. Other values of β were chosen so that they form a geometric sequence increasing and decreasing by factors of 2 around this value. If $\beta < 0.091$ darcies^{-2}, the minimization of J_{SM}, which is started from the result of the non-regularized estimation, is completed in one iteration, since the regularization component (βJ_{ST}) is negligible compared to J_{LS}. If $\beta > 11.74$ darcies^{-2}, the values of J_{LS} become very large, and the algorithm experiences convergence difficulties. For $\beta = 0.734$ darcies^{-2}, the algorithm converges faster than any of the other cases. On the whole, J_{LS} increases and J_{ST} and its component terms (except ${J_{ST}}^{(0)}$) decrease as β increases. Figure 6 shows the effect of the values of β on the estimated surface. We note that at the value of β based on our algorithm, neither is the regularization effect negligible nor is there significant data mismatch, and the estimated surface shown in Figure 6 approximates the true surface shown in Figure 2.c.

6.5 Stability of Regularized Solution

The most important feature of regularization is the stability of the solution so that small perturbations in measured data (random measurement error in the pressure data) imply small perturbations in the parameter estimates. To explore the stability of the parameter estimates, we use the absolute permeability given by Eq. (19) and three different simulated noisy pressure sequences scaled so that the root mean-square observation error is about 0.3×10^5 Pa. Figure 7 shows that the non-regularized estimates are unstable over the entire reservoir domain while the regularized estimates exhibit instability only in the regions near the boundaries ($x = 0$ and $x = x_L$) of the reservoir where the flow is negligible. Table VI shows the performance data for the three different data sets. Note that the difference between the values of J_{ST} and its terms (except ${J_{ST}}^{(0)}$) for the different data sets

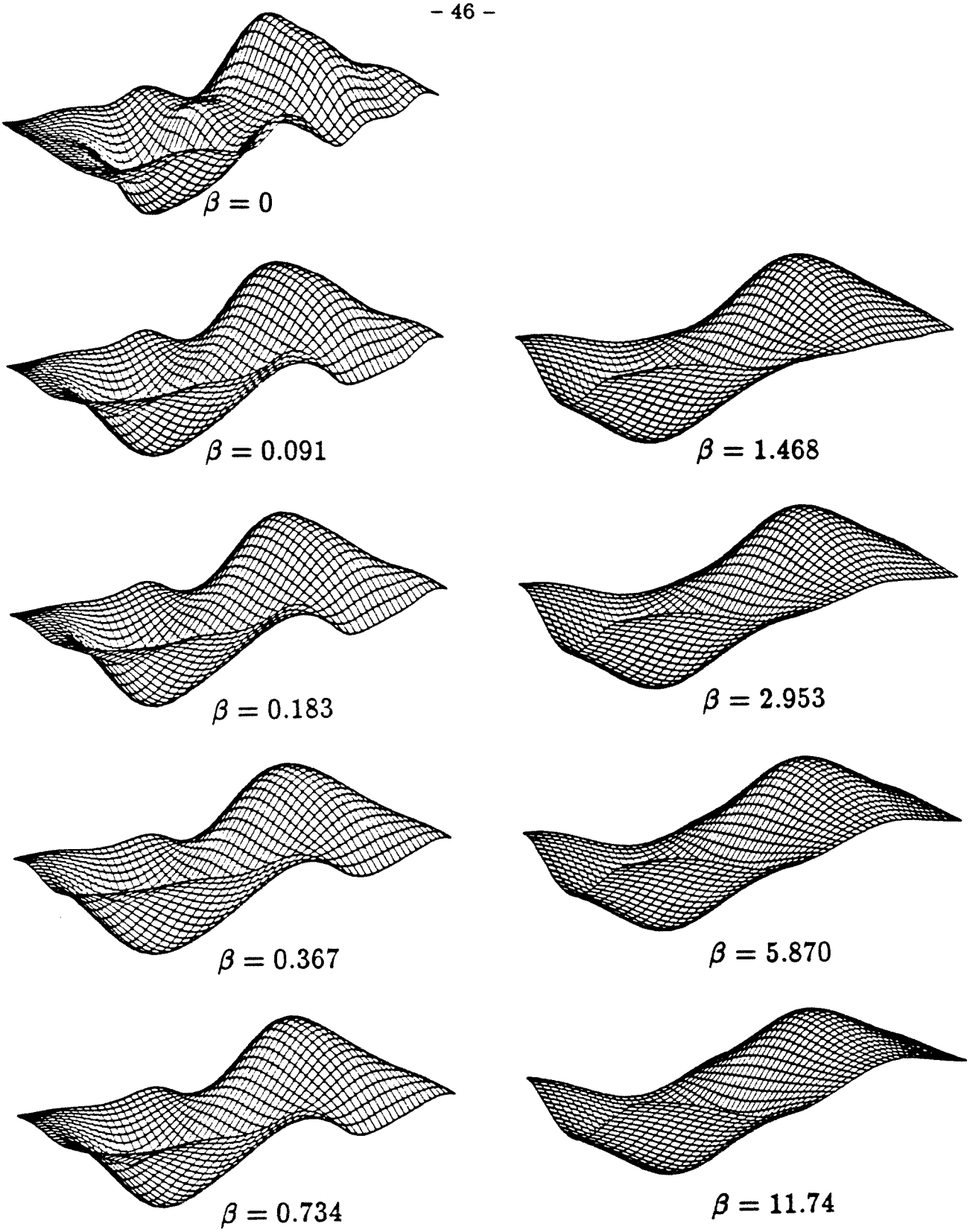

Figure 6 Effect of regularization parameter on the estimation of k given by Eq. (21) (Units are darcies^{-2}.)

Table VI Stability of Solution for the Estimation of k given by Eq. (19)

Data Set	β darcies^{-2}	J_{SM}	J_{LS}	J_{ST}	$J_{ST}^{(0)}$	$J_{ST}^{(1)}$	$J_{ST}^{(2)}$	$J_{ST}^{(3)}$	CPU time seconds*
1	0	0.913	0.913†	0.664	13.9	0.127	0.157	0.380	36.5
2	0	0.922	0.922‡	0.922	13.8	0.132	0.202	0.588	35.7
3	0	0.997	0.997**	0.442	13.7	0.088	0.105	0.250	22.0
1	1.0	0.988	0.935†	0.053	14.0	0.030	0.012	0.010	35.4
2	1.0	0.983	0.942‡	0.041	13.9	0.024	0.006	0.015	37.6
3	1.0	1.032	0.997**	0.035	13.9	0.021	0.005	0.007	37.8
True k				0.027	14.0	0.027	0	0	

* CRAY X-MP/48.

† J_{LS} for true k is 1.070.

‡ J_{LS} for true k is 1.041.

** J_{LS} for true k is 1.099.

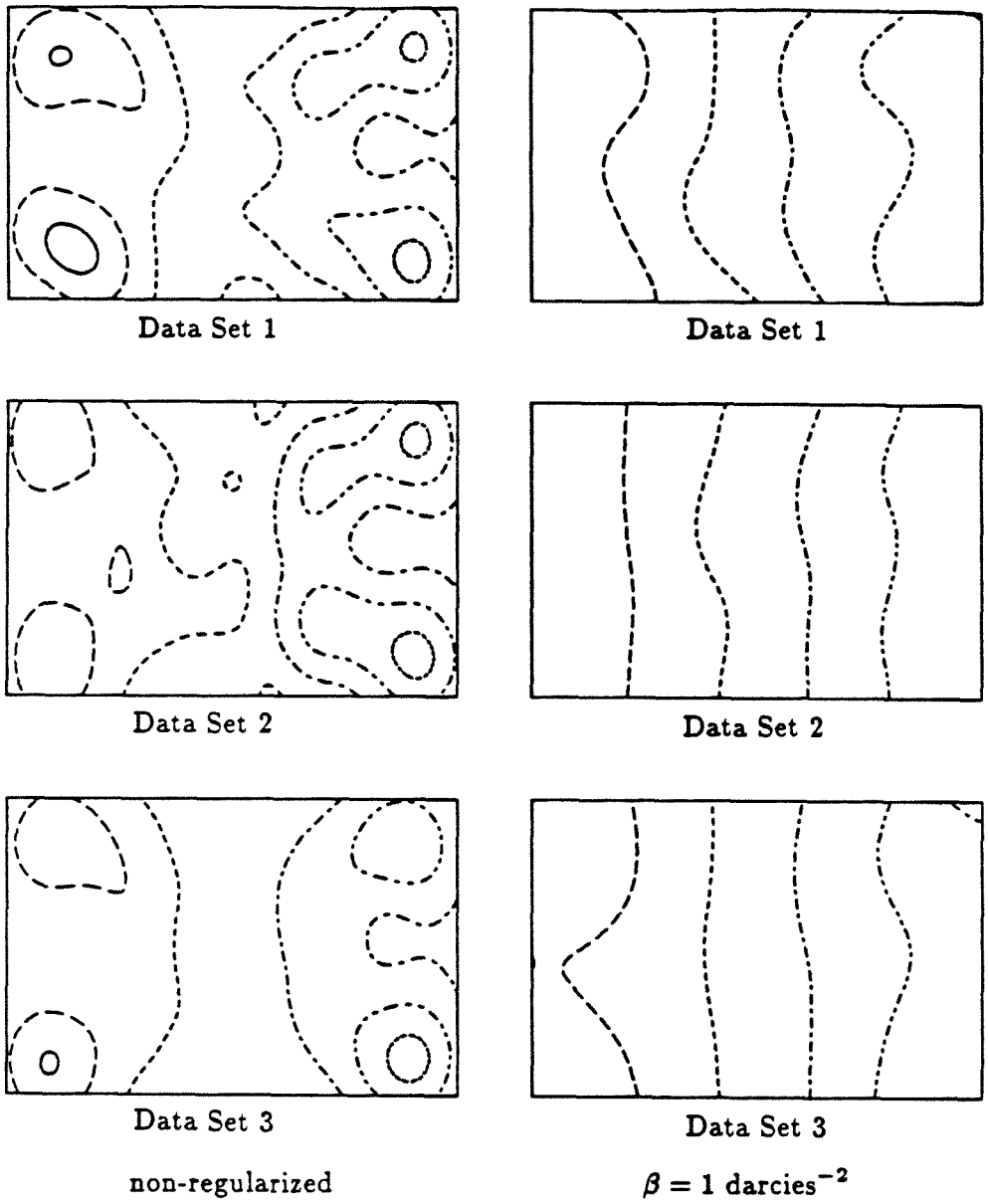

Figure 7 Stability of solution for the estimation of k given by Eq. (19)

Contour values are:

——————— $k = 0.2$ darcies

– – – – – – – $k = 0.24$ darcies

---------- $k = 0.28$ darcies

-·-·-·-·-·- $k = 0.32$ darcies

-·-·-·-·-·- $k = 0.36$ darcies

····· $k = 0.4$ darcies

are reduced by a factor of 10 as a consequence of regularization.

7. Conclusions

The purpose of this study has been to develop an algorithm for parameter estimation by regularization and spline approximation for two-phase petroleum reservoirs.

The algorithm is divided into three steps. Step 1 seeks a flat initial guess of the parameter. This step avoids convergence difficulties that may arise in estimating spatially varying parameters from a poor initial guess. Usually this step converges within a few (4–6) iterative solutions of the reservoir and adjoint equations. Step 2 is devoted to non-regularized ($\beta = 0$) conventional least-squares estimation by spline approximation. The spline grid system is chosen so that the number of spline coefficients is the same as the number of grid cells for the solution of reservoir PDE's, unless the number of observed data is less than the number of unknown coefficients. The parameter estimates from this step are usually ill-conditioned and dependent on the choice of the spline grid. This step usually requires 20–40 iterative solutions of the reservoir and adjoint equations to reduce the gradient value of the performance index to 1/1000 of its starting value. In this step, approximate values of the upper bounds of J_{LS} and J_{ST} are then estimated. In Step 3, parameter estimation by regularization and spline approximation is carried out to obtain the final solution. In this step, the regularization parameter is selected as the ratio of J_{LS} to J_{ST} determined in Step 2, and Locker and Prenter's stabilizing functional is used. The algorithm generally converges after 20–40 iterative solutions of the reservoir and adjoint equations.

For non-regularized estimation, the parameter estimates are sensitive to the choice of the spline grid, whereas for regularized estimation, the results are found to be insensitive to the choice of the spline grid (unless it is too coarse to properly represent the spatial variation). Since the value of the regularization parameter is

dependent on the dimension of the spline grid, it is recommended that one use a grid system for spline approximation such that the number of spline coefficients is approximately equal to the smaller of the number of PDE grid cells or the number of observation data. Locker and Prenter's stabilizing functional with gradient operator was found to be superior to Tikhonov's stabilizing functional from the point of view of numerical performance.

The algorithm does not require any *a priori* information on the parameter to be estimated except that the parameter can be properly represented by a spline approximation. The parameter estimates based on the algorithm are shown to be superior to conventional non-regularized least-squares estimation in the sense of stability to the observation error and initial guess dependency.

Acknowledgment

We wish to gratefully acknowledge Chevron Oil Field Research Company for providing access to their CRAY X-MP/48 for the computations reported here.

References

Aziz, K. and A. Settari, *Petroleum Reservoir Simulation* (Applied Science, London, 1983), p. 204.

Banks, H. T., in *Proceedings 3rd IFAC Symposium on Control of Distributed Parameter Systems, Toulouse, France, 1982* (Pergamon, New York, 1982), p. SP21.

Banks, H. T. and J. M. Crowley, in *American Control Conference, San Francisco, California, 1983*, p.997.

Banks, H. T. and P. D. Lamm, *IEEE Trans. Autom. Control*, **AC-30**, 386 (1985).

Banks, H. T. and K. A. Murphy, "Estimation of Coefficients and Boundary Parameters in Hyperbolic Systems," *Division of Applied Mathematics, Brown University, Report LCDS No. 84-5* (1984).

Van den Bosch, B. and J. H. Seinfeld, *Soc. Pet. Eng. J.*, **17**, 398 (1977).

Chavent, G., M. Dupuy, and P. Lemonnier, *Soc. Pet. Eng. J.*, **15**, 74 (1975).

Chen, W. H., G. R. Gavalas, J. H. Seinfeld, and M. L. Wasserman, *Soc. Pet. Eng. J.*, **14**, 593 (1974).

Craven, P. and G. Wahba, *Numer. Math.*, **31**, 377 (1979).

Kravaris, C. and J. H. Seinfeld, *SIAM J. Control and Optimization*, **23**, 217 (1985).

Kravaris, C. and J. H. Seinfeld, "Identification of Spatially-Varying Parameters in Distributed Parameter Systems by Discrete Regularization," *J. Math. Anal. Appl.*, **119** 128 (1986).

Lee, T., C. Kravaris, and J. H. Seinfeld, "History Matching by Spline Approximation and Regularization in Single-Phase Areal Reservoirs," *SPE Reservoir Engineering*, **1**, 521 (1986).

Locker, J. and P. M. Prenter, *J. Math. Anal. Appl.*, **74**, 504 (1980).

Miller, K., *SIAM J. Math. Anal. Appl.*, **1**, 52 (1970).

Nazareth, L., *J. Opt. Theory Appl.*, **23**, 373 (1977).

Scales L. E., *Introduction to Non-Linear Optimization* (Springer-Verlag, New York, 1985), p. 106.

Shah, P. C., G. R. Gavalas, J. H. Seinfeld, *Soc. Pet. Eng. J.*, **18**, 219 (1978).

Tikhonov, A. N., *Soviet Math. Dokl.*, **4**, 1624 (1963).

Tikhonov, A. N. and V. Y. Arsenin, *Solutions of Ill-posed Problems* (Wiley, New York, 1977), p. 45.

Trummer M. R., *SIAM J. Numer. Anal.*, **21**, 729 (1984).

Wasserman, M. L., A. S. Emanuel, and J. H. Seinfeld, *Soc. Pet. Eng. J.*, **15**, 347 (1975).

Appendix A. Finite Difference Reservoir Equations

The basic model consists of two coupled nonlinear PDE's for pressure p and

water saturation S_w. It is customary to discretize them using finite difference approximations to yield a set of nonlinear algebraic equations. We solve these equations sequentially at each time step, i.e., solve the equations for pressure first, then for water saturation, and repeat these procedures until the solution converges (Aziz and Settari, 1983).

In order to solve the reservoir PDE's, Eqs. (2), (3), and (7) are discretized to give implicit time finite difference approximation by

$$\begin{aligned} R_{w_i}^n \equiv & - Q_t \frac{\phi_{SC_i}}{B_{f_i}^{n-1}}(c_w + c_f) S_{w_i}^n (p_i^n - p_i^{n-1}) - Q_t \frac{\phi_{SC_i}}{B_{f_i}^{n-1}}(S_{w_i}^n - S_{w_i}^{n-1}) \\ & - \sum_{j \in \mathbf{J}_i} Q_{i,j} \lambda_{w_{i,j}}^n (p_i^n - p_j^n) + \sum_{k=1}^{N_w} q_{w_k}^n \frac{\delta_{i,i_k}}{h} \\ & = 0 \end{aligned} \tag{A.1}$$

$$\begin{aligned} R_{o_i}^n \equiv & - Q_t \frac{\phi_{SC_i}}{B_{f_i}^{n-1}}(c_o + c_f)(1 - S_{w_i}^n)(p_i^n - p_i^{n-1}) + Q_t \frac{\phi_{SC_i}}{B_{f_i}^{n-1}}(S_{w_i}^n - S_{w_i}^{n-1}) \\ & - \sum_{j \in \mathbf{J}_i} Q_{i,j} \lambda_{o_{i,j}}^n (p_i^n - p_j^n) + \sum_{k=1}^{N_w} q_{o_k}^n \frac{\delta_{i,i_k}}{h} \\ & = 0 \end{aligned} \tag{A.2}$$

for $n = 1, \ldots, N_t$ and $i \in \mathbf{N}$ defined by

$$\begin{aligned} \mathbf{N} & \equiv \{ i \mid i = i_x + N_x(i_y - 1),\ i_x = 1, \ldots, N_x,\ i_y = 1, \ldots, N_y \} \\ & = \{ 1, \ldots, N \} \end{aligned} \tag{A.3}$$

where $N = N_x N_y$ and i_x and i_y denote PDE grid blocks along x- and y-direction, respectively, and the index set $\mathbf{J}_i$, defined for each $i \in \mathbf{N}$ by

$$\mathbf{J}_i = \{ j \mid j = i - N_x, i - 1, i + 1, i + N_x \} \bigcap \mathbf{N}\,, \tag{A.4}$$

is introduced for simplicity, with initial conditions

$$p_i^0 = p_0 \tag{A.5}$$

$$S_{wi}^{0} = S_{iw}. \tag{A.6}$$

In Eqs. (A.1) and (A.2) the mobilities $\lambda_{wi,j}^{n}$ and $\lambda_{oi,j}^{n}$, $i = 1, \ldots, N$ are given by

$$\lambda_{wi,j}^{n} = \frac{k_{i,j} k_{rwi,j}^{n}}{\mu_w} \tag{A.7}$$

$$\lambda_{oi,j}^{n} = \frac{k_{i,j} k_{roi,j}^{n}}{\mu_o} \tag{A.8}$$

where the algebraic average is used for the absolute permeability

$$k_{i,j} = \frac{k_i + k_j}{2} \tag{A.9}$$

and upstream weighting is used for the relative permeabilities for the stability of numerical integration given by

$$\begin{aligned} k_{rwi,j}^{n} &= k_{rw}(S_{wi}^{n}) \quad \text{and} \quad k_{roi,j}^{n} = k_{ro}(S_{wi}^{n}) \qquad \text{if} \quad p_i^n \geq p_j^n \\ k_{rwi,j}^{n} &= k_{rw}(S_{wj}^{n}) \quad \text{and} \quad k_{roi,j}^{n} = k_{ro}(S_{wj}^{n}) \qquad \text{otherwise.} \end{aligned} \tag{A.10}$$

The porosity distribution at pressure p_{SC}, denoted by ϕ_{SC}, is known where SC denotes "standard condition." Compressibility effects are included by using the so-called formation volume factor of rock B_f,

$$B_f(p) = e^{c_f(p_{SC} - p)} \tag{A.11}$$

where in evaluating B_f an explicit time difference scheme is used in the finite difference approximation.

First-order variations of Eqs. (A.1–2) with respect to S_w are given by

$$\begin{aligned} \delta R_{wi}^{n} \equiv & - Q_t \frac{\phi_{SCi}}{B_{fi}^{n-1}} (c_w + c_f) \delta S_{wi}^{n} (p_i^n - p_i^{n-1}) - Q_t \frac{\phi_{SCi}}{B_{fi}^{n-1}} \delta S_{wi}^{n} \\ & - \sum_{j \in J_i} Q_{i,j} \left(\frac{\partial \lambda_{wi,j}^{n}}{\partial S_{wi}^{n}} \delta S_{wi}^{n} + \frac{\partial \lambda_{wi,j}^{n}}{\partial S_{wj}^{n}} \delta S_{wj}^{n} \right) (p_i^n - p_j^n) \\ & + \sum_{k=1}^{N_w} \frac{dq_{wk}^{n}}{dS_{wi}^{n}} \delta S_{wi}^{n} \frac{\delta_{i,i_k}}{h} \end{aligned} \tag{A.12}$$

$$\delta R_{o_i}^n \equiv + Q_t \frac{\phi_{SC_i}}{B_{f_i}^{n-1}} (c_o + c_f) \delta S_{w_i}^n (p_i^n - p_i^{n-1}) + Q_t \frac{\phi_{SC_i}}{B_{f_i}^{n-1}} \delta S_{w_i}^n$$
$$- \sum_{j \in \mathbf{J}_i} Q_{i,j} \left(\frac{\partial \lambda_{o_{i,j}}^n}{\partial S_{w_i}^n} \delta S_{w_i}^n + \frac{\partial \lambda_{o_{i,j}}^n}{\partial S_{w_j}^n} \delta S_{w_j}^n \right) (p_i^n - p_j^n) \qquad (A.13)$$
$$+ \sum_{k=1}^{N_w} \frac{dq_{o_k}^n}{dS_{w_i}^n} \delta S_{w_i}^n \frac{\delta_{i,i_k}}{h}$$

to solve the finite difference equations for S_w.

At time step $t_n = n\Delta t$, $n = 1, \ldots, N_t$, take initial guesses of $p_i^n = p_i^{n-1}$ and $S_{w_i}^n = S_{w_i}^{n-1}$ for $i = 1, \ldots, N$ and solve

$$R_{w_i}^n + R_{o_i}^n = 0 \qquad (A.14)$$

for p_i^n, $i = 1, \ldots, N$ where R_w's and R_o's are given in Eqs. (A.1) and (A.2), respectively. Eq. (A.14) does not include time-derivative terms of S_w, and is a linear pentadiagonal system with respect to p, so that it is easily solved by the Iterative Alternate Direction Implicit (IADI) method.

Secondly, solve

$$\frac{(c_o + c_f)(1 - S_{w_i}^n)}{c_{t_i}^n} R_{w_i}^n - \frac{(c_w + c_f) S_{w_i}^n}{c_{t_i}^n} R_{o_i}^n = 0 \qquad (A.15)$$

for $S_{w_i}^n$, $i = 1, \ldots, N$ by Newton's method, since Eq. (A.15) is nonlinear with respect to S_w. Eq. (A.15) does not include time-derivative terms of p, and the total compressibility, $c_{t_i}^n$ is given by

$$c_{t_i}^n = (c_w + c_f) S_{w_i}^n + (c_o + c_f)(1 - S_{w_i}^n) \, . \qquad (A.16)$$

Taylor series expansion of Eq. (A.15) up to first order gives

$$\frac{(c_o + c_f)(1 - S_{w_i}^n)}{c_{t_i}^n} (R_{w_i}^n + \delta R_{w_i}^n) - \frac{(c_w + c_f) S_{w_i}^n}{c_{t_i}^n} (R_{o_i}^n + \delta R_{o_i}^n) = 0 \qquad (A.17)$$

for $i = 1, \ldots, N$, where the first-order variation terms, δR_w's and δR_o's, are given in Eqs. (A.12) and (A.13), respectively. Eq. (A.17) is a linear pentadiagonal system with respect to δS_w and solved for $\delta S_{w_i}^n$, $i = 1, \ldots, N$ by the IADI method.

Then we compare the current iterate of p_i^n and $S_{w_i}^n$, $i = 1, \ldots, N$ with the previous ones, and repeat solving Eqs. (A.14–17) until convergence.

Appendix B. Functional Derivative of J_{LS}

We present the finite difference version of the first-order necessary condition for a minimum of the least-squares discrepancy function defined by

$$\begin{aligned} J_{LS} = & \frac{1}{N_t N_o} \sum_{n=1}^{N_t} \sum_{\nu=1}^{N_o} \Bigg[W_p \left(p(x_\nu, y_\nu, t_n) - p^{\mathrm{obs}^n_\nu} \right)^2 \\ & + W_F \left(F_{wo}(x_\nu, y_\nu, t_n) - F_{wo}^{\mathrm{obs}^n_\nu} \right)^2 \Bigg] \end{aligned} \tag{B.1}$$

where $p^{\mathrm{obs}^n_\nu}$ and $F_{wo}^{\mathrm{obs}^n_\nu}$ are the pressure and water-to-oil ratio ($\equiv S_w/S_o$) data measured from the ν-th observation well located at (x_ν, y_ν), $\nu = 1, \ldots, N_o$, at time t_n, $n = 1, \ldots, N_t$. The corresponding Hamiltonian of the conventional least-squares problem is

$$\widetilde{J_{LS}} = J_{LS} + \sum_{n=1}^{N_t} \sum_{i=1}^{N} (\psi_{w_i}^n R_{w_i}^n + \psi_{o_i}^n R_{o_i}^n) \,. \tag{B.2}$$

Collecting terms that include δp_i^n yields

$$\begin{aligned} R_{p_i}^n \equiv & Q_t \frac{\phi_{SC_i}}{B_{f_i}^n} \left((c_w + c_f) S_{w_i}^{n+1} \psi_{w_i}^{n+1} + (c_o + c_f)(1 - S_{w_i}^{n+1}) \psi_{o_i}^{n+1} \right) \\ & - Q_t \frac{\phi_{SC_i}}{B_{f_i}^{n-1}} \left((c_w + c_f) S_{w_i}^n \psi_{w_i}^n + (c_o + c_f)(1 - S_{w_i}^n) \psi_{o_i}^n \right) \\ & - \sum_{j \in \mathbf{J}_i} Q_{i,j} \left(\lambda_{w_{i,j}}^n (\psi_{w_i}^n - \psi_{w_j}^n) + \lambda_{o_{i,j}}^n (\psi_{o_i}^n - \psi_{o_j}^n) \right) \\ & + \frac{2W_p}{N_t N_o} \sum_{\nu=1}^{N_o} (p_i^n - p^{\mathrm{obs}^n_\nu}) \delta_{i,i_\nu} \\ & = 0 \,, \end{aligned} \tag{B.3}$$

and terms that include $\delta S_{w_i}^n$ yield

$$
\begin{aligned}
R_{s_i}^n \equiv & Q_t \left(\frac{\phi_{SC_i}}{B_{f_i}^n} (\psi_{w_i}^{n+1} - \psi_{o_i}^{n+1}) - \frac{\phi_{SC_i}}{B_{f_i}^{n-1}} (\psi_{w_i}^n - \psi_{o_i}^n) \right) \\
& - ((c_w + c_f)\psi_{w_i}^n - (c_o + c_f)\psi_{o_i}^n) \, Q_t \frac{\phi_{SC_i}}{B_{f_i}^{n-1}} (p_i^n - p_i^{n-1}) \\
& - \sum_{j \in \mathbf{J}_i} Q_{i,j} \left(\frac{\partial \lambda_{w_{i,j}}^n}{\partial S_{w_i}^n} (\psi_{w_i}^n - \psi_{w_j}^n) + \frac{\partial \lambda_{o_{i,j}}^n}{\partial S_{w_i}^n} (\psi_{o_i}^n - \psi_{o_j}^n) \right) (p_i^n - p_j^n) \\
& + \frac{2W_F}{N_t N_o} \frac{dF_{wo_i}^n}{dS_{w_i}^n} \sum_{\nu=1}^{N_o} (F_{wo_i}^n - F_{wo_\nu}^{\mathrm{obs}\,n}) \delta_{i,i_\nu} + (\psi_{w_i}^n - \psi_{o_i}^n) \sum_{k=1}^{N_w} \frac{dq_{w_k}^n}{dS_{w_i}^n} \frac{\delta_{i,i_k}}{h} \\
& = 0
\end{aligned}
\tag{B.4}
$$

for $i \in \mathbf{N}$ and $n = N_t, N_t - 1, \ldots, 2, 1$ with terminal constraints

$$
\psi_{w_i}^{N_t+1} = 0 \tag{B.5}
$$

$$
\psi_{o_i}^{N_t+1} = 0 \tag{B.6}
$$

for $i \in \mathbf{N}$. The functional derivative of J_{LS} with respect to k_i, $i \in \acute{\mathbf{N}}$ is given by

$$
\frac{\partial J_{LS}}{\partial k_i} = -\frac{1}{2} \sum_{n=1}^{N_t} \sum_{j \in \mathbf{J}_i} Q_{i,j} \left(\frac{k_{rw}{}_{i,j}^n}{\mu_w} (\psi_{w_i}^n - \psi_{w_j}^n) + \frac{k_{ro}{}_{i,j}^n}{\mu_o} (\psi_{o_i}^n - \psi_{o_j}^n) \right) (p_i^n - p_j^n) \, . \tag{B.7}
$$

The adjoint system equations are solved sequentially; i.e., Eq. (B.3) is solved for a new variable ψ_p defined by

$$
\psi_{p_i}^n \equiv \frac{(c_w + c_f) S_{w_i}^n}{c_{t_i}^n} \psi_{w_i}^n + \frac{(c_o + c_f)(1 - S_{w_i}^n)}{c_{t_i}^n} \psi_{o_i}^n \tag{B.8}
$$

and Eq. (B.4) for ψ_s defined by

$$
\psi_{s_i}^n \equiv \psi_{w_i}^n - \psi_{o_i}^n \tag{B.9}
$$

where the IADI method is employed for the solution of each equation, repeating this procedure until the solution converges. From $\partial J_{LS}/\partial k_i$, $i = 1, \ldots, N$ and the derivative of J_{ST} with respect to the spline coefficients we can compute the derivative of J_{SM} with respect to each spline coefficient (Lee et al., 1986).

List of Symbols

a_o	maximum value of oil phase relative permeability
a_w	maximum value of water phase relative permeability
B_f	formation volume factor of rock
b_o	power index of oil phase relative permeability function
b_w	power index of water phase relative permeability function
b_x	function given in Eq. (17)
b_y	function given in Eq. (18)
c_f	compressibility of rock, Pa^{-1}
c_o	compressibility of oil, Pa^{-1}
c_t	total compressibility defined by $(c_w + c_f)S_w + (c_o + c_f)(1 - S_w)$, Pa^{-1}
c_w	compressibility of water, Pa^{-1}
h	thickness of reservoir, m
$H^3(\Omega)$	Sobolev space of functions that are square-integrable and have square-integrable derivatives up to order 3
$H^{(L)}(\Omega)$	Sobolev space associated with the differential operator L
$\mathbf{J}_i$	index set defined by Eq. (A.4)
J_{LS}	least-squares discrepancy term
$\overline{J_{LS}}$	upper bound of J_{LS}
$\widetilde{J_{LS}}$	Hamiltonian of J_{LS} associated with reservoir PDE's Eqs. (A.1–2)
J_{SM}	smoothing functional
J_{ST}	stabilizing functional
$\overline{J_{ST}}$	upper bound of J_{ST}
K	nonlinear operator defined by Eq. (9)
k	absolute permeability, darcies
k_{ro}	relative permeability of oil
k_{rw}	relative permeability of water

L	differential operator
N	number of PDE grid cells given by $N_x N_y$
$\mathbf{N}$	index set defined by Eq. (A.3)
$\mathbf{n}$	outward normal vector defined at the reservoir boundary, m
N_o	number of observation wells
N_t	number of observations at each well
N_w	number of injection-production wells
N_x	number of PDE grid cells along x-direction
N_{xs}	number of spline grid points along x-direction
N_y	number of PDE grid cells along y-direction
N_{ys}	number of spline grid points along y-direction
p	pressure, Pa
p_0	initial pressure, Pa
p_{SC}	pressure at standard condition, Pa
$Q_{i,j}$	quantity defined by $\Delta y/\Delta x$ if $i-j=\pm 1$; $\Delta x/\Delta y$ if $i-j=\pm N_x$; 0 otherwise
q_κ	total volumetric flow rate at injection-production well, m^3/s
$q_{o\kappa}$	volumetric flow rate of oil at injection-production well, m^3/s
Q_t	quantity defined by $\Delta x \Delta y/\Delta t$, m^2/s
$q_{w\kappa}$	volumetric flow rate of water at injection-production wells, m^3/s
R_o	residue of oil phase equation defined by Eq. (2.b)
R_w	residue of water phase equation defined by Eq. (2.a)
S_{iw}	irreducible water saturation
S_o	oil saturation
S_{ro}	residual oil saturation
S_w	water saturation
T	total time period of observation, s

t	time, s
t_n	time of observation, s
u_δ	noisy measured data
v_o	linear velocity of oil, m/s
v_w	linear velocity of water, m/s
W_F	weighting coefficient for water-to-oil ratio discrepancy term in J_{LS}
W_{l_x,l_y}	spline coefficient for parameter α at spline grid point (l_x, l_y)
W_p	weighting coefficient for pressure discrepancy term in J_{LS}
x	space variable, m
x_κ	x-coordinate of κ-th injection-production well, m
x_L	width of reservoir, m
x_ν	x-coordinate of ν-th observation well, m
y	space variable, m
y_κ	y-coordinate of κ-th injection-production well, m
y_L	length of reservoir, m
y_ν	y-coordinate of ν-th observation well, m

Greek Letters

α	unknown parameter to be estimated
β	regularization parameter, darcies^{-2}
$\delta(\cdot)$	Dirac delta function
δR_o	first-order variation of R_o defined by Eq. (A.12)
δR_w	first-order variation of R_w defined by Eq. (A.11)
$\delta_{i,j}$	Kronecker delta
δS_w	first-order variation of S_w
Δt	time interval of each observation, s
Δx	PDE grid size along x-direction, m

Δx_s	spline grid size along x-direction, m
Δy	PDE grid size along y-direction, m
Δy_s	spline grid size along y-direction, m
$\partial\Omega$	boundary of reservoir
ς_m	weighting coefficient in stabilizing functional, $m = 0, \ldots, 3$
η	dimensionless space variable defined by $y/\Delta y$
λ_o	mobility of oil defined by kk_{ro}/μ_o, darcies/Pa $\cdot$ s
λ_w	mobility of water defined by kk_{rw}/μ_w, darcies/Pa $\cdot$ s
μ_o	viscosity of oil, Pa $\cdot$ s
μ_w	viscosity of water, Pa $\cdot$ s
ξ	dimensionless space variable defined by $x/\Delta x$
ρ_o	density of oil, Kg/m^3
ρ_w	density of water, Kg/m^3
ϕ	porosity of rock
ϕ_{SC}	porosity of rock at standard condition
χ^{*4}	cubic B-spline function
ψ_o	adjoint variable associated with oil phase equation
ψ_p	quantity defined by Eq. (B.8)
ψ_s	quantity defined by Eq. (B.9)
ψ_w	adjoint variable associated with water phase equation
Ω	reservoir domain

Subscripts

f	rock
i	grid cell for the solution of PDE, $\in \mathbf{N}$
i_κ	PDE grid cell at which κ-th injection-production well is located
i_ν	PDE grid cell at which ν-th observation well is located
j	grid cell for the solution of PDE, $\in \mathbf{J}_i$

n	time step, $\in \{1, 2, \ldots, N_t\}$
m	order of derivative of parameter
o	oil phase
SC	standard condition
w	water phase
κ	injection-production well, $\in \{1, 2, \ldots, N_w\}$
ν	observation well, $\in \{1, 2, \ldots, N_o\}$

Superscripts

m	order of derivative of parameter
n	time step, $\in \{1, 2, \ldots, N_t\}$

Chapter IV

Estimation of Absolute and Relative Permeabilities in Petroleum Reservoirs

Abstract. The estimation of absolute and relative permeabilities for petroleum reservoirs on the basis of noisy data at wells is considered. The spatially varying absolute permeability is estimated by regularization combined with a bicubic spline approximation. Relative permeability is represented by a given function of saturation with unknown coefficients. Numerical results provide an indication of the estimability of the two permeabilities in conventional petroleum production operations.

The text of Chapter 4 consists of an article coauthored with J. H. Seinfeld, which has been submitted to *Inverse Problems*.

1. Introduction

Once wells have been drilled down into a reservoir containing recoverable petroleum, the local properties of the reservoir rocks and fluids must be determined. A variety of complex acoustical, electronic and magnetic techniques are available that, when lowered into the well, can be used to determine the local properties of the formation and fluids in the neighborhood of the well. Estimates of the reservoir properties are needed, however, throughout the entire reservoir, not just at the wells, in order to simulate various production strategies to try to optimize the recovery of the petroleum. To estimate the properties on the reservoir, past production histories are simulated. The properties are determined as those that produce the closest possible match of the observed and predicted histories. This so-called history-matching process has been addressed in the petroleum, hydrology, and mathematics literature for some 20 years or so (Jacquard and Jain, 1965, Carter et al., 1974, Chen et al., 1974, Chavent et al., 1975, Wasserman et al., 1975, Chen and Seinfeld, 1975, Gavalas et al., 1976, Shah et al., 1978, Neuman and Yakowitz, 1979, Yakowitz and Duckstein, 1980, Neuman and Carrera, 1985, Neuman, 1973, Sun and Yeh, 1985, Yeh, 1986, Yeh and Yoon, 1981, Yeh et al., 1983, Carrera and Neuman, 1986, Seinfeld and Chen, 1978, Yoon and Yeh, 1976, Tang and Chen, 1984, Van den Bosch and Seinfeld, 1977, Watson et al., 1984, Lee et al., 1986, and Lee and Seinfeld, 1986).

In the early stages of production of a petroleum reservoir, it can often be assumed that the reservoir contains only a single fluid, oil. In that case the reservoir behavior is described by a single linear parabolic PDE for pressure. The reservoir parameters that enter the equation, and are subject to estimation, are the rock porosity ϕ and the absolute permeability k, both of which vary with location in the reservoir. Most of the above cited references are addressed to the case of a single-phase reservoir. (In case of an aquifer, although the reservoir fluid is water, the pressure is governed by the same PDE as in the case of an oil reservoir.)

Generally, one must account for the fact that oil and water are present together in petroleum reservoirs, and the resulting reservoir model consists of two coupled nonlinear PDE's. In addition to the porosity ϕ and absolute permeability k, the two-phase case is characterized by the *relative permeabilities* k_{ro} and k_{rw} ("o" referring to oil — "w" referring to water) that are presumed to be functions of the local fluid saturation in the medium. The precise values of the two relative permeabilities are usually not known.

The essential difficulties in the petroleum reservoir inverse problem are twofold. First, the reservoir properties are spatially varying, and the estimation of a spatially varying permeability is well known to be an ill-posed problem (Chavent, 1979ab, Seinfeld and Kravaris, 1982, Kravaris and Seinfeld, 1985). Second, the oil-water reservoir is a highly nonlinear system, for which rigorous results concerning its inverse problems do not exist.

The ill-posed nature of the single-phase permeability estimation problem has been attacked by Bayesian approaches (Gavalas et al., 1976, Shah et al., 1978) regularization (Tang and Chen, 1984, Seinfeld and Kravaris, 1982, Kravaris and Seinfeld, 1985, 1986, Lee et al., 1986, Neuman and de Marsily, 1976) and spline approximation (Banks and Lamm, 1985). While the Bayesian approach requires *a priori* statistical information on the unknown parameters that may not be generally available and spline approximation, in and of itself, does not guarantee well-posedness, the regularization approach offers both rigorous stability and convenient computational implementation. The first step of the regularization formulation is to measure the non-smoothness of the parameter by its norm in an appropriate Hilbert space, called the stabilizing functional, and then to seek the value of the parameter that minimizes the weighted sum of the least-squares discrepancy term and the stabilizing functional. In previous applications of regularization to the petroleum reservoir inverse problem, Lee et al. (1986) estimated absolute permeability and porosity in

a single-phase reservoir and Lee and Seinfeld (1986) estimated the absolute permeability in a two-phase reservoir.

The object of the present paper is to develop an algorithm for the simultaneous estimation of absolute and relative permeabilities in two-phase petroleum reservoirs. In related work on two-phase reservoirs Van den Bosch and Seinfeld (1977) investigated the estimation of constant absolute permeability and porosity and relative permeabilities near a single producing well where radial symmetry can be exploited. Watson et al. (1984) estimated absolute permeability, porosity and relative permeabilities simultaneously, assuming that the absolute permeability and porosity are each a constant independent of location. The present paper addresses the more practical case in which the absolute permeability is spatially varying. (Since the porosity is generally less variable than the permeability and also is better identified, we do not consider its estimation here.)

The next section defines the mathematical model of the oil-water petroleum reservoir. Section 3 then defines the inverse problem associated with estimating absolute and relative permeabilities. In Section 4 we present a numerical regularization algorithm, and section 5 is devoted to a detailed computational example.

2. Mathematical Model of Two-Phase Petroleum Reservoir

Consider a two-dimensional oil-water reservoir that has sufficiently large areal extent so that we can assume that the pressure change and hence the flow in the vertical direction is negligible compared to that in the other two directions (Aziz and Settari, 1983, pp. 204 – 243). Assuming that the oil and water phases are immiscible, the equations of mass conservation for the oil and water phases are

$$\frac{\partial}{\partial t}(\rho_o \phi S_o) + \nabla \cdot (\rho_o \mathbf{v}_o) = \sum_{\kappa=1}^{N_w} \rho_o q_{o\kappa} \frac{\delta(x - x_\kappa)\delta(y - y_\kappa)}{h} \tag{1}$$

$$\frac{\partial}{\partial t}(\rho_w \phi S_w) + \nabla \cdot (\rho_w \mathbf{v}_w) = \sum_{\kappa=1}^{N_w} \rho_w q_{w\kappa} \frac{\delta(x - x_\kappa)\delta(y - y_\kappa)}{h} \tag{2}$$

for $(x, y) \in \Omega$ and $0 < t < T$, where S_o and S_w, the volume fractions of oil and water with respect to the total fluid volume, called oil and water saturations, respectively, satisfy $S_o \equiv 1 - S_w$. The oil-water reservoirs that do not include gas phase generally are slightly compressible systems; i.e., the porosity, ϕ, and the density of oil, ρ_o, and water, ρ_w, are weak functions of pressure. It is customary that the functional dependencies are given by $c_f = (1/\phi)(d\phi/dp)$, $c_o = (1/\rho_o)(d\rho_o/dp)$, and $c_w = (1/\rho_w)(d\rho_w/dp)$ where c_f, c_o, and c_w denote the compressibilities of rock, oil, and water and are assumed to be constant over the entire region of pressure change of the reservoir (Aziz and Settari, 1983, p. 13). The volumetric flow rates of the water and oil phases at the wells located at (x_κ, y_κ) are denoted by $q_{o\kappa}$ and $q_{w\kappa}$, $\kappa = 1, \ldots, N_w$. For injection wells, $q_o = 0$ and $q_w > 0$. For production wells, q_o and q_w are negative, and the ratio q_w/q_o is proportional to the ratio of local flow velocities of water to oil at the bottom of wells. The thickness of the reservoir, h, is assumed to be constant over the whole reservoir domain.* The linear velocities of the oil and water phases are assumed to be described by Darcy's Law,

$$\mathbf{v}_o = -\frac{k k_{ro}}{\mu_o} \nabla p \tag{3}$$

$$\mathbf{v}_w = -\frac{k k_{rw}}{\mu_w} \nabla p \,, \tag{4}$$

where the absolute permeability k is a parameter characterizing the fluid conductivity of a porous medium, μ_o and μ_w are the viscosities of oil and water, respectively, and the relative permeabilities of oil and water, k_{ro} and k_{rw}, respectively, are assumed to be functions of fluid (water) saturation within the porous medium independent of flow rate and fluid properties. Widely used functional forms of the

* If h is spatially varying, then the integrated properties hk and $h\phi$ are subject to estimation instead of k and ϕ, respectively, in the reservoir parameter estimation problem, but it does not change the structure of problems.

relative permeabilities, and those employed in this study, are

$$k_{ro}(S_w) = a_o \left(\frac{1 - S_{ro} - S_w}{1 - S_{ro} - S_{iw}} \right)^{b_o} \tag{5}$$

$$k_{rw}(S_w) = a_w \left(\frac{S_w - S_{iw}}{1 - S_{ro} - S_{iw}} \right)^{b_w} \tag{6}$$

for $S_{iw} \leq S_w \leq 1 - S_{ro}$ where irreducible (or connate) water saturation, S_{iw}, and residual oil saturation, S_{ro}, are the lower bounds of S_w and S_o, respectively, under which water and oil, respectively, become immobile with reasonable pressure gradients. The relative permeabilities are each less than unity, and typically, their sum is also less than unity for $S_{iw} < S_w < 1 - S_{ro}$ (Collins, 1961, pp. 53 - 55). Eqs. (1 - 6) together with the no-flux boundary condition,

$$\mathbf{n} \cdot \nabla p = 0 \,, \tag{7}$$

for $(x, y) \in \partial\Omega$ and $0 < t < T$, and the given initial conditions

$$p(x, y, 0) = p_0(x, y) \tag{8}$$

$$S_w(x, y, 0) = S_{w0}(x, y) \tag{9}$$

for $(x, y) \in \Omega$ describe the water-driven oil recovery process for a petroleum reservoir with an impermeable boundary. Eqs. (1 - 9) are solved numerically using finite difference approximation. Physically, these equations describe the movement of both phases, usually as water is intentionally pumped down certain wells to drive the oil in place toward other wells where it is produced. When the water breaks through at the production wells, the displacement process is considered to be complete.

3. The Inverse Problem

It is desired to estimate simultaneously the absolute permeability k and the relative permeabilities, k_{ro} and k_{rw}, from data normally available at wells that have been

drilled into the reservoir. Since k_{ro} and k_{rw} are assumed to be given by Eqs. (5) and (6), their estimation reduces to that of the two unknown constant parameters b_o and b_w. The measured data consist of the pressure at N_o wells and at N_t discrete times over $0 < t < T$ and of the water fraction of the total flow at each well,

$$f_w = \frac{k_{rw}/\mu_w}{k_{rw}/\mu_w + k_{ro}/\mu_o} . \tag{10}$$

The usual least-squares objective function consists of two contributions, one each from the pressure and the water flow observations. We define σ_p^2 as the mean-square error between the calculated and measured pressure data

$$\sigma_p^2 = \frac{1}{N_o N_t} \sum_{n=1}^{N_t} \sum_{\nu=1}^{N_o} \left(p(x_\nu, y_\nu, t_n) - p^{\text{obs}}{}_\nu^n \right)^2 \tag{11}$$

where $(x_\nu, y_\nu) \in \Omega$, $\nu = 1, \ldots, N_o$ denote the locations of the observations, that is the wells, and t_n, $n = 1, \ldots, N_t$ are the observation times. Similarly, we define σ_f^2 as the mean-square error in the water flow data,

$$\sigma_f^2 = \frac{1}{N_o N_t} \sum_{n=1}^{N_t} \sum_{\nu=1}^{N_o} \left(f_w(x_\nu, y_\nu, t_n) - f_w^{\text{obs}}{}_\nu^n \right)^2 . \tag{12}$$

Then the least-squares objective function is given by a weighted sum of the two contributions

$$J_{LS}(k, b_o, b_w) = W_p \sigma_p^2 + W_f \sigma_f^2 \tag{13}$$

where W_p and W_f are the weighting coefficients for the pressure and flow-rate terms, respectively.

The conventional least-squares identification problem is to estimate $k(x, y)$, b_o and b_w to minimize J_{LS}. The spatial variation of k leads to an ill-posed inverse problem, and hence we turn to a regularization formulation. Kravaris and Seinfeld (1985, 1986) extended the concept of regularization to the estimation of coefficients in PDE's. Regularization of a problem refers to solving a problem related to the original problem, called the regularized problem, the solution of which

is both more "regular" and approximates the solution of the original problem. In Tikhonov's regularization formulation (Tikhonov and Arsenin, 1977), the measure of non-smoothness of the parameter being estimated, called the stabilizing functional, is represented by a norm of the parameter in an appropriate Hilbert space, for example,

$$J_{ST}(k) = ||k||^2_{H^3(\Omega)} , \tag{14}$$

where the Sobolev space $H^3(\Omega)$ is the set of functions that are square-integrable over Ω and have square-integrable derivatives up to order 3. More precisely, Tikhonov's stabilizing functional is given by

$$J_{ST}(k) = \sum_{m=0}^{3} \varsigma_m \iint_{\Omega} \sum_{\nu=0}^{m} \binom{m}{\nu} \left(\frac{\partial^m k(\xi,\eta)}{\partial \xi^\nu \partial \eta^{m-\nu}} \right)^2 d\xi d\eta \tag{15}$$

where convenient dimensionless variables are $\xi = N_x x/x_L$ and $\eta = N_y y/y_L$, where x_L and y_L are the lateral reservoir dimensions, and N_x and N_y are the number of PDE grid cells employed along x- and y-directions, respectively. The conditions for the coefficients ς_m are $\varsigma_0 > 0$, $\varsigma_1 > 0$, $\varsigma_2 > 0$, and $\varsigma_3 > 0$ (Tikhonov, 1963); or $\varsigma_0 \geq 0$, $\varsigma_1 \geq 0$, $\varsigma_2 \geq 0$, and $\varsigma_3 > 0$ (Tikhonov and Arsenin, 1977, pp. 69 – 70). As Trummer (1984) has pointed out, using the stabilizing functional that includes the Euclidean norm of the parameter itself leads to the underestimation of the parameter. Locker and Prenter (1980) suggested the use of a stabilizing functional with a differential operator. Lee and Seinfeld (1986) used the stabilizing functional with the gradient operator (∇) so that it does not include the Euclidean norm term ($\varsigma_0 \equiv 0$ in Eq. (15)) for the estimation of absolute permeability.

The regularization formulation of the inverse problem seeks the minimum of the smoothing functional,

$$J_{SM}(k, b_o, b_w; \beta) = J_{LS}(k, b_o, b_w) + \beta J_{ST}(k) , \tag{16}$$

where β is the regularization parameter that represents the relative importance given to J_{ST}. In the present problem, J_{LS} is composed of the two terms as shown

in Eq. (13); hence, J_{SM} includes three quantities, $W_p\sigma_p^2$, $W_f\sigma_f^2$, and βJ_{ST}, where two of the three weighting coefficients W_p, W_f, and β must be determined independently. W_f/W_p can be chosen as the ratio $\overline{\sigma}_p^2/\overline{\sigma}_f^2$, where $\overline{\sigma}_p^2$ and $\overline{\sigma}_f^2$ denote the variances associated with the pressure and production data measurements, respectively (Watson et al., 1980). In the present study, $\overline{\sigma}_p^2/\overline{\sigma}_f^2$ is assumed to be known and W_f/W_p is chosen as that value. An important question regarding the regularization method is determining a suitable value of β for the given noisy data, especially where the noise level may or may not be known. The value of β is chosen in several different ways (Miller, 1970; Tikhonov and Arsenin, 1977, pp. 87 – 94; and Craven and Wahba, 1979). Miller suggests that β be determined from the ratio of an upper bound of the measurement error to an upper bound of the measure of non-smoothness. Craven and Wahba (1979) used the method of generalized cross validation (GCV) to determine the regularization parameter. Since GCV requires parametric sensitivity information, this method is not practical for such a large-scale problem like reservoir parameter estimation. Lee and Seinfeld (1986) developed an algorithm based on Miller's idea, which determines the regularization parameter automatically during the estimation process without requiring *a priori* information.

The absolute permeability in a two-phase reservoir is primarily estimated from the pressure data (Van den Bosch and Seinfeld, 1977; Watson et al., 1984). Thus, we can determine β/W_p from the ratio of an upper bound of σ_p^2 to an upper bound of J_{ST}. In practice, these values are usually not known and Lee and Seinfeld (1986) used the values of J_{ST} and the pressure discrepancy of the results of the non-regularized ($\beta = 0$) estimation to determine β. Without loss of generality W_p will be specified as $1/\overline{\sigma}_p^2$.

Spline approximation of spatially varying parameters has several merits including a built-in smoothing and computational convenience (Banks and Lamm, 1985; Kravaris and Seinfeld, 1986) The spline approximation of the spatially varying ab-

solute permeability is given by

$$k(x,y) = \sum_{l_y=1}^{N_{ys}} \sum_{l_x=1}^{N_{xs}} \chi^{*4}\left(4 - l_x + \frac{x}{\Delta x_s}\right) \chi^{*4}\left(4 - l_y + \frac{y}{\Delta y_s}\right) W_l \qquad (17)$$

where $\chi^{*4}(\theta)$ is cubic B-spline function,

$$\chi^{*4}(\theta) = \begin{cases} \theta^3/6 & \theta \in [0,1] \\ 1/6 + (\theta-1)/2 + (\theta-1)^2/2 + (\theta-1)^3/2 & \theta \in [1,2] \\ 4/6 - (\theta-2)^2 + (\theta-2)^3/2 & \theta \in [2,3] \\ 1/6 - (\theta-3)/2 + (\theta-3)^2/2 - (\theta-3)^3/6 & \theta \in [3,4] \\ 0 & \text{otherwise,} \end{cases} \qquad (18)$$

Δx_s and Δy_s are the grid spacings for the spline approximation and $l = l_x + N_{xs}(l_y - 1)$ for $l_x = 1, \ldots, N_{xs}$ and $l_y = 1, \ldots, N_{ys}$. In applying the spline approximation to the parameter estimation problem, if the number of spline coefficients, $N_{xs} \times N_{ys} (= N_s)$, is too few then the spline approximation cannot represent the spatial details properly. On the other hand, the number of spline coefficients should not exceed the number of grid cells for the solution of the PDE's. When the spline approximation is used together with regularization, the smoothing power of the spline approximation becomes less important than in its absence and N_{xs} and N_{ys} can be chosen as large as the numbers of grid cells along x- and y-directions for the solution of the PDE's (Lee and Seinfeld, 1986). The unknown parameters characterizing $k(x,y)$ are now W_l, $l = 1, \ldots, N_s$.

4. Numerical Algorithm

The reservoir parameter estimation problem is a large nonlinear least-squares problem. The number of unknown parameters to be estimated is the same magnitude as the number of grid cells for the discretization of the PDE's. That number is of order of at least one hundred in the field applications. In general, because of the size

of the estimation problem, a minimization method that requires the first derivative of the objective function is preferred over one that requires the second derivatives. The first order derivatives of the least-squares performance index can be derived using optimal control theory (Chen et al., 1974 and Chavent et al., 1975). The functional derivative of J_{LS} with respect to $k(x,y)$ is

$$\frac{\delta J_{LS}}{\delta k} = -\int_0^T \left(\frac{k_{rw}}{\mu_w} \nabla\psi_w \cdot \nabla p + \frac{k_{ro}}{\mu_o} \nabla\psi_o \cdot \nabla p \right) dt \tag{19}$$

and the partial derivatives of J_{LS} with respect to b_o and b_w are

$$\begin{aligned} \frac{\partial J_{LS}}{\partial b_o} = -\int_0^T \iint_\Omega dxdydt \Bigg[& \frac{k}{\mu_o} \frac{\partial k_{ro}}{\partial b_o} \nabla\psi_o \cdot \nabla p \\ & + \sum_{\kappa=1}^{N_w} \left(\psi_w \frac{\partial q_{w\kappa}}{\partial b_o} + \psi_o \frac{\partial q_{o\kappa}}{\partial b_o} \right) \frac{\delta(x-x_\kappa)\delta(y-y_\kappa)}{h} \\ & + \frac{2W_f}{N_o N_t} \sum_{n=1}^{N_t} \sum_{\nu=1}^{N_o} (f_w - f_w^{\mathrm{obs}^n_\nu}) \frac{\partial f_w}{\partial b_o} \delta(x-x_\nu)\delta(y-y_\nu)\delta(t-t_n) \Bigg] \end{aligned} \tag{20}$$

$$\begin{aligned} \frac{\partial J_{LS}}{\partial b_w} = -\int_0^T \iint_\Omega dxdydt \Bigg[& \frac{k}{\mu_w} \frac{\partial k_{rw}}{\partial b_w} \nabla\psi_w \cdot \nabla p \\ & + \sum_{\kappa=1}^{N_w} \left(\psi_w \frac{\partial q_{w\kappa}}{\partial b_w} + \psi_o \frac{\partial q_{o\kappa}}{\partial b_w} \right) \frac{\delta(x-x_\kappa)\delta(y-y_\kappa)}{h} \\ & + \frac{2W_f}{N_o N_t} \sum_{n=1}^{N_t} \sum_{\nu=1}^{N_o} (f_w - f_w^{\mathrm{obs}^n_\nu}) \frac{\partial f_w}{\partial b_w} \delta(x-x_\nu)\delta(y-y_\nu)\delta(t-t_n) \Bigg] \end{aligned} \tag{21}$$

The adjoint variables ψ_o and ψ_w satisfy the following adjoint equations

$$\begin{aligned} & -(c_w + c_f)\frac{\partial}{\partial t}(\phi S_w \psi_w) - (c_o + c_f)\frac{\partial}{\partial t}(\phi S_o \psi_o) \\ & -\nabla \cdot \left(\frac{k k_{rw}}{\mu_w} \nabla\psi_w + \frac{k k_{ro}}{\mu_o} \nabla\psi_o \right) \\ & = \frac{2W_p}{N_o N_t} \sum_{n=1}^{N_t} \sum_{\nu=1}^{N_o} \left(p - p^{\mathrm{obs}^n_\nu} \right) \delta(x-x_\nu)\delta(y-y_\nu)\delta(t-t_n) \end{aligned} \tag{22}$$

from the terms including the variation of p and

$$
\begin{aligned}
&-\frac{\partial}{\partial t}[\phi(\psi_w-\psi_o)]+\phi((c_w+c_f)\psi_w-(c_o+c_f)\psi_o)\frac{\partial p}{\partial t}\\
&+\frac{k}{\mu_w}\frac{\partial k_{rw}}{\partial S_w}\nabla\psi_w\cdot\nabla p+\frac{k}{\mu_o}\frac{\partial k_{ro}}{\partial S_w}\nabla\psi_o\cdot\nabla p\\
&-\sum_{\kappa=1}^{N_w}\left(\psi_w\frac{\partial q_{w\kappa}}{\partial S_w}+\psi_o\frac{\partial q_{o\kappa}}{\partial S_w}\right)\frac{\delta(x-x_\kappa)\delta(y-y_\kappa)}{h} \qquad (23)\\
&=\frac{2W_f}{N_oN_t}\sum_{n=1}^{N_t}\sum_{\nu=1}^{N_o}\left(f_w-f_w^{\mathrm{obs}\,n}{}_{\nu}\right)\frac{\partial f_w}{\partial S_w}\delta(x-x_\nu)\delta(y-y_\nu)\delta(t-t_n)
\end{aligned}
$$

from the terms including the variation of S_w for $(x,y)\in\Omega$ and $0<t<T$ with the terminal constraints

$$\psi_o(x,y,T)=0 \qquad (24)$$

$$\psi_w(x,y,T)=0 \qquad (25)$$

for $(x,y)\in\Omega$ and the boundary condition

$$\mathbf{n}\cdot\left(\frac{kk_{rw}}{\mu_w}\nabla\psi_w+\frac{kk_{ro}}{\mu_o}\nabla\psi_o\right)=0 \qquad (26)$$

for $(x,y)\in\partial\Omega$ and $0<t<T$.

Shah et al. (1978) have evaluated the sensitivities of the reservoir state variables (p and f_w) to the parameters. It is considerably more difficult to simultaneously estimate k, b_o, and b_w than to estimate k only or to estimate k_{ro} and k_{rw} only. Since the quantities appear as kk_{ro} and kk_{rw}, p and f_w are especially insensitive to changes in k, b_o, and b_w. This observation suggests that k and (b_o,b_w) should be estimated separately during the minimization process.

The problem is to estimate the spline coefficients, W_l, $l=1,\ldots,N_s$, and the dimensionless exponents, b_o and b_w, in the relative permeability expressions, that minimize the smoothing functional J_{SM}. Consider the minimization of J_{SM} by a steepest descent technique. The gradient of J_{SM} with respect to W_l, $l=1,\ldots,N_s$ is

$$\mathbf{g}_w=\begin{pmatrix}\partial J_{SM}/\partial W_1\\ \vdots\\ \partial J_{SM}/\partial W_{N_s}\end{pmatrix} \qquad (27)$$

The partial derivatives $\partial J_{SM}/\partial W_l$, $l = 1, \ldots, N_s$ can be directly calculated from (the finite difference approximation of) the functional derivative $\delta J_{LS}/\delta k$ and the partial derivatives $\partial J_{ST}/\partial W_l$. The gradient of J_{SM} with respect to (b_o, b_w) is simply

$$\mathbf{g}_b = \begin{pmatrix} \partial J_{LS}/\partial b_o \\ \partial J_{LS}/\partial b_w \end{pmatrix} . \tag{28}$$

In the following discussion we will refer to $(W_1, \ldots, W_{N_s})$ and (b_o, b_w) as $\mathbf{W}$ and $\mathbf{b}$, respectively. The line search step in the steepest descent method starting at $(\mathbf{W}, \mathbf{b})$ along the descent direction $\mathbf{d}_W = -\mathbf{g}_w(\mathbf{W}, \mathbf{b})$ and $\mathbf{d}_b = -\mathbf{g}_b(\mathbf{W}, \mathbf{b})$ is to find the step length s such that

$$\mathbf{g}_w(\mathbf{W} + s\mathbf{d}_W, \mathbf{b} + s\mathbf{d}_b) \cdot \mathbf{d}_W + \mathbf{g}_b(\mathbf{W} + s\mathbf{d}_W, \mathbf{b} + s\mathbf{d}_b) \cdot \mathbf{d}_b = 0 . \tag{29}$$

In its practical application, the line search step represented by Eq. (29) is dependent on the linear scale (unit) of absolute permeability and thus is not unique. To see this, let $\widehat{k} = ck$, where c is an arbitrary positive constant. Then $\widehat{\mathbf{W}} = c\mathbf{W}$ and the line search step is to find $\widehat{s}$ such that

$$\frac{1}{c^2}\mathbf{g}_w\left(\frac{\widehat{\mathbf{W}}}{c} + \widehat{s}\frac{\mathbf{d}_W}{c}, \mathbf{b} + \widehat{s}\mathbf{d}_b\right) \cdot \mathbf{d}_W + \mathbf{g}_b\left(\frac{\widehat{\mathbf{W}}}{c} + \widehat{s}\frac{\mathbf{d}_W}{c}, \mathbf{b} + \widehat{s}\mathbf{d}_b\right) \cdot \mathbf{d}_b = 0 . \tag{30}$$

The arbitrariness of c suggests a modification of the line search step that finds the set of step lengths (r, s) such that

$$\mathbf{g}_w(\mathbf{W} + r\mathbf{d}_W, \mathbf{b} + s\mathbf{d}_b) \cdot \mathbf{d}_W = 0 \tag{31}$$

$$\mathbf{g}_b(\mathbf{W} + r\mathbf{d}_W, \mathbf{b} + s\mathbf{d}_b) \cdot \mathbf{d}_b = 0 \tag{32}$$

independent of the linear scale c.

To estimate (k, b_o, b_w) simultaneously, the following three-step algorithm will be used assuming that no *a priori* information is available for the spatial variation of $k(x, y)$ and β.

Step 1 Assuming that $k(x,y) = \bar{k}$ over the whole domain, find $(\bar{k}, b_o, b_w)$ that minimize J_{LS}.

Step 2 Starting from $W_l = \bar{k}$, $l = 1, \ldots, N_s$, calculated from step 1, minimize J_{LS} with respect to $(\mathbf{W}, b_o, b_W)$. Compute $\beta = W_p \sigma_p^2 / J_{ST}$ at convergence.

Step 3 Using β and starting from $(\mathbf{W}, b_o, b_w)$ determined in step 2, minimize J_{SM} with respect to $\mathbf{W}$, b_o, and b_w.

In each step, the minimization of J_{LS} or J_{SM} will be carried out by the steepest descent method using Eqs. (31 – 32).

Step 2 of the algorithm is the conventional least-squares estimation of k by spline approximation, and of b_o and b_w, that gives the best fit of observed pressure and flow data. The major contribution of step 3 in the algorithm is to alleviate the ill-conditioning of the estimated k by a regularization. Generally, the exponents of the relative permeabilities, b_o and b_w, will not change significantly in step 3. In practice, therefore, step 3 can usually be replaced by

Step 3′ Using β, b_o, and b_w and starting from $\mathbf{W}$ determined in step 2, minimize J_{SM} with respect to $\mathbf{W}$.

In step 3′ the smoothing functional J_{SM} is minimized with respect to the single set of parameters, $\mathbf{W}$, and the minimization can be carried out by a general multivariate gradient algorithm. The partial conjugate gradient method of Nazareth (1977) is chosen, as it is suitable for a large-scale minimization.

For the numerical implementation of the stabilizing functional with the gradient operator, J_{ST} with $\varsigma_0 = 0$ in Eq. (15), the weighting coefficients ς_m, $m = 1$, 2, and 3, need to be specified. Since the integration in Eq. (15) is based on the length scales of discretization of the PDE's, x_L/N_x and y_L/N_y, the grid spacings for the reservoir PDE, ς_m's of the derivative terms can be chosen as $\varsigma_1 = \varsigma_2 = \varsigma_3 = 1$.

5. Computational Examples

In order to test the performance of the algorithm thoroughly, we will introduce a hypothetical reservoir for which the true properties are assumed to be known. The assumed fluid and reservoir properties are shown in Table I. The assumed true absolute permeability distribution is given by

$$k(x,y) = 0.3 - 0.1 \sin\left(\frac{2\pi x}{x_L}\right) \sin\left(\frac{\pi y}{y_L}\right) \tag{33}$$

in units of darcies (1 darcy = 0.987×10^{-12} m^2) for $(x,y) \in \Omega$. The location of wells and the true absolute permeability contour map are shown in Figure 1. The governing PDE's (1 – 9) are solved on a 15 × 10 mesh with the time stepsize of 23.1 days. The observation data are taken from nine observation wells that include two production wells with observation time interval 23.1 days and perturbed by uniformly distributed random numbers (generated by IMSL subroutine GGNML on VAX 11/780), with zero mean and standard deviations 0.34 atm and 0.0085 for p and f_w, respectively. These noisy data are then used to attempt to recover (k, b_o, b_w).

Water-breakthrough time has an important significance in the identifiabilities of the parameters. Watson et al. (1984) have shown, in the two-phase one-dimensional reservoir where water is injected at one end and oil is produced at the other end, that absolute permeability can be estimated from the data up to the water-breakthrough time and that the prebreakthrough production data carry little information about the relative permeabilities. Figure 2 shows the transient pressure and fractional flow of water at the production wells located at (450 m, 550 m) and (1050 m, 550 m) calculated on the basis of the true (k, b_o, b_w). We note that, for the conditions of this example, the water-breakthrough time of this reservoir model occurs at about 6.4 years after the inception of water injection. In the following examples, two different time periods of the observed data will be chosen, one of 9.5 and the other of 6.4 years.

Table I Specification of Reservoir Model

Properties of Water and Oil

$a_w = 0.9$	$a_o = 1.0$
$b_w = 2.5$	$b_o = 2.0$
$S_{iw} = 0.1$	$S_{ro} = 0.2$
$\mu_w = 10^{-3}$ Pa · s	$\mu_o = 3 \times 10^{-3}$ Pa · s
$c_w = 1.94 \times 10^{-9}$ Pa^{-1}	$c_o = 0.97 \times 10^{-9}$ Pa^{-1}
Production Wells	
$q_w = 0.003\ f_w$ m^3/s	$q_o = 0.003\ (1 - f_w)$ m^3/s
Injection Wells	
$q_w = 0.001$ m^3/s	$q_o = 0$

Properties of Reservoir

$$c_f = 2.91 \times 10^{-9}\ \text{Pa}^{-1}$$

$$\phi = 0.2 - 0.05 \sin(2\pi x/x_L) \sin(\pi y/y_L)$$

$$x_L \times y_L \times h = 1500 \times 1000 \times 10\ \text{m}^3$$

$$p(x, y, 0) = 1.52 \times 10^7\ \text{Pa}$$

$$S_w(x, y, 0) = 0.1$$

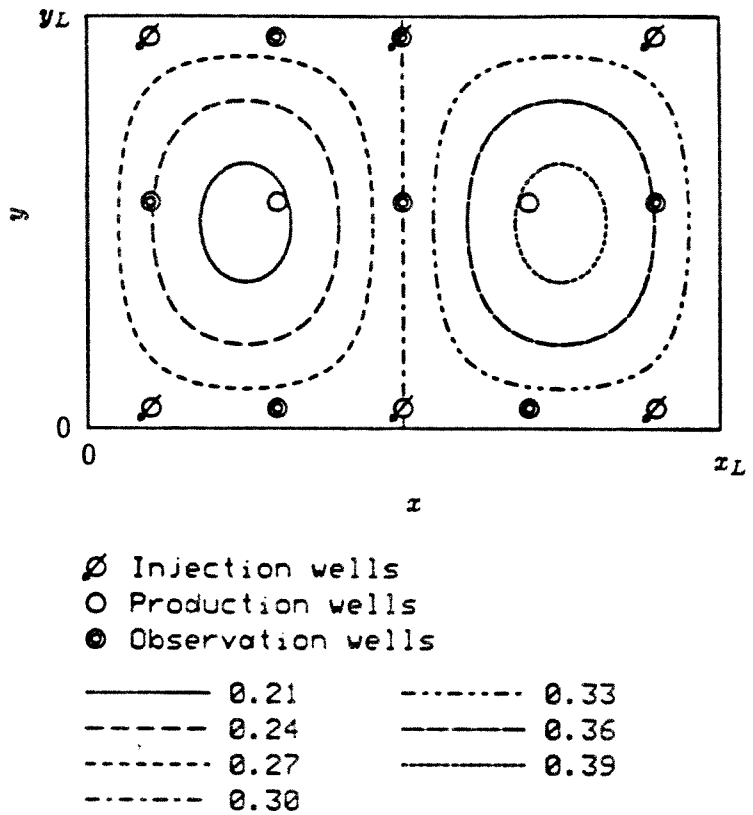

Figure 1 Contours of the assumed true absolute permeability profile and location of wells

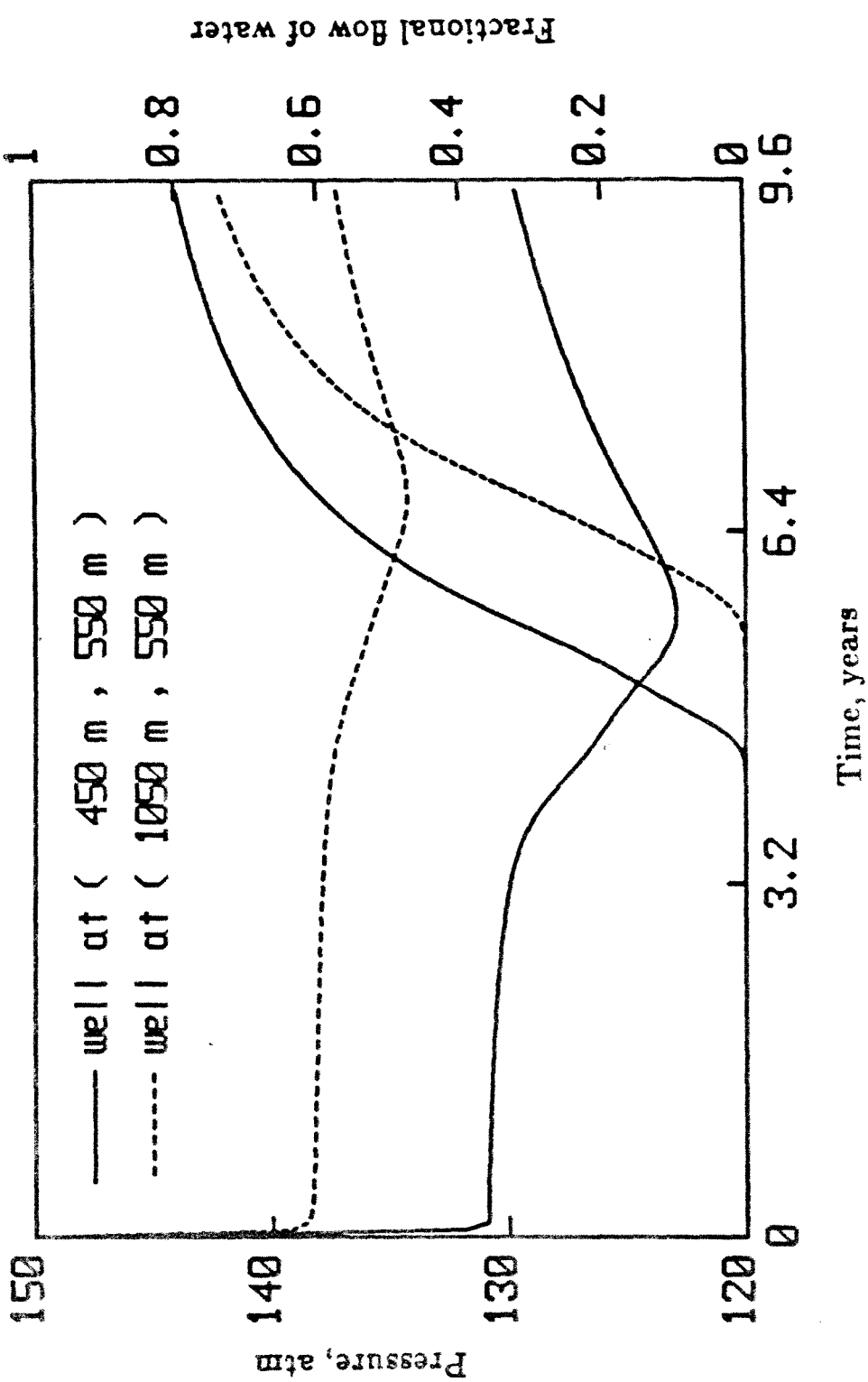

Figure 2 Transient pressure and fractional flow of water at the two production wells

The convergence criteria of the minimization are

$$\left|\frac{\partial J_{LS}}{\partial \bar{k}}\right| < 10 \quad \text{and} \quad ||\mathbf{g}_b||_\infty < 10 \tag{34}$$

for step 1 and

$$||\mathbf{g}_w||_\infty < 2 \quad \text{and} \quad ||\mathbf{g}_b||_\infty < 5 \tag{35}$$

for steps 2 and 3. Although the same conditions are used for steps 2 and 3, they are in effect more strict for step 3, due to the additional term βJ_{ST}. In case of step 3′, only the first criterion in Eq. (35) is used to terminate the iteration.

Over a period of 9.5 years, 150 pressure and 150 production data are taken at each of the 9 observation wells and $(\mathbf{W}, b_o, b_w)$ is estimated using the suggested 3-step algorithm. The results of the estimation are summarized in Table II. The first step is to estimate the set $(\bar{k}, b_o, b_w)$ that minimizes J_{LS}, where $\bar{k}$ denotes a spatially uniform k. Although the resultant $\bar{k}$ is not an acceptable estimate of a spatially varying k in most cases, it is a reasonable average of the spatially varying k. Two different sets of $(\bar{k}, b_o, b_w)$'s, (0.2 darcies, 1.5, 1.5) and (0.4 darcies, 3.0, 3.0) were chosen as the starting point of this step. The convergent results, (0.289 darcies, 2.09, 2.51) and (0.286 darcies, 2.06, 2.48), show good agreement indicating the robustness of this step. In Figure 3, $\bar{k}k_{rw}(S_w)$, $\bar{k}k_{ro}(S_w)$, and $f_w(S_w)$ calculated from these values are depicted by the solid lines. This step makes the remainder of the algorithm to be insensitive to the choice of the initial guess $(\bar{k}, b_o, b_w)$. The next step is the pure least-squares estimation of (k, b_o, b_w) with $\beta = 0$, where k is represented by the set of spline coefficients $\mathbf{W}$. In this step, σ_p and σ_f decrease substantially and approach those calculated from the true (k, b_o, b_w). The estimated k is shown in Figure 4 and $(b_o, b_w) = (1.98, 2.50)$. From the resultant $W_p\sigma_p^2$ and J_{ST}, $\beta = 2.63$ darcies^{-2}. Step 3 is the final regularized estimation of (k, b_o, b_w) with β determined from step 2. The resultant k is shown in Figure 4 and $(b_o, b_w) = (1.98, 2.50)$. Table II shows that, in step 3, J_{ST} is reduced significantly due to its inclusion, J_{LS} is reduced slightly due to continued minimization, and J_{SM} is increased

Table II Performance of estimation of (k, b_o, b_w) from 9×150 data

	$\bar{k}$	b_o	b_w	β	σ_p	σ_f	J_{LS}	J_{ST}	J_{SM}	CPU time[a]	Number of[b]
	darcies			darcies^{-2}	atm			darcies^2		s	Iterations
Initial Guess (a)	0.2	1.5	1.5		2.98	0.0896	181				
Step 1 (from a)	0.289	2.09	2.51		2.20	0.0378	59.3			71	19
Initial Guess (b)	0.4	3.0	3.0		2.51	0.0621	104				
Step 1 (from b)	0.286	2.06	2.48		2.20	0.0380	59.6			116	30
Step 2		1.98	2.50	0.0	0.37	0.0095	2.34	0.430	2.34	127	31
Step 3		1.98	2.50	2.63	0.36	0.0089	2.14	0.274	2.87	54	13
Step 3′		1.98	2.50	2.63	0.36	0.0086	2.04	0.239	2.67	65	16
True values		2.0	2.5		0.34	0.0087	2	0.144			

(*a*) On Cray X-MP/48

(*b*) Number of solving state and adjoint PDE's

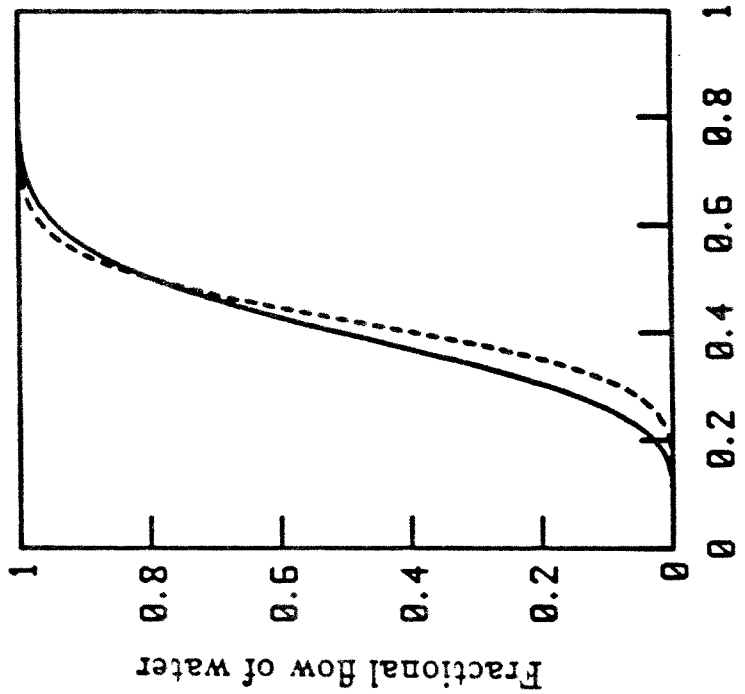

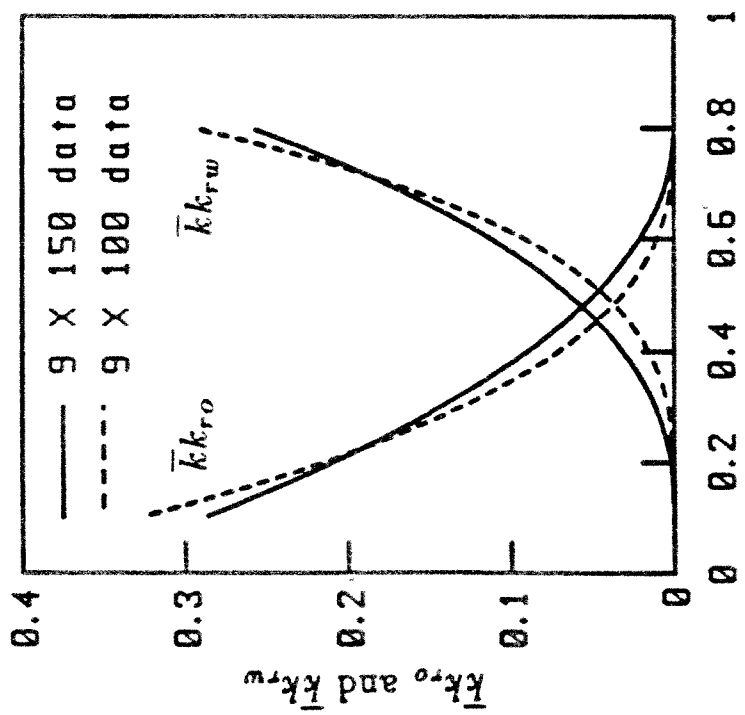

Figure 3 $\bar{k}k_{rw}$, $\bar{k}k_{ro}$, and f_w versus S_w calculated from the resultant $(\bar{k}, b_o, b_w)$'s of Step 1

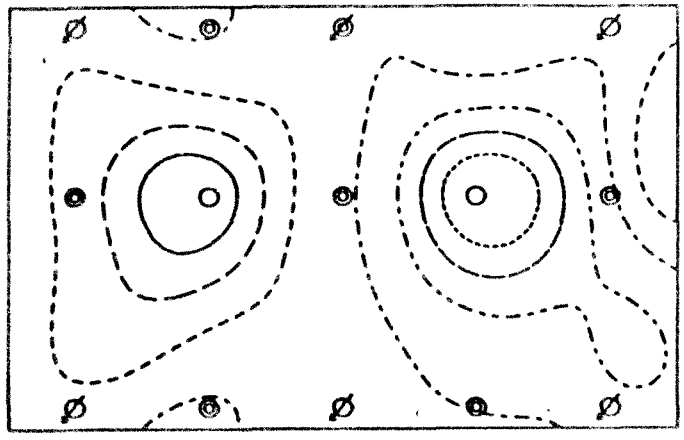

$\beta = 0$ (Step 2)

Ø Injection wells
O Production wells
◎ Observation wells

0.21
0.24
0.27
0.30
0.33
0.36
0.39

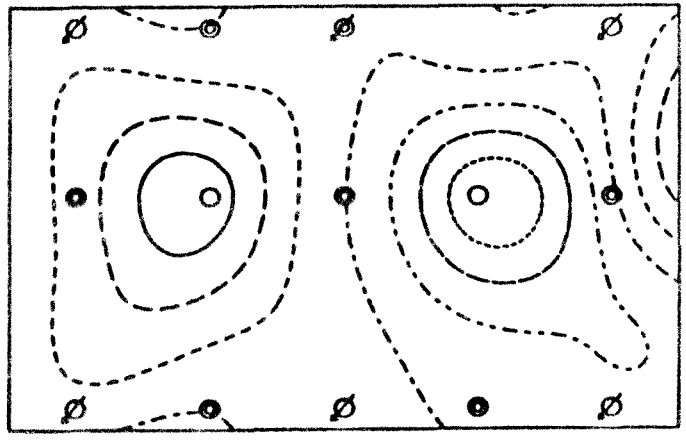

$\beta = 2.63$ darcies^{-2} (Step 3)

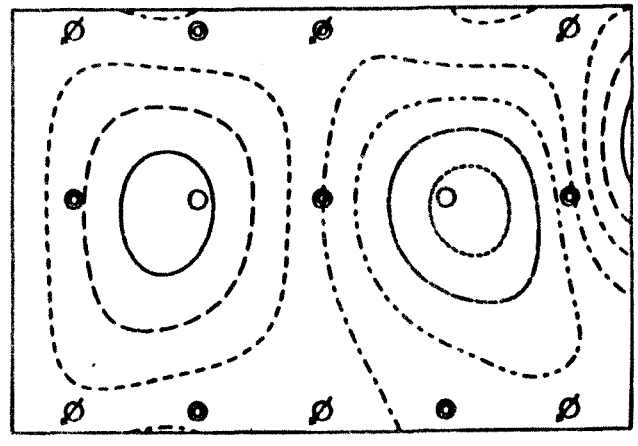

$\beta = 2.63$ darcies^{-2} (Step 3′)

Figure 4 Estimated k surfaces from 150 data points at each well

compared to the values in step 2. Comparison of the k contours in Figure 4 shows the smoothing effect of regularization on the "hump" near the lower right corner of the reservoir. As an alternative of step 3, step 3′ is the regularized estimation of $\mathbf{W}$, while b_o and b_w are fixed to the values determined by step 2 and the same β is used as step 3. The contours of the resultant k are shown in Figure 4, which shows more smoothing effect compared to that of step 3. Both the discrepancy and the stabilizing functional terms are smaller than those of step 3, while step 3′ required more computing time as shown in Table II. Throughout the estimation process, (b_o, b_w) is estimated accurately even in step 1. The entire algorithms, steps 1, 2, and 3, required 63 and 74 iterations (solutions of state and adjoint PDE'S), corresponding to 252 and 297 seconds of computing time and steps 1, 2, and 3′, 66 and 77 iterations corresponding to 263 and 308 seconds (4.0 seconds per iteration) on a Cray X-MP/48 for the given initial guesses (0.2 darcies, 1.5, 1.5) and (0.4 darcies, 3.0 3.0), respectively.

The identifiability condition of relative permeabilities given by Watson et al. (1984) is not directly applicable to the two-dimensional reservoir with multiple injection and multiple production wells considered in this study. To investigate the effect of the observation time period we consider the case in which 100 pressure and 100 production data are taken over a period of 6.4 years. Both of the production wells begin to produce water as well as oil, but flow data after water-breakthrough are not available from the well located at (450 m, 550 m) by the time period of 6.4 years for the given reservoir. As is shown in Table III, this example shows the same tendency as the previous example in terms of the insensitivity of the result of step 1 to the choice of initial guess and the slight improvement of data match in steps 3 and 3′ as compared to step 2. Step 1 is started with (0.2 darcies, 1.5, 1.5) and (0.4 darcies, 3.0, 3.0) and converges to (0.329 darcies, 2.75, 3.49) and (0.328 darcies, 2.74, 3.40), respectively. The resultant $\bar{k}$ (0.328 – 0.329 darcies) is a

Table III Performance of estimation of (k, b_o, b_w) from 9×100 data

	$\bar{k}$	b_o	b_w	β	σ_p	σ_f	J_{LS}	J_{ST}	J_{SM}	CPU time[a]	Number of[b]
	darcies			darcies^{-2}	atm			darcies^2		s	Iterations
Initial Guess (a)	0.2	1.5	1.5		3.20	0.0963	209				
Step 1 (from a)	0.329	2.75	3.49		2.15	0.0502	72.2			50	19
Initial Guess (b)	0.4	3.0	3.0		2.47	0.0555	91.9				
Step 1 (from b)	0.328	2.74	3.40		2.12	0.0481	68.4			61	22
Step 2		1.99	2.53	0.0	0.43	0.0091	2.64	0.464	2.64	114	40
Step 3		1.99	2.51	3.30	0.36	0.0087	2.11	0.222	2.84	115	42
Step 3′		1.98	2.53	3.30	0.38	0.0088	2.22	0.253	3.06	31	11
True values		2.0	2.5		0.34	0.0087	2	0.144			

(*a*) On Cray X-MP/48

(*b*) Number of solving state and adjoint PDE's

reasonable average of spatially varying k given in Eq. (33), although it is 0.4 darcies higher than that estimated in the previous case. In contrast to the previous case, however, the values of (b_o, b_w) are far from the true ones. Nevertheless, as shown in Figure 3 by the dashed line, $\bar{k}k_{rw}(S_w)$, $\bar{k}k_{ro}(S_w)$, and $f_w(S_w)$ do not disagree substantially from those values calculated in the previous case. Step 2 is started with (0.329 darcies, 2.75, 3.49) and $\beta = 0$. The resultant k surface is shown in Figure 5 and (b_o, b_w) is (1.99, 2.53), where (b_o, b_w) shows good agreement with the true one. Comparison of (b_o, b_w) in steps 1 and 2 shows that the flow data up to the water-breakthrough can be fitted by the wide range of different values of (b_o, b_w), and in this case the estimation of (b_o, b_w) should be carried out based on the k that matches the observed data accurately. The value of β estimated by the algorithm is 3.30 darcies^{-2}. The final (b_o, b_w) is (1.99, 2.51) for step 3, and the estimated k's for steps 3 and 3′ are shown in Figure 5. The discrepancy and the stabilizing functional terms of step 3 are smaller than those of step 3′ (See Table III.), but Figure 5 shows about the same degree of smoothing effect for the two different regularization steps. The algorithm required 101 and 104 iterations corresponding 279 and 290 seconds of computing time (2.8 seconds per iteration) for step 3 and 70 and 73 iterations corresponding to 195 and 206 seconds for step 3′ for the given initial guesses (0.2 darcies, 1.5, 1.5) and (0.4 darcies, 3.0 3.0), respectively.

6. Conclusions

Two numerical algorithms are developed to estimate the spatially varying absolute permeability, k, and the exponents in the relative permeability expressions for two-phase petroleum reservoirs, based on noisy pressure and flow data. The spatially varying absolute permeability is estimated by regularization with bicubic spline approximation. The algorithms developed suggest the choice of the regularization parameter based on the ratio of the level of the observation error in pressure data to

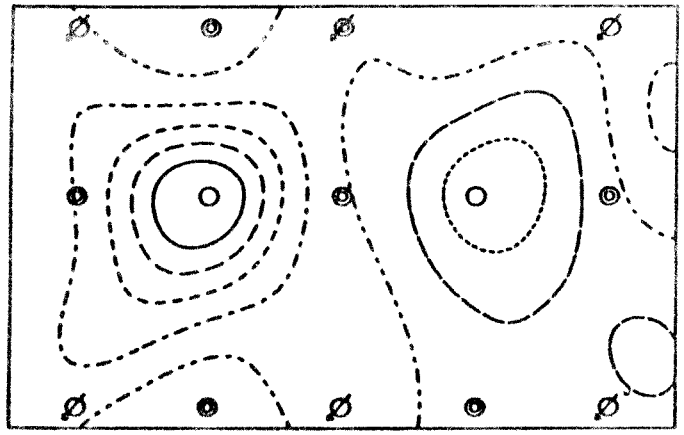

$\beta = 0$ (Step 2)

Ø Injection wells
O Production wells
◎ Observation wells

0.21
0.24
0.27
0.30
0.33
0.36
0.39

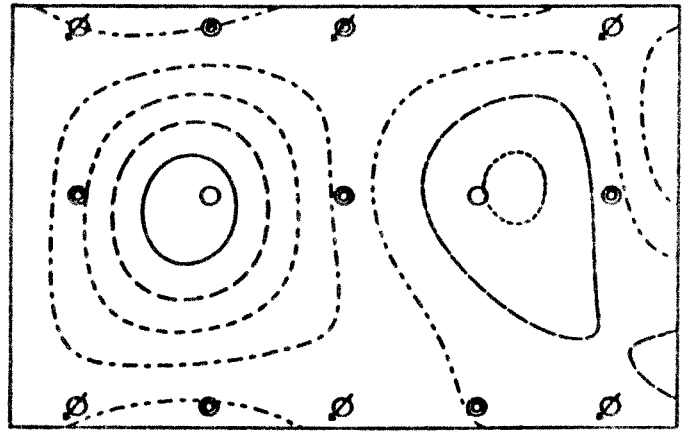

$\beta = 3.30$ darcies^{-2} (Step 3)

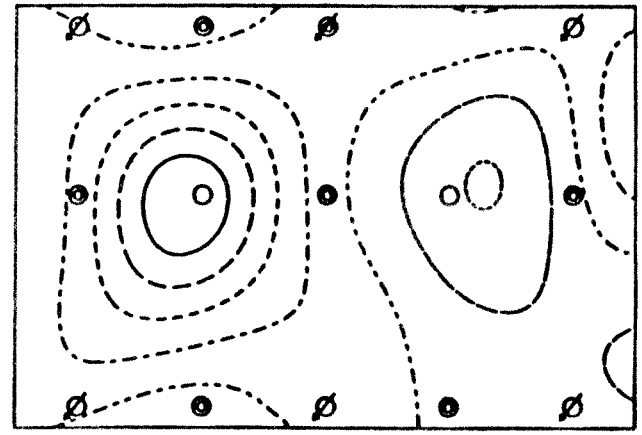

$\beta = 3.30$ darcies^{-2} (Step 3′)

Figure 5 Estimated k surfaces from 100 data points at each well

the measure of non-smoothness of parameter. The regularized estimation alleviates the ill-conditioning that resulted from the conventional least-squares estimation. We demonstrate conditions under which the absolute and relative permeabilities can be estimated simultaneously.

References

Aziz, K. and A. Settari, *Petroleum Reservoir Simulation* (Applied Science, London, 1983) pp. 204 – 243.

Banks, H. T. and P. D. Lamm, Estimation of Variable Coefficients in Parabolic Distributed Systems, *IEEE Trans. Automat. Control,* **AC-30,** 386 – 398 (1985).

Carrera, J. and S. P. Neuman, Estimation of Aquifer Parameters Under Transient and Steady-State Conditions: 2 Uniqueness, Stability and Solution Algorithms, *Water Resour. Res.,* **22,** 211 – 227 (1986).

Carter, R. D., L. F. Kemp Jr., A. C. Pierce, and D. L. Williams, Performance Matching with Constraints, *Soc. Pet. Eng. J.,* **14,** 187 – 196 (1974).

Chavent, G., About the Stability of the Optimal Control Solution of Inverse Problems, in *Inverse and Improperly Posed Problems in Differential Equations,* ed. G. Anger, *Proceedings of the Conference on Mathematical and Numerical Method, May 29 – June 2, Halle/Salle, GDR* (Akademie-Verlag, Berlin, 1979a) pp. 45 – 78.

Chavent, G., Identification of Distributed Parameter Systems: About the Output Least Squares Method, Its Implementation and Identifiability in *Identification and System Parameter Estimation* ed. R. Isermann, *Proceedings of the Fifth IFAC Symposium, September 24 – 28, Darmstadt, FRG* (Pergamon Press, New York, 1979b) pp. 85 – 97.

Chavent, G., M. Dupuy, and P. Lemonnier, History Matching by Use of Optimal Theory, *Soc. Pet. Eng. J.,* **15,** 74 – 86 (1975).

Chen, W. H., G. R. Gavalas, J. H. Seinfeld, and M. L. Wasserman, A New Algorithm for Automatic History Matching, *Soc. Pet. Eng. J.,* **14,** 593 – 608 (1974).

Chen, W. H. and J. H. Seinfeld, Estimation of the Location of the Boundary of a Petroleum Reservoir, *Soc. Pet. Eng. J.,* **15,** 19 – 38 (1975).

Collins, R. E., *Flow of Fluids through Porous Materials* (Reinhold, London, 1961) pp. 53 – 55.

Craven, P. and G. Wahba, Smoothing Noisy Data with Spline Functions, *Numer. Math.*, **31**, 377 – 403 (1979).

Gavalas, G. R., P. C. Shah, and J. H. Seinfeld, Reservoir History Matching by Bayesian Estimation, *Soc. Pet. Eng. J.*, **16**, 337 – 350 (1976).

Jacquard, P. and C. Jain, Permeability Distribution from Field Pressure Data, *Soc. Pet. Eng. J.*, **5**, 281 – 294 (1965).

Kravaris, C. and J. H. Seinfeld, Identification of Parameters in Distributed Parameter Systems by Regularization, *SIAM J. Control Optim.*, **23**, 217 – 241 (1985).

Kravaris, C. and J. H. Seinfeld, Identification of Spatially Varying Parameters in Distributed Parameter Systems by Discrete Regularization, *J. Math. Anal. Appl.*, **119**, 128 – 152 (1986).

Lee, T., C. Kravaris, and J. H. Seinfeld, History Matching by Spline Approximation and Regularization in Single-Phase Areal Reservoirs, *SPE Reservoir Engineering*, **1**, 521 – 534 (1986).

Lee, T. and J. H. Seinfeld, Estimation of Properties of Two-Phase Petroleum Reservoirs by Regularization, *J. Comp. Phys.*, in press (1986).

Locker, J. and P. M. Prenter, Regularization with Differential Operator. I. General Theory, *J. of Math. Anal. Appl.*, **74**, 504 – 529 (1980).

Miller, K., Least-Squares Method for Ill-Posed Problems with a Prescribed Bound, *SIAM J. Math. Anal. Appl.*, **1**, 52 – 74 (1970).

Nazareth, L., A Conjugate Gradient Algorithm Without Line Searches, *J. Opt. Theory. Appl.*, **23**, 373 – 387 (1977).

Neuman, S. P. and S. Yakowitz, A statistical Approach to the Inverse Problem of Aquifer Hydrology. 1 Theory, *Water Resour. Res.*, **15**, 845 – 860 (1979).

Neuman, S. P., Calibration of Distributed Parameter Groundwater Flow Models Viewed as a Multiple-Objective Decision Process Under Uncertainty, *Water Resour. Res.*, **9**, 1006 – 1021 (1973).

Neuman, S. P. and J. Carrera, Maximum-Likelihood Adjoint-State Finite-Element Estimation of Groundwater Parameter under Steady- and Nonsteady-State Conditions, *Appl. Math. Comput.*, **17**, 405 – 432 (1985).

Neuman, S. P. and G. de Marsily, Identifiability of Linear Systems Response by Parametric Programming, *Water Resour. Res.*, **12**, 253 – 262 (1976).

Seinfeld, J. H. and W. H. Chen, Identification of Petroleum Reservoir Properties ets W. H. Ray and D. G. Lainiotis *Distributed Parameter System: Identification, Estimation and Control* (Marcel Dekker, New York, 1978) pp. 497 – 554.

Seinfeld, J. H. and C. Kravaris, Distributed Parameter Identification in Geophysics — Petroleum Reservoirs and Aquifers *Distributed Parameter Control Systems* ed S. G. Tzafestas. *International Series on Systems and Control* **6** *University of Patras, Greece* (Pergamon Press, New York, 1982) pp 357 – 390.

Shah, P. C., G. R. Gavalas, and J. H. Seinfeld, Error Analysis in History Matching: Optimum Level of Parametrization, *Soc. Pet. Eng. J.*, **18**, 219 – 228 (1978).

Sun, N. Z. and W. W.-G. Yeh, Identification of Parameter Structure in Groundwater Inverse Problem, *Water Resour. Res.*, **21**, 869 – 883 (1985).

Tang, Y. N. and Y. M. Chen, Application of GPST Algorithm to History Matching of Single-Phase Simulator Models, *Inst. Math. Appl. Conf. Ser. Lehigh*, (Oxford, New York, 1984)

Tikhonov, A. N., Regularization of Incorrectly Posed Problems, *Soviet Math. Dokl.*, **4**, 1624 – 1627 (1963).

Tikhonov, A. N. and V. Y. Arsenin, *Solutions of Ill-Posed Problems* (Winston, Washington D. C., 1977)

Trummer, M. R., A Method for Solving Ill-Posed Linear Operator Equations, *SIAM*

J. Numer. Anal., **21**, 729 – 737 (1984).

Van den Bosch, B. and J. H. Seinfeld, History Matching in Two-Phase Petroleum Reservoirs: Incompressible Flow, *Soc. Pet. Eng. J.*, **17**, 398 – 406 (1977).

Wasserman, M. L., A. S. Emanuel, and J. H. Seinfeld, Practical Application of Optimal-Control Theory to History-Matching Multiphase Simulator Models, *Soc. Pet. Eng. J.*, **15**, 347 – 355 (1975).

Watson, A. T., G. R. Gavalas, and J. H. Seinfeld, Identifiability of Estimates of Two-Phase Reservoir Properties in History Matching, *Soc. Pet. Eng. J.*, **24**, 697 – 706 (1984).

Watson, A. T., J. H. Seinfeld, G. R. Gavalas, and P. T. Woo, History Matching in Two-Phase Petroleum Reservoirs, *Soc. Pet. Eng. J.*, **20**, 521 – 532 (1980).

Yakowitz, S. and L. Duckstein, Instability in Aquifer Identification: Theory and Case Studies, *Water Resour. Res.*, **16**, 1045 – 1064 (1980).

Yeh, W. W.-G., Review of Parameter Identification Procedures in Groundwater Hydrology: The Inverse Problem, *Water Resour. Res.*, **22**, 95 – 108 (1986).

Yeh, W. W.-G. and Y. S. Yoon, Aquifer Parameter Identification with Optimum Dimensions in Parametrization, *Water Resour. Res.*, **17**, 664 – 672 (1981).

Yeh, W. W.-G., Y. S. Yoon, and K. S. Lee, Aquifer Parameter Identification with Kriging and Optimum Parametrization, *Water Resour. Res.*, **19** 225 – 233 (1983).

Yoon, Y. S. and W. W.-G. Yeh, Parameter Identification in an Inhomogeneous Medium with the Finite Element Method, *Soc. Pet. Eng. J.*, **16**, 217 – 226 (1976).

Chapter V

Conclusion

In this dissertation, automatic history-matching algorithms are developed to estimate the petroleum reservoir properties from the noisy measured data by regularization and spline approximation. Since no rigorous mathematical guide is available in formulating the estimation problem as a regularized problem, extensive numerical tests were carried out and the algorithms are developed based on the numerical tests. In Chapter II, absolute permeability and porosity are estimated in single-phase reservoirs, and it was demonstrated that the use of a uniform value of parameter that gives the best fit of observed data serves as a good starting point of spatially varying parameter estimation. The choice of the regularization parameter was restricted by the inclusion of the Euclidean norm in the stabilizing functional and the restriction leads to the use of a rather coarse spline grid system. In Chapters III and IV, 3-step history matching algorithms are developed to estimate the absolute permeability (Chapter III) and absolute and relative permeabilities simultaneously (Chapter IV) in two-phase reservoirs. The non-smoothness of the parameter estimate is better measured as a Sobolev norm of gradient of the parameter in the absence of the Euclidean norm of parameter itself. The number of spline coefficients was chosen as much as the number of PDE meshes to represent the spatial details of parameters. The regularization parameter determined from the pressure discrepancy and stabilizing functional with gradient operator always provided a reasonable regularization effect, so that the algorithm gave physically meaning estimates. For the simultaneous estimation of parameters in Chapter IV, a minimization technique is suggested that calculates the parametric sensitivity of smoothing functional along the given descent direction.

In Chapter IV, the regularization parameter for the estimation of absolute permeability is determined from the ratio of the pressure discrepancy to the non-

smoothness of an absolute permeability estimate. This idea can be applied to the estimation of porosity by determining the regularization parameter from the ratio of the flow data discrepancy to the non-smoothness of porosity estimates and can be extended to the simultaneous estimation of absolute permeability and porosity by combining two stabilizing functionals in the smoothing functional. Since the form of the stabilizing functional and the degree of spline approximation do not have any relation with specific properties of absolute permeability, they can be directly used to the estimation of porosity. If the idea of a rough parametric sensitivity analysis is applied to the general class of multivariate minimization algorithms such as conjugate gradient and variable metric algorithms, the rate of convergence of minimization can be accelerated.

Appendix A

Estimation of Absolute Permeability with Stiff Spatial Variation

1. Description of Example

In Chapter III, a history matching algorithm has been developed to estimate the spatially varying absolute permeability, k, of two-phase two-dimensional petroleum reservoirs. The algorithm was tested for the reservoirs with known absolute permeability distributions, that can be represented by combinations of polynomials and elementary transcendental functions. The distributions were fitted by spline approximation. In this section we will try to estimate an absolute permeability distribution that varies more stiffly. The reservoir domain is divided into a 10×10 mesh, and 100 values of the absolute permeability k are given on the mesh. (See Figure 1.) This example was suggested by the Chevron Oil Field Research Company with the reservoir specification shown in Table I and the locations of wells depicted in Figure 2. The minimum and maximum values of k are 0.5 and 5.5 darcies, where with a maximum difference of two consecutive mesh values of 3.0 darcies. The spline approximation of the distribution is calculated on a 10×10 spline grid and the contour map of that approximation is shown in Figure 2. The root-mean-square error of the spline fit on the mesh is 0.31 darcies. In this example, the oil recovery policy is different from the previous ones in Chapter III; in that the oil production rate of each production well is specified and kept constant, and as a result, the water production rate ($q_w = [f_w/(1 - f_w)]q_o$), and thus the total production rate of the well, increases after the water-breakthrough time so that the overall pressure inside the reservoir decreases. In Chapter III, the total production rate of each well was kept constant.

In this study we will consider the effects of a number of observation points

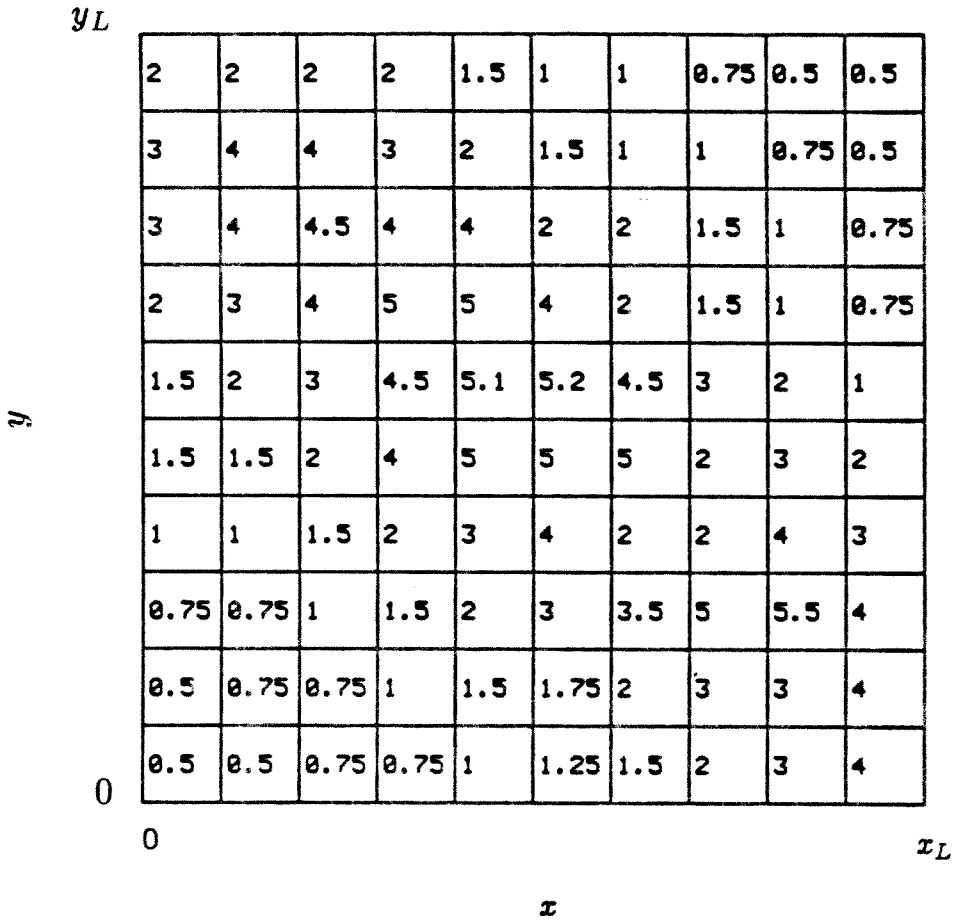

2	2	2	2	1.5	1	1	0.75	0.5	0.5
3	4	4	3	2	1.5	1	1	0.75	0.5
3	4	4.5	4	4	2	2	1.5	1	0.75
2	3	4	5	5	4	2	1.5	1	0.75
1.5	2	3	4.5	5.1	5.2	4.5	3	2	1
1.5	1.5	2	4	5	5	5	2	3	2
1	1	1.5	2	3	4	2	2	4	3
0.75	0.75	1	1.5	2	3	3.5	5	5.5	4
0.5	0.75	0.75	1	1.5	1.75	2	3	3	4
0.5	0.5	0.75	0.75	1	1.25	1.5	2	3	4

Figure 1 Original absolute permeability distribution in darcies given on 10×10 mesh

Table I Specification of Reservoir Model

Properties of Water and Oil

$a_w = 1.0$	$a_o = 1.0$
$b_w = 2.0$	$b_o = 2.0$
$= 0.0$	$= 0.0$
$\mu_w = 10^{-3}$ Pa · s	$\mu_o = 0.5 \times 10^{-3}$ Pa · s
$c_w = 1.45 \times 10^{-9}$ Pa^{-1}	$c_o = 0.15 \times 10^{-9}$ Pa^{-1}
Production Wells	
$q_w = 0.00184\ f_w/(1 - f_w)$ m^3/s	$q_o = 0.00184$ m^3/s
Injection Wells	
$q_w = 0.00276$ m^3/s	$q_o = 0$

Properties of Reservoir

$c_f = 0$
$\phi = 0.2$
$x_L \times y_L \times h = 1220 \times 1220 \times 6.2$ m^3
$p(x, y, 0) = 2,07 \times 10^7$ Pa
$S_w(x, y, 0) = 0.2$

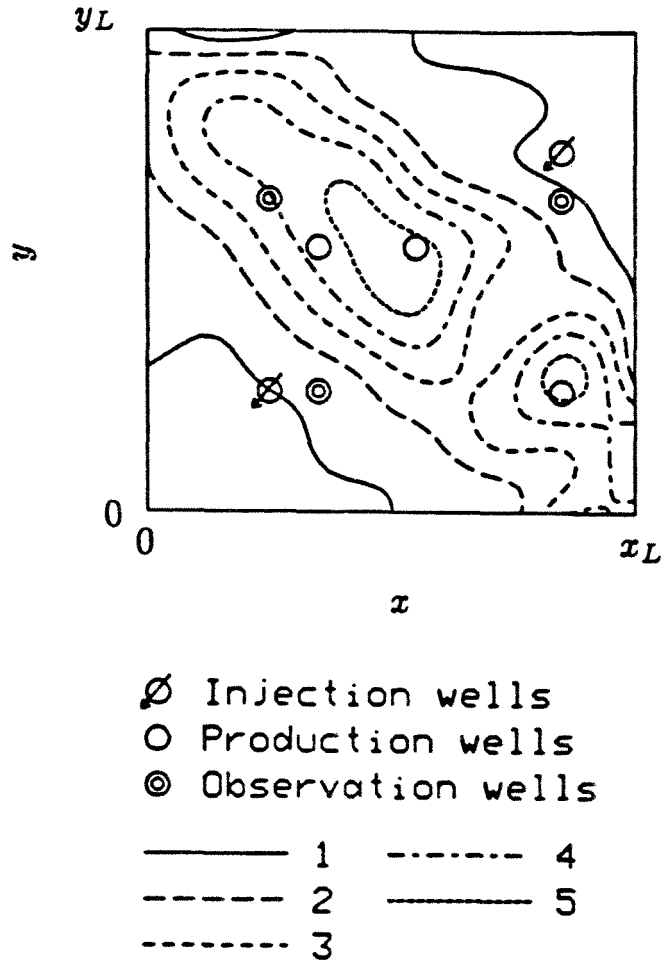

Figure 2 Location of wells and contours of the spline approximated absolute permeability in darcies by 10×10 spline grid

and the noise in observation as well as the effect of regularization on the ability to estimate the absolute permeability k. Three production wells will be used as the observation points for the estimation and three pure observation points will be added to test the effect of number of observation wells. The regularization parameter is chosen by the algorithm suggested in Chapter III.

2. Computational Results

Seventeen pressure data and 17 flow data points are measured at each of 6 or 3 observation wells over a time period of 170 days with a time interval of 10 days, giving a total of 102 (6 wells) or 51 (3 wells) each of pressure and flow data for the estimation. In the case of noisy observation data, the root-mean-square error of pressure data (σ_p) is 0.029 atm, and the of the error of water-to-oil ratio data (σ_F) is 0.007. The value of J_{LS} calculated from these data is 2.01. Throughout, to test the robustness of the algorithm the 3-step history-matching algorithm was started with two different initial guesses of uniform absolute permeabilities, $\overline{k}$, 5 and 1 darcies. The following 4 cases are considered:

Case 1 Noisy data from 6 wells.

Case 2 Noiseless data from 6 wells.

Case 3 Noisy data from 3 wells.

Case 4 Noiseless data from 3 wells.

In Case 1, the absolute permeability was estimated from the noisy 102 pressure and 102 flow data measured at the 6 observation points that include 3 production wells and 3 pure observation wells. For the given initial guesses of $\overline{k} = 5$ and 1 darcies, $J_{LS} = 97.7$ and 540, respectively, and Step 1 converged to $\overline{k} = 2.42 - 2.43$ darcies with $J_{LS} = 32.0$. (See Table II.) In the next step k is estimated with $\beta = 0$. The resultant k is shown in Figure 3a with a corresponding value of $J_{LS} = 1.78$. Figure 3a shows that the estimated k contour map agrees reasonably with the map

Table II Performance of absolute permeability estimation with noisy data from 6 wells

	$\overline{k}$ darcies	β darcies^{-2}	σ_p atm	σ_F	J_{LS}	J_{ST}	J_{SM}	CPU time[a] s
Initial guess (a)	5		0.248	0.034	97.7			
Step 1 (from a)	2.42		0.086	0.034	32.0			4.9
Initial guess (b)	1		0.651	0.034	540.0			
Step 1 (from b)	2.43		0.086	0.034	32.0			5.2
Step 2		0	0.027	0.007	1.78	565	1.78	48.7
Step 3		0.0016	0.028	0.007	1.82	241	2.11	37.1
True k			0.029	0.007	2.01	2309		

(*a*) On Cray X-MP/48

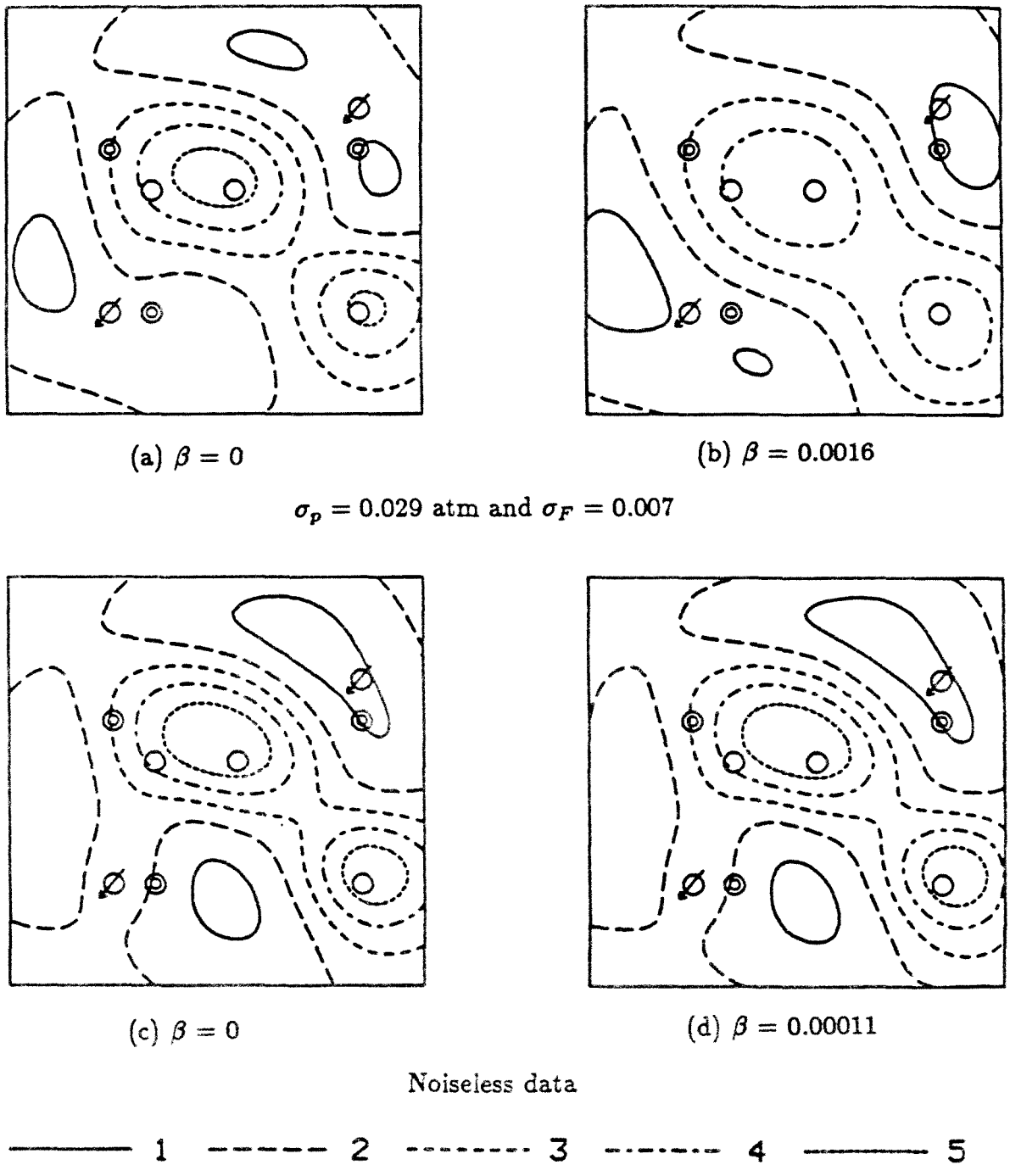

Figure 3 Contours of the estimated absolute permeabilities in darcies from the data observed at 6 points

in Figure 2 in the middle of the reservoir, where the observation wells are located. β is determined from the ratio of the pressure discrepancy term ($W_p\sigma_p^2$) to J_{ST}, that is, 0.0016 darcies^{-2}. The regularized estimation of k is shown in Figure 3b, where the contour of 5 darcies is lost as a result of the smoothing effect of regularization. Comparison of Figures 3a and 3b shows that there exist regions around the contours of 1 and 2 darcies where the estimates are neither correct nor show a consistent effect of regularization with the regions of contours 3, 4, and 5. The algorithm required 90.7 – 91 seconds of computing time on a Cray X-MP/48.

Case 2 is the same as Case 1 except that the measured data do not include an observation error. Table III shows that the results of Steps 1 and 2 do not differ significantly from the previous case except for the values of the discrepancy terms that represent the effect of random error in the data used in Case 1. From the results of Step 2, β is chosen as 0.00011 darcies^{-2}, that is, 7 % of the value of β of Case 1. Step 3 finished immediately since the term βJ_{ST} is negligible compared to J_{LS}; consequently Figure 3d does not show a significant change compared to Figure 3c. In Step 3 J_{ST} increased by 2 % (corresponding to 1 % of J_{SM}) after regularization, but the estimated k satisfied the given tolerable limit,

$$|\partial J_{SM}/\partial W_{l_x,l_y}| \leq 0 \qquad \text{for all } l_x = 1,\ldots,N_{xs} \text{ and } l_y = 1,\ldots,N_{ys}. \quad (A.1)$$

The absolute permeabilities were not estimated correctly in the regions around the contours of 1 and 2 darcies in Figures 3c and 3d. Also the shapes of the contours of 1 and 2 darcies are different from those in Case 1. Comparison of four contour maps in Figure 3 shows that the estimates in these regions were not improved by the reduction of the noise level or by regularization, since the unidentifiability results from the lack of fluid flow in that region for the given configuration of injection and production wells. The total fluid velocity vectors on the mesh at the end of 170 days are depicted in Figure 4. This case required 53.2 – 53.4 seconds of CPU time, 37.5 seconds less than that of Case 1. The difference was attributed to regularization in

Table III Performance of absolute permeability estimation with noiseless data from 6 wells

	$\overline{k}$ darcies	β darcies^{-2}	σ_p atm	σ_F	J_{LS}	J_{ST}	J_{SM}	CPU time[a] s
Initial guess (a)	5		0.246	0.034	97.7			
Step 1 (from a)	2.42		0.082	0.034	30.7			4.9
Initial guess (b)	1		0.649	0.034	532.2			
Step 1 (from b)	2.42		0.082	0.034	30.7			5.1
Step 2		0	0.0089	0.00025	0.097	853	0.097	46.0
Step 3		0.00011	0.0089	0.00025	0.097	873	0.195	2.3

(*a*) On Cray X-MP/48

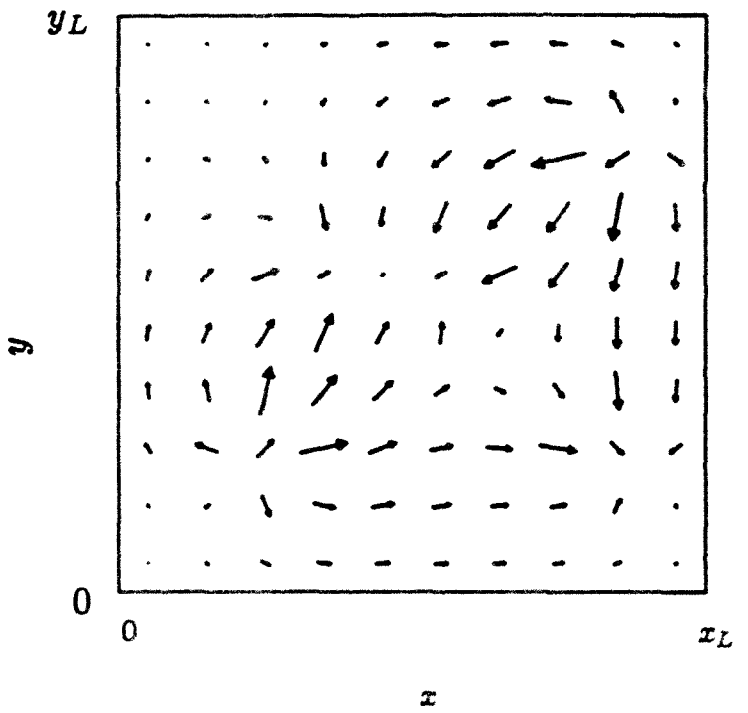

Figure 4 Total fluid velocity at 170 days (The length and the head of arrows indicate the magnitude and the direction of the velocity vectors, respectively.)

Table IV Performance of absolute permeability estimation with noisy data from 3 wells

	$\overline{k}$ darcies	β darcies^{-2}	σ_p atm	σ_F	J_{LS}	J_{ST}	J_{SM}	CPU time[a] s
Initial guess (a)	5		0.250	0.006	76.3			
Step 1 (from a)	2.64		0.034	0.006	2.2			5.5
Initial guess (b)	1		0.864	0.006	903.7			
Step 1 (from b)	2.64		0.034	0.006	2.2			5.5
Step 2		0	0.027	0.006	1.63	3.4	1.63	5.9
Step 3		0.26	0.029	0.006	1.73	0.33	1.81	13.6
True k			0.029	0.007	2.00	2309		

(*a*) On Cray X-MP/48

Case 1.

Now we consider the 17 pressure and flow data measured at the three production wells. This is Case 3. At the initial guesses of $\overline{k} = 5$ and 1 darcies, the discrepancy in pressure data (σ_p) shown in Table IV is about the same as that of the corresponding 6 observation point case. Step 1 converged to $\overline{k} = 2.64$ darcies and $J_{LS} = 2.2$. Although the uniform k estimated by Step 1 is far from the true k in its spatial detail, the adequate data match with the given observed data indicates the insufficiency of the observations. Estimation of spatially varying k in Step 2 converged to the k shown in Figure 5a that more resembles the uniform k estimated by Step 1 than it does the true k while the discrepancy terms are less than those calculated from the true k. β determined by Step 2 was 0.26 darcies^{-2} and the estimation was continued to Step 3, although the estimation in Step 2 was poor. Figure 5b shows the resulting k. As shown in Table IV, the resulting J_{ST} is only 10 % of the starting J_{ST}, and the reduction in J_{ST} indicates that the relative importance of the stabilizing functional term was emphasized by the algorithm. In this case, the discrepancy in flow data (σ_F) was kept constant at 0.006 indicating the insensitivity of flow data to variation of the absolute permeability. The computing time required for Case 3 was 25 seconds, that reflecting the fact that the observed data used in this case easy to match by the algorithm regardless of the accuracy of the estimation of k itself.

In Case 4, the same number of data and the same observation points are used as in Case 3, but the data are error free. Table V shows that the flow data mismatch was negligible during the estimation even for initial guesses of $\overline{k} = 5$ and 1 darcies. The results of Steps 1 and 2 in this case are the same as those in Case 3. Although it is possible that different k's will fit the observed data (the true k as an example), Step 2 in Cases 3 and 4 converged to the same but incorrect k, since the k shown in Figure 3a and 3c are close to the initial guess of k (= 2.63 darcies). β estimated

Table V Performance of absolute permeability estimation with noiseless data from 3 wells

	$\overline{k}$ darcies	β darcies^{-2}	σ_p atm	σ_F	J_{LS}	J_{ST}	J_{SM}	CPU time[a] s
Initial guess (a)	5		0.251	0.00004	76.1			
Step 1 (from a)	2.63		0.022	0.00004	0.6			5.6
Initial guess (b)	1		0.861	0.00004	897.3			
Step 1 (from b)	2.63		0.022	0.00004	0.6			5.5
Step 2		0	0.011	0.00004	0.142	2.1	0.142	4.6
Step 3		0.00011	0.012	0.00004	0.163	0.67	0.208	4.0

(*a*) On Cray X-MP/48

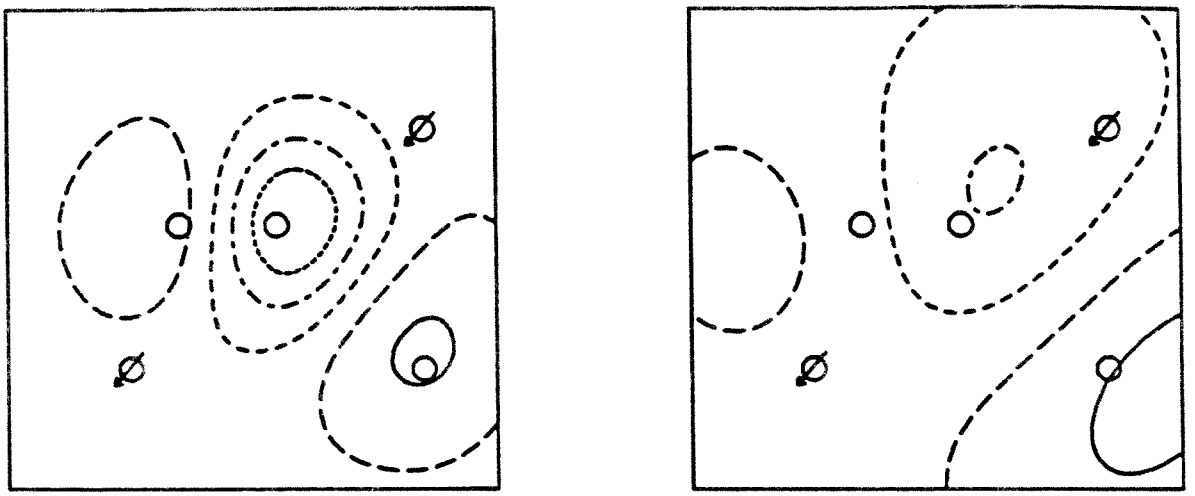

(a) $\beta = 0$ (b) $\beta = 0.26$

$\sigma_p = 0.029$ atm and $\sigma_F = 0.007$

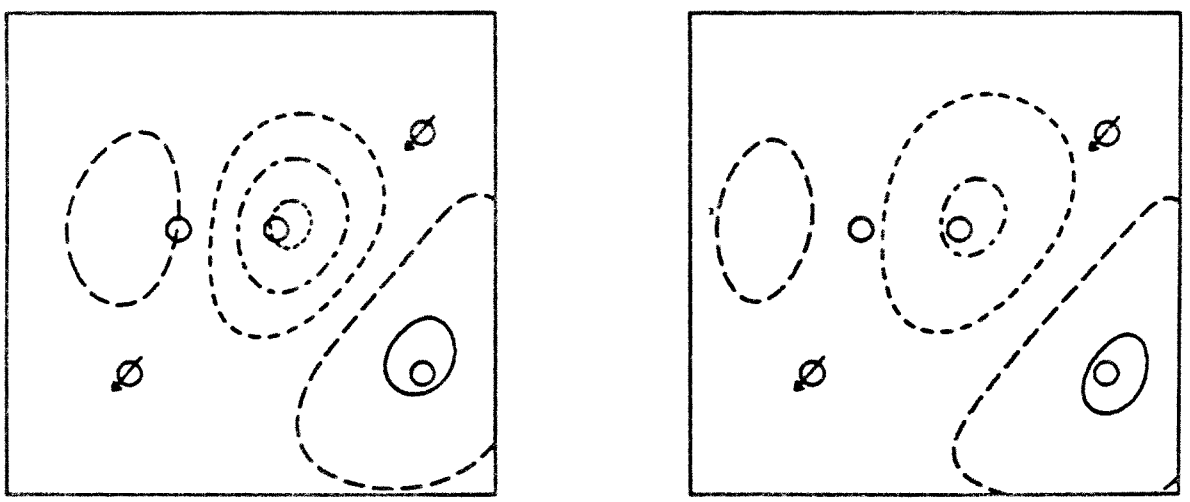

(c) $\beta = 0$ (d) $\beta = 0.067$

Noiseless data

2.5 2.6 2.7 2.8 2.9

Figure 5 Contours of the estimated absolute permeabilities in darcies from the data observed at 3 points

in this step was 0.011 darcies^{-2}, which is 42 % of β in Case 3. In comparison with the fact that β in Case 2 is only 7 % of that in Case 1, β in Step 4 determined by the algorithm is relatively large reflecting the relative importance of the stabilizing functional for estimation with insufficient data. As a result of regularization, the estimated k shown in Figure 5d is smoother than that in Figure 5c. This case required 14.5 – 14.6 seconds of computing time smaller than that for Case 3. The reduction is mainly due to less computing time for the regularization in Step 3.

The time period of observation in this study, 170 days, is relatively short compared to the total time period of oil recovery in this reservoir. Since the goal of reservoir parameter estimation is to be able to predict the future behavior of the reservoir, it is worthwhile to investigate how the estimated absolute permeabilities will enable prediction of future pressures. Figure 6 shows the true and predicted transient pressures at the production well located at (670 m, 670 m) up to 850 days, which are calculated from the true k and 8 different estimated k's. The 4 predicted transient pressures from Cases 1 and 2 are indistinguishable from each other with the same being true for the Cases 3 and 4. The errors in pressures prediction at 850 days after the observation started is 7 atm for the 6 observation point cases and 40 atm for the 3 observation cases

3. Conclusion

In this study, some new results are demonstrated, that we did not consider in Chapter 3. An example configuration of the observation points shows that, with the pressure histories observed at those points, we could not get a meaningful estimation of absolute permeability. The estimates were improved by using additional pressure histories. The effect of random observation error was investigated. With noiseless data, the regularization parameter β determined by the 3-step algorithm was small enough so that regularization does not change the parameter estimated

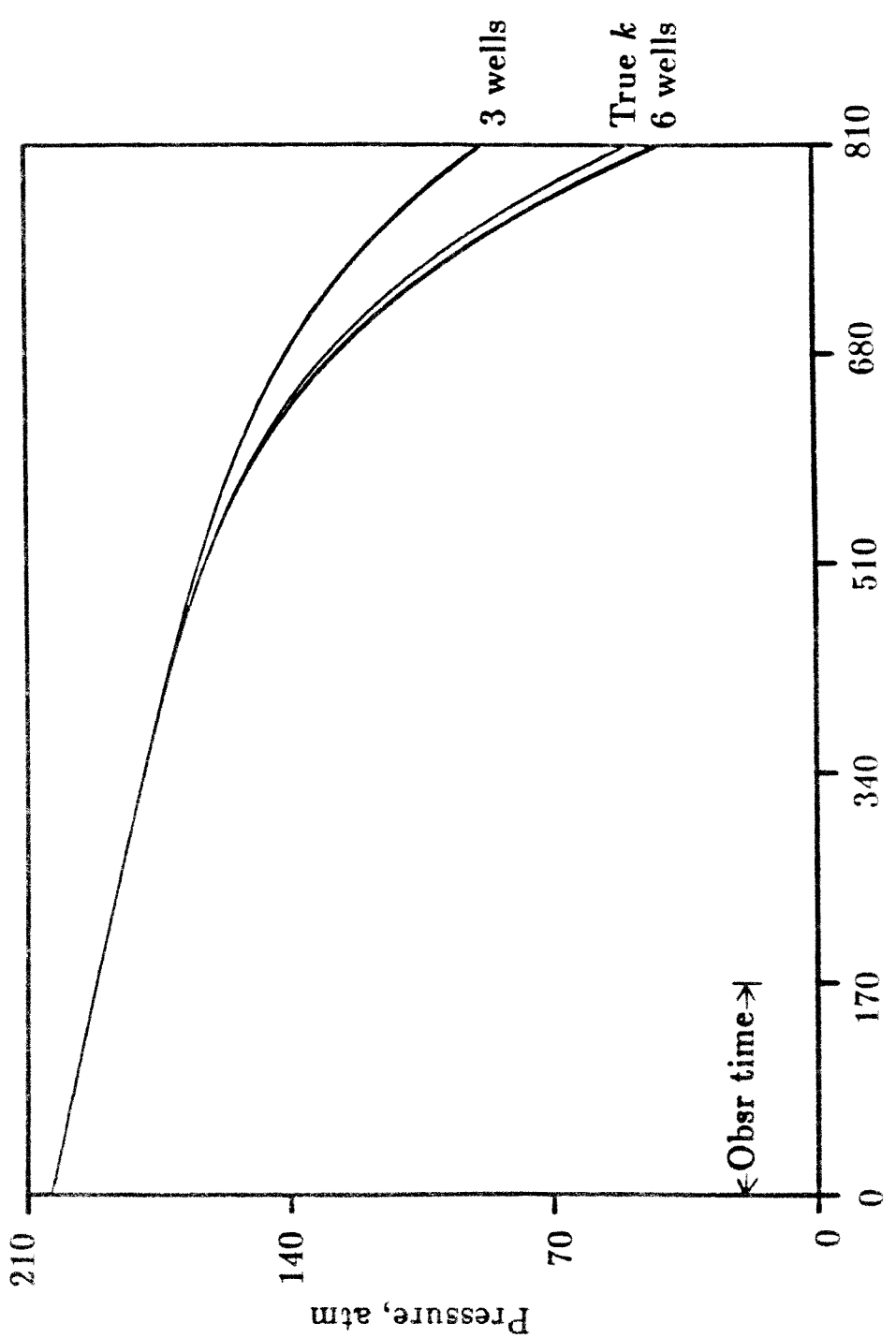

Figure 6 Pressures predicted from the true and the estimated absolute permeabilities

by the conventional least-squares estimation. But if the observation points are not sufficient to estimate the parameter, the estimation was affected by regularization.

Appendix B

Numerical Description of Derivation of History Matching Algorithms

1. Derivation of Reservoir Equations

Consider a two-dimensional (areal) oil-water reservoir with uniform thickness h that is much smaller than the other two dimensions. Assuming that the oil and water phases are immiscible, the equations of mass conservation for oil and water phases are

$$R_o = -\frac{\partial}{\partial t}(\rho_o \phi S_o) - \nabla \cdot (\rho_o \mathbf{v}_o) + \sum_{\kappa=1}^{N_w} \rho_o q_{o\kappa} \frac{\delta(x-x_\kappa)\delta(y-y_\kappa)}{h} = 0 \qquad (B.1)$$

$$R_w = -\frac{\partial}{\partial t}(\rho_w \phi S_w) - \nabla \cdot (\rho_w \mathbf{v}_w) + \sum_{\kappa=1}^{N_w} \rho_w q_{w\kappa} \frac{\delta(x-x_\kappa)\delta(y-y_\kappa)}{h} = 0 \qquad (B.2)$$

for $(x,y) \in \Omega$, and $0 < t < T$. S_o and S_w denote the saturations of oil and water, and $S_o \equiv 1 - S_w$. The porosity, ϕ, and the density of oil, ρ_o, and water, ρ_w, are weak functions of pressure. Define the compressibility of rock, c_f, oil, c_o, and water, c_w, by

$$c_f = \frac{1}{\phi}\frac{d\phi}{dp} \qquad (B.3)$$

$$c_o = \frac{1}{\rho_o}\frac{d\rho_o}{dp} \qquad (B.4)$$

$$c_w = \frac{1}{\rho_w}\frac{d\rho_w}{dp} \qquad (B.5)$$

and assume that the compressibilities be constant over the entire region of pressure change in this reservoir model. The formation volume factor of rock is defined by

$$B_f = \frac{\phi_{sc}}{\phi} . \qquad (B.6)$$

The linear fluid velocities of oil and water, $\mathbf{v}_o$ and $\mathbf{v}_w$, respectively, are assumed to obey Darcy's law in porous medium

$$\mathbf{v}_o = -\frac{kk_{ro}}{\mu_o}\nabla p \tag{B.7}$$

$$\mathbf{v}_w = -\frac{kk_{rw}}{\mu_w}\nabla p \tag{B.8}$$

where k denotes absolute permeability, and k_{ro} and k_{rw} denote relative permeabilities of oil and water, respectively, which are assumed to be functions of saturation given by

$$k_{ro} = a_o\left(\frac{1 - S_{ro} - S_w}{1 - S_{ro} - S_{iw}}\right)^{b_o} \tag{B.9}$$

$$k_{rw} = a_w\left(\frac{S_w - S_{iw}}{1 - S_{ro} - S_{iw}}\right)^{b_w} \tag{B.10}$$

for $S_{iw} \leq S_w \leq 1 - S_{ro}$. S_{ro} and S_{iw} denote residual oil and irreducible (connate) water saturations, respectively, and a_o, a_w, b_o, and b_w are constants. By combining Eqs. (B.1) and (B.7), the divergence term in the oil phase equation becomes

$$\nabla\cdot\left(\rho_o\frac{kk_{ro}}{\mu_o}\nabla p\right) = \rho_o\nabla\cdot\left(\frac{kk_{ro}}{\mu_o}\nabla p\right) + c_o\rho_o\nabla p\cdot\left(\frac{kk_{ro}}{\mu_o}\nabla p\right) \tag{B.11}$$

and the second term on righthand side is ignored. The injection and production rates of oil and water, $q_{o\kappa}$ and $q_{w\kappa}$ at wells $\kappa = 1,\ldots,N_w$ located at (x_κ, y_κ) are specified as

$$\begin{cases} q_{o\kappa} = 0 & \text{and } q_{w\kappa} = q_\kappa & \text{for injection wells} \\ q_{o\kappa} = (1 - f_w)q_\kappa & \text{and } q_{w\kappa} = f_w q_\kappa & \text{for production wells} \end{cases} \tag{B.12}$$

for Chapters III and IV, where q_κ, $\kappa = 1,\ldots,N_w$ denote the total injection (> 0) or total production (< 0) rates. For the example reported in Appendix A, the oil production rates are specified and the water production rates are given by

$$q_{w\kappa} = [f_w/(1 - f_w)]q_{o\kappa}\,. \tag{B.13}$$

Using above assumptions, Eqs. (1) and (2) become

$$R_o = -\frac{\phi_{sc}}{B_f}(c_o + c_f)(1 - S_w)\frac{\partial p}{\partial t} + \frac{\phi_{sc}}{B_f}\frac{\partial S_w}{\partial t} + \nabla \cdot \left(\frac{k k_{ro}}{\mu_o}\nabla p\right) + \sum_{\kappa=1}^{N_w} q_{o\kappa}\frac{\delta(x - x_\kappa)\delta(y - y_\kappa)}{h} \tag{B.14}$$

$$R_w = -\frac{\phi_{sc}}{B_f}(c_w + c_f)S_w\frac{\partial p}{\partial t} - \frac{\phi_{sc}}{B_f}\frac{\partial S_w}{\partial t} + \nabla \cdot \left(\frac{k k_{rw}}{\mu_w}\nabla p\right) + \sum_{\kappa=1}^{N_w} q_{w\kappa}\frac{\delta(x - x_\kappa)\delta(y - y_\kappa)}{h} \tag{B.15}$$

for $(x, y) \in \Omega$ and $0 < t < T$. The no-flux boundary condition at the impermeable boundary is

$$\mathbf{n} \cdot \nabla p = 0 \tag{B.16}$$

for $(x, y) \in \partial\Omega$ and $0 < t < T$. Initial conditions are given by

$$p(x, y, 0) = p^0(x, y) \tag{B.17}$$

$$S_w(x, y, 0) = {S_w}^0(x, y) \tag{B.18}$$

for $(x, y) \in \Omega$. Eqs. (B.14 – 18) are discretized by implicit time finite difference approximation. Define sets of integers

$$\begin{aligned} \mathcal{N} &= \{\, i \mid i = i_x + N_x(i_y - 1),\ i_x = 1, \ldots, N_x,\ i_y = 1, \ldots, N_y,\ \} \\ &= \{\, 1, \ldots, N \,\}, \end{aligned} \tag{B.19}$$

where N_x and N_y denote the numbers of grid cells along x- and y-directions for PDE's and $N = N_x N_y$, and

$$J_i = \{\, i - N_x, i - 1, i + 1, 1 + N_x \,\} \bigcap \mathcal{N} \tag{B.20}$$

for $i \in \mathcal{N}$.

$$\begin{aligned} R_{o_i}^n = &-Q_t\frac{\phi_{sc_i}}{{B_f}_i^{n-1}}(c_o + c_f)(1 - {S_w}_i^n)\left(p_i^n - p_i^{n-1}\right) \\ &+ Q_t\frac{\phi_{sc_i}}{{B_f}_i^{n-1}}\left({S_w}_i^n - {S_w}_i^{n-1}\right) \\ &- \sum_{j \in J_i} Q_{i,j}\frac{k_{i,j}{k_{ro}}_{i,j}^n}{\mu_o}\left(p_i^n - p_j^n\right) + \sum_{\kappa=1}^{N_w} q_{o\kappa}\frac{\delta_{i,i_\kappa}}{h} \\ =&0 \end{aligned} \tag{B.21}$$

$$
\begin{aligned}
R_{w_i}^{\,n} = & - Q_t \frac{\phi_{sc\,i}}{B_{f_i}^{\,n-1}} (c_w + c_f) S_{w_i}^{\,n} \left(p_i^n - p_i^{n-1} \right) \\
& - Q_t \frac{\phi_{sc\,i}}{B_{f_i}^{\,n-1}} \left(S_{w_i}^{\,n} - S_{w_i}^{\,n-1} \right) \\
& - \sum_{j \in J_i} Q_{i,j} \frac{k_{i,j} k_{rw_{i,j}}^{\,n}}{\mu_w} \left(p_i^n - p_j^n \right) + \sum_{\kappa=1}^{N_w} q_{w\kappa} \frac{\delta_{i,i_\kappa}}{h} \\
= & 0
\end{aligned}
\tag{B.22}
$$

for $i \in \mathcal{N}$ and $n = 1, \ldots, N_t$ where $Q_t = \Delta x \Delta y / \Delta t$ and

$$
Q_{i,j} = \begin{cases} \Delta y / \Delta x & \text{for } j \in \{ i-1, i+1 \} \bigcap \mathcal{N} \\ \Delta x / \Delta y & \text{for } j \in \{ i-N_x, i+N_x \} \bigcap \mathcal{N} \\ 0 & \text{otherwise.} \end{cases} \tag{B.23}
$$

Initial conditions are

$$
p_i^0 = p^0 \tag{B.24}
$$

$$
S_{w_i}^{\,0} = S_w{}^0 \tag{B.25}
$$

for $i \in \mathcal{N}$. In Eqs. (B.21) and (B.22), the arithmetic average is used for the absolute permeability

$$
k_{i,j} = \frac{k_i + k_j}{2} \tag{B.26}
$$

and upstream weighting is used for the relative permeabilities (Settari and Aziz, 1975)

$$
\begin{cases} k_{ro_{i,j}}^{\,n} = k_{ro}(S_{w_i}^{\,n}) \text{ and } k_{rw_{i,j}}^{\,n} = k_{rw}(S_{w_i}^{\,n}) & \text{if } p_i^n \geq p_j^n \\ k_{ro_{i,j}}^{\,n} = k_{ro}(S_{w_j}^{\,n}) \text{ and } k_{rw_{i,j}}^{\,n} = k_{rw}(S_{w_j}^{\,n}) & \text{if } p_i^n < p_j^n. \end{cases} \tag{B.27}
$$

2. Solution of Reservoir Equations

To solve the finite difference reservoir equations, it is convenient to define the "expansion equation"

$$
R_{o_i}^{\,n} + R_{w_i}^{\,n} = 0 \tag{B.28}
$$

to solve for the pressure and

$$
\frac{(c_o + c_f)(1 - S_{w_i}^{\,n})}{c_{t_i}^n} R_{w_i}^{\,n} - \frac{(c_w + c_f) S_w}{c_{t_i}^n} R_{o_i}^{\,n} = 0 \tag{B.29}
$$

Step 4 Solve Eq. (B.31) for $\delta \mathbf{S}_w{}^n$ by the IADI method.

Step 5 If Eq. (B.29) is not satisfied then repeat Step 4.

Step 6 If $||\mathbf{p}^n - \mathbf{p}^{n,\text{old}}||_\infty > \epsilon_1$ or $||\mathbf{S}_w{}^n - \mathbf{S}_w{}^{n,\text{old}}||_\infty > \epsilon_2$, repeat Step 2.

3. Derivation of Adjoint System

The least-squares discrepancy function J_{LS} consists of two contributions, the pressure and the flow measurements, given by

$$J_{LS} = \int_0^T \iint_\Omega dxdydt \frac{1}{N_t N_o} \sum_{n=1}^{N_t} \sum_{\nu=1}^{N_o} \Bigg[W_p \left(p(x_\nu, y_\nu, t_n) - p^{\text{obs}}{}_\nu^n \right)^2 + W_f \left(f_w(x_\nu, y_\nu, t_n) - f_w^{\text{obs}}{}_\nu^n \right)^2 \Bigg] \delta(x - x_\nu)\delta(y - y_\nu)\delta(t - t_n) \tag{B.34}$$

where $p^{\text{obs}}{}_\nu^n$ and $f_w^{\text{obs}}{}_\nu^n$ denote the pressure and fractional flow of water data measured at wells $\nu = 1, \ldots, N_o$ located at (x_ν, y_ν) and at time $t_n = n\Delta t$, $n = 1, \ldots, N_t$. The fractional flow of water is defined by

$$f_w = \frac{k_{rw}/\mu_w}{k_{rw}/\mu_w + k_{ro}/\mu_o} \,. \tag{B.35}$$

By adjoining the Eqs. (B.14) and (B.15) by means of adjoint variables, ψ_o and ψ_w, we get

$$\widetilde{J_{LS}} = J_{LS} + \int_0^T \iint_\Omega \left(\psi_o R_o + \psi_w R_w \right) dxdydt \,. \tag{B.36}$$

From the first variation of Eq. (B.36), the adjoint equations are given by

$$\begin{aligned} R_p =& (c_w + c_f)\frac{\partial}{\partial t}(\phi S_w \psi_w) + (c_o + c_f)\frac{\partial}{\partial t}(\phi(1 - S_w)\psi_o) \\ &+ \nabla \cdot \left(\frac{k k_{rw}}{\mu_w} \nabla \psi_w + \frac{k k_{ro}}{\mu_o} \nabla \psi_o \right) \\ &+ \frac{2W_p}{N_o N_t} \sum_{n=1}^{N_t} \sum_{\nu=1}^{N_o} \left(p - p^{\text{obs}}{}_\nu^n \right) \delta(x - x_\nu)\delta(y - y_\nu)\delta(t - t_n) \\ =& 0 \end{aligned} \tag{B.37}$$

from the terms including the variation of p and

$$\begin{aligned} R_s =& \frac{\partial}{\partial t}\left[\phi(\psi_w - \psi_o)\right] - \phi((c_w + c_f)\psi_w - (c_o + c_f)\psi_o)\frac{\partial p}{\partial t} \\ & - \frac{k}{\mu_w}\frac{\partial k_{rw}}{\partial S_w}\nabla\psi_w \cdot \nabla p - \frac{k}{\mu_o}\frac{\partial k_{ro}}{\partial S_w}\nabla\psi_o \cdot \nabla p \\ & + \sum_{\kappa=1}^{N_w}\left(\psi_w \frac{\partial q_{w\kappa}}{\partial S_w} + \psi_o \frac{\partial q_{o\kappa}}{\partial S_w}\right)\frac{\delta(x - x_\kappa)\delta(y - y_\kappa)}{h} \\ & + \frac{2W_f}{N_o N_t}\sum_{n=1}^{N_t}\sum_{\nu=1}^{N_o}\left(f_w - f_w^{\mathrm{obs}\,n}{}_\nu\right)\frac{\partial f_w}{\partial S_w}\delta(x - x_\nu)\delta(y - y_\nu)\delta(t - t_n) \\ =& 0 \end{aligned} \tag{B.38}$$

from the terms including the variation of S_w for $(x, y) \in \Omega$ and $0 < t < T$ with the terminal constraints

$$\psi_o(x, y, T) = 0 \tag{B.39}$$

$$\psi_w(x, y, T) = 0 \tag{B.40}$$

for $(x, y) \in \Omega$ and the boundary condition

$$\mathbf{n} \cdot \left(\frac{k k_{rw}}{\mu_w}\nabla\psi_w + \frac{k k_{ro}}{\mu_o}\nabla\psi_o\right) = 0 \tag{B.41}$$

for $(x, y) \in \partial\Omega$ and $0 < t < T$. The functional derivative of J_{LS} with respect to $k(x, y)$ is

$$\frac{\delta J_{LS}}{\delta k} = -\int_0^T \left(\frac{k_{rw}}{\mu_w}\nabla\psi_w \cdot \nabla p + \frac{k_{ro}}{\mu_o}\nabla\psi_o \cdot \nabla p\right) dt\,, \tag{B.42}$$

and the partial derivatives of J_{LS} with respect to b_o and b_w are

$$\begin{aligned} \frac{\partial J_{LS}}{\partial b_o} =& -\int_0^T \iint_\Omega dxdydt\left[\frac{k}{\mu_o}\frac{\partial k_{ro}}{\partial b_o}\nabla\psi_o \cdot \nabla p\right. \\ & + \sum_{\kappa=1}^{N_w}\left(\psi_w \frac{\partial q_{w\kappa}}{\partial b_o} + \psi_o \frac{\partial q_{o\kappa}}{\partial b_o}\right)\frac{\delta(x - x_\kappa)\delta(y - y_\kappa)}{h} \\ & \left. + \frac{2W_f}{N_o N_t}\sum_{n=1}^{N_t}\sum_{\nu=1}^{N_o}(f_w - f_w^{\mathrm{obs}\,n}{}_\nu)\frac{\partial f_w}{\partial b_o}\delta(x - x_\nu)\delta(y - y_\nu)\delta(t - t_n)\right] \end{aligned} \tag{B.43}$$

$$\frac{\partial J_{LS}}{\partial b_w} = -\int_0^T \iint_\Omega dxdydt \left[\frac{k}{\mu_w} \frac{\partial k_{rw}}{\partial b_w} \nabla\psi_w \cdot \nabla p \right.$$
$$+ \sum_{\kappa=1}^{N_w} \left(\psi_w \frac{\partial q_{w\kappa}}{\partial b_w} + \psi_o \frac{\partial q_{o\kappa}}{\partial b_w} \right) \frac{\delta(x-x_\kappa)\delta(y-y_\kappa)}{h} \qquad (B.44)$$
$$\left. + \frac{2W_f}{N_o N_t} \sum_{n=1}^{N_t} \sum_{\nu=1}^{N_o} (f_w - f_w^{\mathrm{obs}\,n}_{\nu}) \frac{\partial f_w}{\partial b_w} \delta(x-x_\nu)\delta(y-y_\nu)\delta(t-t_n) \right] .$$

4. Solution of Adjoint Equations

The finite difference correspondences of Eqs. (B.34) and (B.36) are

$$J_{LS} = \frac{1}{N_t N_o} \sum_{n=1}^{N_t} \sum_{\nu=1}^{N_o} \sum_{i=1}^{N} \left[W_p \left(p_i^n - p^{\mathrm{obs}\,n}_{\nu} \right)^2 + W_f \left(f_{w_i}^n - f_w^{\mathrm{obs}\,n}_{\nu} \right)^2 \right] \delta_{i,i_\nu} \qquad (B.45)$$

and

$$\widetilde{J_{LS}} = J_{LS} + \sum_{n=1}^{N_t} \sum_{i=1}^{N} (\psi_{w_i}^n R_{w_i}^n + \psi_{o_i}^n R_{o_i}^n) . \qquad (B.46)$$

Collecting terms that include the first variation of p_i^n yields

$$R_{p_i}^n = Q_t \frac{\phi_{sc\,i}}{B_{f_i}^n} \left((c_w + c_f) S_{w_i}^{n+1} \psi_{w_i}^{n+1} + (c_o + c_f)(1 - S_{w_i}^{n+1}) \psi_{o_i}^{n+1} \right)$$
$$- Q_t \frac{\phi_{sc\,i}}{B_{f_i}^{n-1}} \left((c_w + c_f) S_{w_i}^n \psi_{w_i}^n + (c_o + c_f)(1 - S_{w_i}^n) \psi_{o_i}^n \right)$$
$$- \sum_{j \in J_i} \left(\frac{k_{i,j} k_{rw}{}_{i,j}^n}{\mu_w} (\psi_{w_i}^n - \psi_{w_j}^n) + \frac{k_{i,j} k_{ro}{}_{i,j}^n}{\mu_o} (\psi_{o_i}^n - \psi_{o_j}^n) \right) \qquad (B.47)$$
$$+ \frac{2W_p}{N_t N_o} \sum_{\nu=1}^{N_o} (p_i^n - p^{\mathrm{obs}\,n}_{\nu}) \delta_{i,i_\nu}$$
$$= 0 ,$$

and terms that include the first variation of ${S_{w_i}}^n$ yield

$$
\begin{aligned}
{R_{s_i}}^n =& Q_t \left(\frac{\phi_{sc\,i}}{{B_{f_i}}^n} ({\psi_{w_i}}^{n+1} - {\psi_{o_i}}^{n+1}) - \frac{\phi_{sc\,i}}{{B_{f_i}}^{n-1}} ({\psi_{w_i}}^n - {\psi_{o_i}}^n) \right) \\
& - ((c_w + c_f){\psi_{w_i}}^n - (c_o + c_f){\psi_{o_i}}^n)\, Q_t \frac{\phi_{sc\,i}}{{B_{f_i}}^{n-1}} ({p_i}^n - {p_i}^{n-1}) \\
& - \sum_{j \in J_i} \left(\frac{k_{i,j}}{\mu_w} \frac{\partial {k_{rw}}_{i,j}^n}{\partial {S_{w_i}}^n} ({\psi_{w_i}}^n - {\psi_{w_j}}^n) + \frac{k_{i,j}}{\mu_o} \frac{\partial {k_{ro}}_i j^n}{\partial {S_{w_i}}^n} ({\psi_{o_i}}^n - {\psi_{o_j}}^n) \right) ({p_i}^n - {p_j}^n) \\
& + \frac{2W_f}{N_t N_o} \frac{\partial {f_{w_i}}^n}{\partial {S_{w_i}}^n} \sum_{\nu=1}^{N_o} ({f_{w_i}}^n - {f_w^{\mathrm{obs}}}_\nu^n) \delta_{i,i_\nu} + \sum_{\kappa=1}^{N_w} \left({\psi_{w_i}}^n \frac{\partial q_{w\kappa}}{\partial {S_{w_i}}^n} + {\psi_{o_i}}^n \frac{\partial q_{o\kappa}}{\partial {S_{w_i}}^n} \right) \delta_{i,i_\nu} \\
=& 0
\end{aligned}
\tag{B.48}
$$

for $i \in \mathcal{N}$ and $n = N_t, N_t - 1, \ldots, 2, 1$ with terminal constraints

$${\psi_{w_i}}^{N_t+1} = 0 \tag{B.49}$$

$${\psi_{o_i}}^{N_t+1} = 0 \tag{B.50}$$

for $i \in \mathcal{N}$. The functional derivatives of J_{LS} with respect to k_i, $i \in \mathcal{N}$, are given by

$$
\frac{\partial J_{LS}}{\partial k_i} = -\frac{1}{2} \sum_{n=1}^{N_t} \sum_{j \in J_i} \left(\frac{{k_{rw}}_{i,j}^n}{\mu_w} ({\psi_{w_i}}^n - {\psi_{w_j}}^n) + \frac{{k_{ro}}_{i,j}^n}{\mu_o} ({\psi_{o_i}}^n - {\psi_{o_j}}^n) \right) ({p_i}^n - {p_j}^n)
\tag{B.51}
$$

$$
\begin{aligned}
\frac{\partial J_{LS}}{\partial b_o} = & -\frac{1}{2} \sum_{n=1}^{N_t} \left[\sum_{i=1}^{N} \sum_{j \in J_i} \frac{k_{i,j}}{\mu_o} \frac{\partial {k_{ro}}_{i,j}^n}{\partial b_o} ({\psi_{o_i}}^n - {\psi_{o_j}}^n)({p_i}^n - {p_j}^n) \right. \\
& + \sum_{\kappa=1}^{N_w} \left({\psi_{w_i}}^n \frac{\partial q_{w\kappa}}{\partial b_o} + {\psi_{o_i}}^n \frac{\partial q_{o\kappa}}{\partial b_o} \right) \frac{\delta_{i,i_\kappa}}{h} \\
& \left. + \frac{2W_f}{N_t N_o} \sum_{\nu=1}^{N_o} \left({f_{w_i}}^n - {f_w^{\mathrm{obs}}}_\nu^n \right) \frac{\partial {f_{w_i}}^n}{\partial b_o} \delta_{i,i_\nu} \right]
\end{aligned}
\tag{B.52}
$$

$$
\begin{aligned}
\frac{\partial J_{LS}}{\partial b_w} = & -\frac{1}{2} \sum_{n=1}^{N_t} \left[\sum_{i=1}^{N} \sum_{j \in J_i} \frac{k_{i,j}}{\mu_w} \frac{\partial {k_{rw}}_{i,j}^n}{\partial b_o} ({\psi_{w_i}}^n - {\psi_{w_j}}^n)({p_i}^n - {p_j}^n) + \right. \\
& \sum_{\kappa=1}^{N_w} \left({\psi_{w_i}}^n \frac{\partial q_{w\kappa}}{\partial b_w} + {\psi_{o_i}}^n \frac{\partial q_{o\kappa}}{\partial b_w} \right) \frac{\delta_{i,i_\kappa}}{h} \\
& \left. + \frac{2W_f}{N_t N_o} \sum_{\nu=1}^{N_o} \left({f_{w_i}}^n - {f_w^{\mathrm{obs}}}_\nu^n \right) \frac{\partial {f_{w_i}}^n}{\partial b_w} \delta_{i,i_\nu} \right]
\end{aligned}
\tag{B.53}
$$

It is convenient to solve Eqs. (B.47) and (B.48) for a new set of variables ψ_p and ψ_s defined by

$$\psi_{p_i}^{\ n} = \frac{(c_w + c_f)S_{w_i}^{\ n}}{c_{t_i}^{\ n}}\psi_{w_i}^{\ n} + \frac{(c_o + c_f)(1 - S_{w_i}^{\ n})}{c_{t_i}^{\ n}}\psi_{o_i}^{\ n} \qquad (B.54)$$

$$\psi_{s_i}^{\ n} = \psi_{w_i}^{\ n} - \psi_{o_i}^{\ n} . \qquad (B.55)$$

Define $\Psi_p{}^n = (\psi_{p1}^{\ n}, \ldots, \psi_{pN}^{\ n})$ and $\Psi_s{}^n = (\psi_{s1}^{\ n}, \ldots, \psi_{sN}^{\ n})$; then the numerical scheme to solve the adjoint equations and to compute the derivatives of J_{LS} for $n = N_t, N_t - 1, \ldots, 2, 1$ is as follows

Step 1 Let $\Psi_p{}^n = \Psi_p{}^{n+1}$ and $\Psi_s{}^n = \Psi_s{}^{n+1}$.

Step 2 Let $\Psi_p{}^{n,\mathrm{old}} = \Psi_p{}^n$ and $\Psi_s{}^{n,\mathrm{old}} = \Psi_s{}^n$.

Step 3 Solve Eq. (B.47) for Ψ_p by the IADI method.

Step 4 Solve Eq. (B.48) for Ψ_s by the IADI method.

Step 5 If $||\Psi_p{}^n - \Psi_p{}^{n,\mathrm{old}}||_\infty > \epsilon_3$ or $||\Psi_s{}^n - \Psi_s{}^{n,\mathrm{old}}||_\infty > \epsilon_4$ then repeat Step 2.

Step 6 Compute the contribution of n-th time step values of $\partial J_{LS}/\partial k_i$, $i \in \mathcal{N}$ and of $\partial J_{LS}/\partial b_o$ and $\partial J_{LS}/\partial b_w$.

5. Calculation of Derivatives of J_{SM} w.r.t. W_{l_x,l_y}

To apply the spline approximation of the absolute permeability to the history-matching algorithms, we need the expression of the derivatives of J_{SM} with respect to the spline coefficients, W_{l_x,l_y}, $l_x = 1, \ldots, N_{xs}$ and $l_y = 1, \ldots, N_{ys}$. From the derivatives of J_{LS} to k_i, $i \in \mathcal{N}$, the derivative of J_{LS} with respect to the spline coefficients can be calculated by

$$\frac{\partial J_{LS}}{\partial W_{l_x,l_y}} = \sum_{i_x=1}^{N_x}\sum_{i_y=1}^{N_y} \frac{\partial J_{LS}}{\partial k_i} \chi^{*4}\left(4 - l_x + \frac{x}{\delta x_s}\right)\chi^{*4}\left(4 - l_y + \frac{y}{\delta y_s}\right) \qquad (B.56)$$

for $l_x = 1, \ldots, N_{xs}$ and $l_y = 1, \ldots, N_{ys}$, and $i = i_x + N_x(i_y - 1)$. The derivatives $\partial J_{ST}/\partial W_{l_x,l_y}$, $l_x = 1, \ldots, N_{xs}$ and $l_y = 1, \ldots, N_{ys}$, can be calculated exactly

(Kravaris, 1984). Finally we have

$$\frac{\partial J_{SM}}{\partial W_{l_x,l_y}} = \frac{\partial J_{LS}}{\partial W_{l_x,l_y}} + \beta \frac{\partial J_{ST}}{\partial W_{l_x,l_y}} . \qquad (B.57)$$

6. Minimization Algorithms

In this dissertation, two different minimization techniques are employed. The partial conjugate gradient algorithm of Nazareth (1977) is used for the minimization of a single set of parameters, and the steepest descent algorithm is used for the minimization of two sets of parameters, that are spline coefficients to represent absolute permeability and the exponents of relative permeability expressions. To simplify the following discussion, we will use new sets of variables in this section. Let $\mathbf{x}$ be an n-dimensional vector, $F(\mathbf{x})$ be a function to be minimized over $\mathbf{x}$, and $\mathbf{g}(\mathbf{x})$ be the gradient of F at $\mathbf{x}$. Let $\mathbf{d}$ denote the descent direction vector, which will be determined during the minimization. The partial conjugate gradient algorithms are generally preferable for large-scale problems that have hundreds of variables. To maximize the overall efficiency, the Nazareth algorithm terminates the line search step early without exact search, and to keep the conjugacy of the search direction, the new descent direction is calculated from two previously determined descent directions given by

$$\mathbf{d}_{j+1} = -\mathbf{h}_j + \frac{\mathbf{h}_{j-1} \cdot \mathbf{h}_j}{\mathbf{h}_{j-1} \cdot \mathbf{d}_{j-1}} \mathbf{d}_{j-1} + \frac{\mathbf{h}_j \cdot \mathbf{h}_j}{\mathbf{h}_j \cdot \mathbf{d}_j} \mathbf{d}_j \qquad (B.58)$$

where $\mathbf{h}_j = \mathbf{g}_{j+1} - \mathbf{g}_j$ and j is the minor iteration count. (See Figure 1.) In the examples reported in this dissertation, the algorithm required usually 2 line search iterations and 5 - 10 minor iterations. The number of the major iterations was much dependent on the given problems but, on the whole, the 3-step history-matching algorithm reported in Chapter III required 20 - 40 solutions of state and adjoint equations.

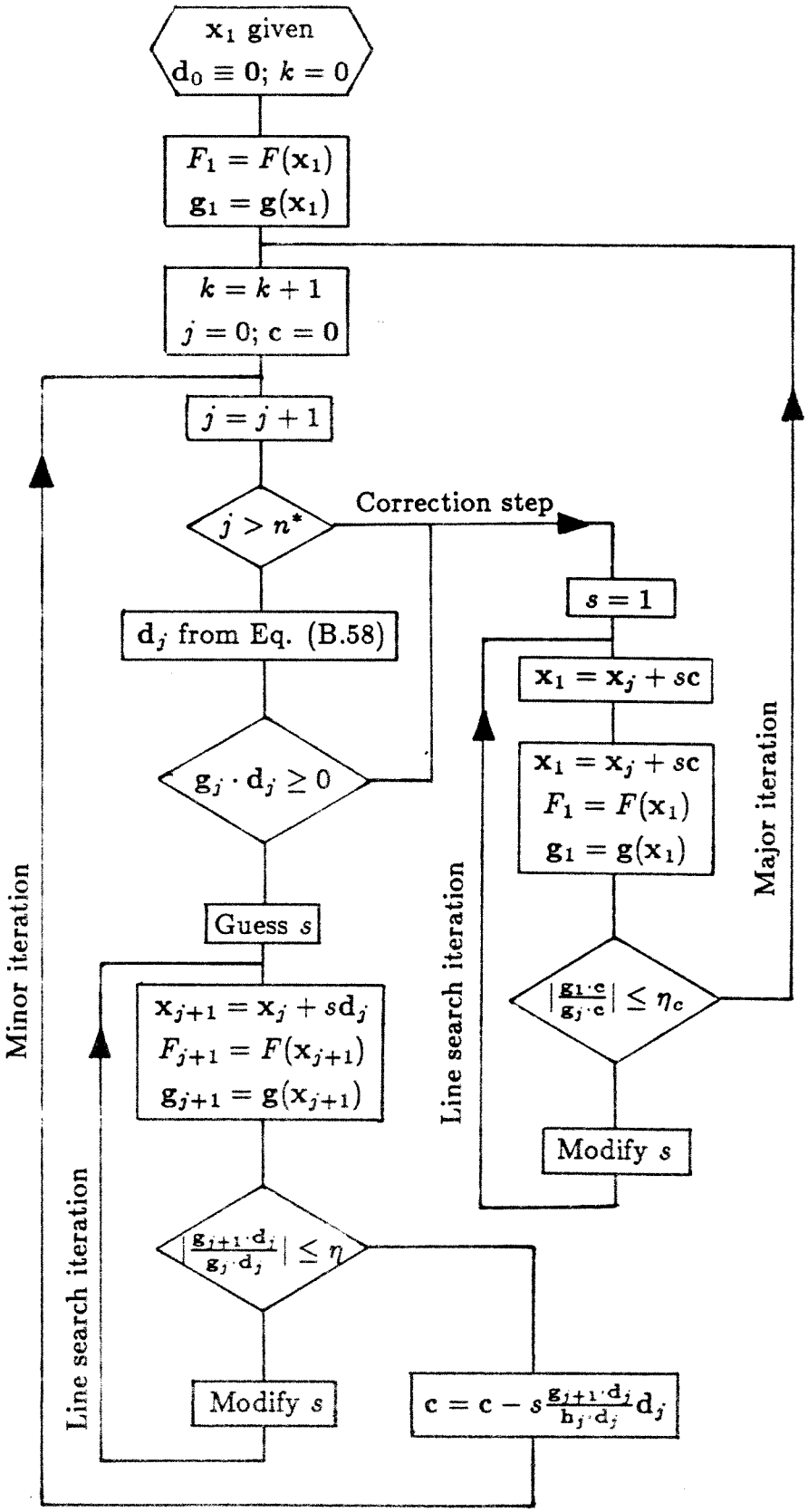

Figure 1 Flow chart of Nazareth's partial conjugate gradient Algorithm

In Chapter IV, the smoothing functional was minimized by an alternative of the steepest descent algorithm, which redefines the descent direction from the rough parametric sensitivity analysis to improve the convergence. Let $\mathbf{y}$, $\mathbf{z}$, $\mathbf{g}^y$, $\mathbf{g}^z$, $\mathbf{d}^y$, and $\mathbf{d}^z$ be n-vectors and let the last $n - m$ $(m < n)$ elements of $\mathbf{y}$ and the first m elements of $\mathbf{z}$ be zero and the same is true for $\mathbf{g}^y$ and $\mathbf{g}^z$, respectively, and for $\mathbf{d}^y$ and $\mathbf{d}^z$, respectively. Let the two vectors $\mathbf{y}$ and $\mathbf{z}$ satisfy $\mathbf{x} = \mathbf{y} + \mathbf{z}$, and $\mathbf{g}^y$ and $\mathbf{g}^z$ satisfy $\mathbf{g} = \mathbf{g}^y + \mathbf{g}^z$. Let $\mathbf{d}^y = -\mathbf{g}^y$ and $\mathbf{d}^z = -\mathbf{g}^z$; then $\mathbf{d}^y + \mathbf{d}^z$ is the usual descent direction of the steepest descent method. Let $\mathbf{y}$ and $\mathbf{z}$ represent two different physical quantities to which F has different sensitivities. This is the case of simultaneous estimation of absolute and relative permeabilities. Define

$$G_y(s_y, s_z) = \mathbf{g}^y(\mathbf{y} + s_y\mathbf{d}^y, \mathbf{z} + s_z\mathbf{d}^z) \cdot \mathbf{d}^y \qquad (B.59)$$

$$G_z(s_y, s_z) = \mathbf{g}^z(\mathbf{y} + s_y\mathbf{d}^y, \mathbf{z} + s_z\mathbf{d}^z) \cdot \mathbf{d}^z \; ; \qquad (B.60)$$

then Eqs. (31) and (32) in Chapter IV can be rewritten as $G_y = G_z = 0$. The stepsizes (s_y, s_z) can be determined from the Taylor series expansions of Eqs. (B.59) and (B.60) given by

$$\begin{pmatrix} \frac{\partial G_y}{\partial s_y} & \frac{\partial G_y}{\partial s_z} \\ \frac{\partial G_z}{\partial s_y} & \frac{\partial G_z}{\partial s_z} \end{pmatrix} \begin{pmatrix} s_y \\ s_z \end{pmatrix} + \begin{pmatrix} G_y \\ G_z \end{pmatrix} = 0 \, , \qquad (B.61)$$

and the descent direction in Figure 2 is given by

$$\mathbf{d} = s_y\mathbf{d}^y + s_z\mathbf{d}^z \, , \qquad (B.62)$$

and the line search is carried out in the direction $\mathbf{d}$.

References

Aziz, K. and A. Settari, *Petroleum Reservoir Simulation* (Applied Sceince, London, 1983).

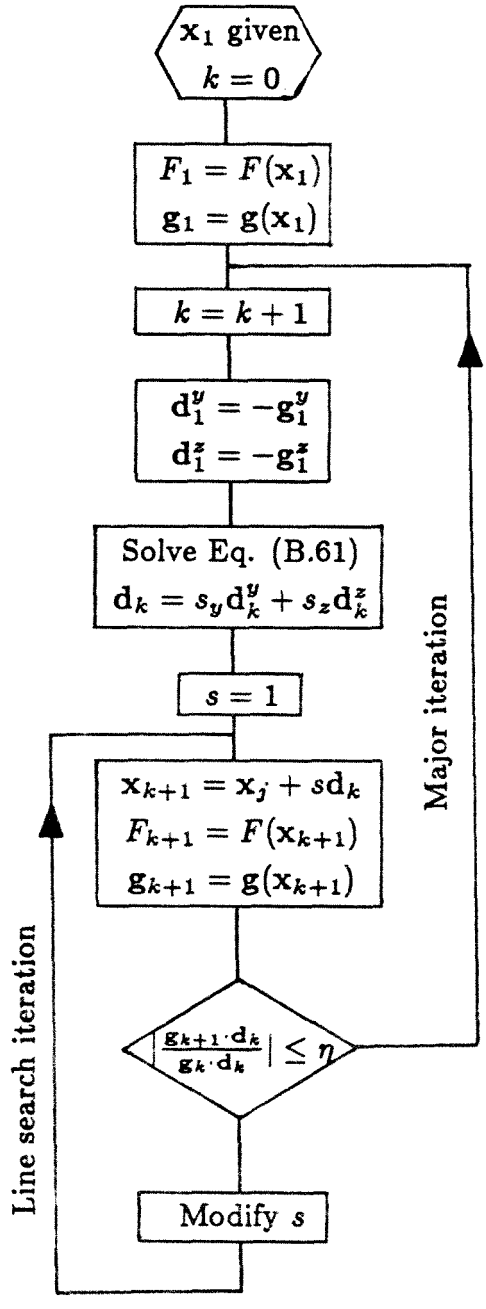

Figure 2 Flow chart of steepest descent algorithm with correction of the descent direction by parametric sensitivity analysis

Briggs J. E. and T. N. Dixon, Some Practical Considerations in the Numerical Solution of Two-Dimensional Reservoir Problems, *Soc. Pet. End. J.*,**8**,185 – 194 (1968).

Kravaris, C., Identification of Spatially-Varying Parameters in Distributed Parameter Systems, *PhD Thesis,* California Institute of Technology (1984).

Nazareth, L., A Conjugate Gradient Algorithm Without Line Searches, *J. Opt. Theory Appl.*, **23**, 373 – 387 (1977).

Settari, A. and K. Aziz, Treatment of Nonlinear Terms in the Numerical Solution of Partial Differential Equations for Multiphase Flow in Porous Media, *Int. J. Multiphase Flow,* **1**, 817 – 844 (1975).